



2014-12-01

Influence of Pile Shape on Resistance to Lateral Loading

Guillermo Bustamante
Brigham Young University - Provo

Follow this and additional works at: <https://scholarsarchive.byu.edu/etd>

 Part of the [Civil and Environmental Engineering Commons](#)

BYU ScholarsArchive Citation

Bustamante, Guillermo, "Influence of Pile Shape on Resistance to Lateral Loading" (2014). *All Theses and Dissertations*. 5630.
<https://scholarsarchive.byu.edu/etd/5630>

This Thesis is brought to you for free and open access by BYU ScholarsArchive. It has been accepted for inclusion in All Theses and Dissertations by an authorized administrator of BYU ScholarsArchive. For more information, please contact scholarsarchive@byu.edu, ellen_amatangelo@byu.edu.

Influence of Pile Shape on Resistance to Lateral Loading

Guillermo Xabier Bustamante

A thesis submitted to the faculty of
Brigham Young University
in partial fulfillment of the requirements for the degree of
Master of Science

Kyle M. Rollins, Chair
Kevin W. Franke
Paul W. Richards

Department of Civil and Environmental Engineering

Brigham Young University

December 2014

Copyright © 2014 Guillermo Xabier Bustamante

All Rights Reserved

ABSTRACT

Influence of Pile Shape on Resistance to Lateral Loading

Guillermo Xabier Bustamante
Department of Civil and Environmental Engineering, BYU
Master of Science

The lateral resistance of pile foundations has typically been based on the resistance of circular pipe piles. In addition, most instrumented lateral load tests and cases history have involved circular piles. However, piles used in engineering practice may also be non-circular cross-section piles such as square and H piles. Some researchers have theorized that the lateral resistance of square piles will be higher than that of circular piles (Reese and Van Impe, 2001; Briaud et al, 1983; Smith, 1987) for various reasons, but there is not test data to support this claims.

To provide basic comparative performance data, lateral load tests were performed on piles with circular, square and H sections. To facilitate comparisons, all the tests piles were approximately 12 inches in width or diameter and were made of steel. The square and circular pipe sections had comparable moments of inertia; however, the H pile was loaded about the weak axis, as is often the case of piles supporting integral abutments, and had a much lower moment of inertia. The granular fill around the pile was compacted to approximately 95% of the standard Proctor maximum density and would be typical of fill for a bridge abutment.

Lateral load was applied with a free-head condition at a height of 1 ft above the ground surface. To define the load-deflection response, load was applied incrementally to produce deflection increments of about 0.25 inches up to a maximum deflection of about 3 inches. Although the square and pipe pile sections had nearly the same moment of inertia, the square pile provided lateral resistance that was 20 to 30% higher for a given deflection. The lateral resistance of the H pile was smaller than the other two pile shapes but higher than what it is expected based on the moment of inertia.

Back analysis with the computer program LPILE indicates that the pile shape was influencing the lateral resistance. Increasing the effective width to account for the shape effect as suggested by Reese and Van Impe (2001) was insufficient to account for the increased resistance. To provide agreement with the measured response, p-multipliers of 1.2 and 1.35 were required for the square pile and H piles, respectively. The analyses suggest that the increased resistance for the square and H pile sections was a result of increases in both the side shear and normal stress components of resistance. Using the back-calculated p-multipliers provided very good agreement between the measured and computed load-deflection curves and the bending moment versus depth curves.

Keywords: lateral load, pile, shape influence, lateral resistance, full-scale test, LPILE, pile geometry, MSE wall, side friction, circular pile, H pile, square pile

ACKNOWLEDGEMENTS

Funding for this study was provided by an FHWA pooled fund study TPF-5(272) “Evaluation of Lateral Pile Resistance Near MSE Walls at a Dedicated Wall Site” supported by Departments of Transportation from the states of Florida, Iowa, Kansas, Massachusetts, Minnesota, Montana, New York, Oregon, Texas and Utah. Utah served as the lead agency with Jason Richards as the project manager. This support is gratefully acknowledged; however, the opinions, conclusions and recommendations in this paper do not necessarily represent those of the sponsoring organizations.

I would also like to thank the following people who generously offered their help, input, and involvement in this process: Dr. Kyle M. Rollins, who inspired me to continue my exploration in the field of geotechnical engineering, but who also provided thoughtful feedback, expertise, knowledge and encouragement throughout my graduate studies; Dr. Kevin W. Franke and Dr. Paul W. Richards for being part of my committee and for their excellent advice; David Anderson and Rodney Mayo for providing their field experience and help during the construction, testing, and data collection for this project; Kim, Jolene, Katelyn and the rest of the secretaries, for always being willing to help. Thanks to my team: Jarell Han, Cody Hatch, Jason Besendorfer, Ryan Budd, and Andrew Luna for their hard work during this research.

Thanks to my parents for teaching me to dream big. Special thanks to my brother Guillermo Ramón and his family for opening the door of their home to me and being great support throughout my career and an infinite source of happiness in my life.

Finally, I am grateful to CoreBrace LLC, my employer during my graduate studies, for providing a work schedule that allowed me to complete my degree.

TABLE OF CONTENTS

LIST OF TABLES	vi
LIST OF FIGURES	vii
1 Introduction.....	1
2 Literature Review	5
2.1 Smith (1987)	5
2.2 Briaud et al (1983)	7
2.3 Reese and Van Impe (2001).....	12
2.4 Filz et al (2013).....	14
3 Test Layout	17
3.1 MSE Wall	18
3.1.1 Backfill.....	18
3.2 Piles.....	22
3.3 Load Apparatus.....	24
4 Instrumentation.....	25
4.1 Load Cell and Pressure Transducer	25
4.2 String Potentiometers.....	26
4.3 Strain Gauges	28
4.4 Digital Image Correlation (DIC) Camera System	29
5 Lateral Load Testing	33
5.1 Load Displacement Curves	34
5.2 Pile Performance.....	37
5.3 Ground Displacement	42
5.4 Heave	45

5.5	Failure Planes.....	46
6	Lateral Load Analysis.....	49
6.1	Pile Material Properties	50
6.2	Pile Load Model.....	51
6.3	Soil Properties Model	51
6.4	Results of LPILE Analysis	57
6.5	Reese and Van Impe Equivalent Diameter	64
6.6	Briaud and Smith F-y/Q-y Mechanism.....	68
6.7	P-multiplier Approach	74
6.8	Bending Moment vs. Depth Curves.....	77
7	Conclusions.....	81
7.1	Test Results.....	81
7.2	Lateral Load Analysis.....	82
7.3	Recommendation For Future Research.....	83
	REFERENCE.....	85
	Appendix A. Reese and Van impe	87
	Appendix B. F-y/Q-y Mechanism.....	89
	Appendix C. LPILE – ROUND PILE.....	91

LIST OF TABLES

Table 3-1: Pile Properties.....	22
Table 4-1: String Potentiometer Distances	28
Table 6-1: Soil Profile Properties Used in LPILE Analysis	56
Table 6-2: Reese and Van Impe Equivalent Diameter (Square & H piles)	65
Table 6-3: P-multipliers	74

LIST OF FIGURES

Figure 2-1: Q-y and F-y Contributions (After Smith 1987)	6
Figure 2-2: Schematic F-y (After Smith 1987).....	7
Figure 2-3: Friction and Front Resistance Forces for Texas A&M U. Drilled Shaft (Briaud et al 1983)	9
Figure 2-4: Sabine 2.5 Deep P-y Curves (Briaud et al 1983).....	11
Figure 2-5: Schematic Drawing Showing Difference in Lateral Resistance Owing to Pile Shape (After Reese and Van Impe, 2001)	12
Figure 2-6: Sign Convention (Fitz et al 2013).....	16
Figure 3-1: Location of Test Site	17
Figure 3-2: Schematic Plan & Elevation View Showing Layout of Test Piles & MSE Wall.....	18
Figure 3-3: Gradation for Select Backfill	19
Figure 3-4: Roller Compaction Between Test Piles and Reaction Piles.....	20
Figure 3-5: Plate Compaction Between MSE Wall and Piles Adjacent to The MSE Wall...	20
Figure 3-6: Jumping Jack Type Compaction Around Test Piles Investigated in This Study	21
Figure 3-7: Nuclear Density Gauge Testing	21
Figure 3-8: Driving Pile with a Diesel Type Hammer.....	23
Figure 3-9: Load Apparatus	24
Figure 4-1: Typical Tie-Rod Cell and Pressure Transducer Layout.....	26
Figure 4-2: String Potentiometer Instrumentation (H-pile)	27
Figure 4-3: H Pile Strain Gauge Instrumentation	29
Figure 4-4: Typical DIC Set Up.....	30
Figure 4-5: Ground Contrast Pattern for DIC Capture	31
Figure 5-1: Plan View of the Lateral Load Tests.....	33

Figure 5-2: Pile Peak Head Load vs. Deflection Curves	35
Figure 5-3: Pile 1 Minute Head Load vs. Deflection Curves	36
Figure 5-4: Bending Moment vs. Depth for Selected Head Loads for the Circular Pile	38
Figure 5-5: Bending Moment vs. Depth for Selected Head Loads for Square2	39
Figure 5-6: Bending Moment vs. Depth for Selected Head Loads for H Pile	40
Figure 5-7: Maximum Bending Moment vs. Depth for the Three Shapes	41
Figure 5-8: Maximum Bending Moment vs. Applied Load for the Three Shapes	42
Figure 5-9: Ground Displacement vs. Distance From Pile Plot for All Piles Tested	43
Figure 5-10: Circular Pile Ground Displacement From DIC	44
Figure 5-11: H Pile Ground Displacement From DIC	45
Figure 5-12: Heave vs. Distance From Pile Face	46
Figure 5-13: Failure Planes for the Distinct Shapes	47
Figure 6-1: LPILE Input Property Window (Round Pile)	51
Figure 6-2: Illustration of Wedge Type Failure Adjacent to Piles at Shallow Depths During Lateral Loading	53
Figure 6-3: Coefficients C1, C2, and C3 as Function of Friction Angle	54
Figure 6-4: Subgrade Reaction Modulus, k Used for API Sand Criteria in p-y Analysis (API, 1982)	55
Figure 6-5: Side View of Soil Layers in LPILE (Round Pile)	56
Figure 6-6: Load vs. Deflection Curve for Various ϕ and k (Round)	57
Figure 6-7: Load-Deflection Curves Comparison of Tested Values and Computed	58
Figure 6-8: Load-Deflection Curves Comparison of Tested Values and Computed (Square & H)	59
Figure 6-9: Bending Moment vs. Depth (Round Pile)	60
Figure 6-10: Bending Moment vs. Depth (Square Pile)	61
Figure 6-11: Bending Moment vs. Depth (H Pile)	62

Figure 6-12: Maximum Computed Bending Moment vs. Applied Load for the Three Shapes	64
Figure 6-13: Load vs. Deflection Curves for Reese & Van Impe’s Approach (H Pile)	67
Figure 6-14: Load vs. Deflection Curves for Reese & Van Impe’s Approach (Square Pile).....	67
Figure 6-15: P-y Curves at Given Depth (Round pile).....	69
Figure 6-16: F-y Curves for Both Round and Square Piles at a Depth of 7 ft.....	70
Figure 6-17: Combined Q-y + F-y = P-y Curves for the Square Pile at 1 ft in Depth.....	71
Figure 6-18: Load vs. Deflection Curves for F-y/Q-y Mechanism (Square Pile)	72
Figure 6-19: Load vs. Deflection Curves for F-y/Q-y Mechanism (H Pile).....	73
Figure 6-20: Comparison of Measured Load-Deflection Curves with Curves Computed Using P-multiplier Approach for Both Square & H piles.....	75
Figure 6-21: Load-Deflection Curve All Approaches Combined (Square).....	76
Figure 6-22: Bending Moment vs. Depth Including P-multiplier (Square).....	78
Figure 6-23: Bending Moment vs. Depth Including P-multiplier (H).....	79

1 INTRODUCTION

Pile foundations are often subjected to lateral loads induced by earthquakes, wind, wave action, landslides, ice flows, ship impacts and other sources. Lateral load test experiments on pile foundation and most case studies have been performed with circular piles. However, piles used in engineering practice may also have a square or an H cross-section. Some researchers have theorized about the influence of pile shape on resistance to lateral loading; however, the technical literature provides almost no lateral load test results comparing the lateral resistance of piles with different shapes at the same site. Typically, one pile shape is selected at a given location and testing only involves that shape with variations in width or diameter. As a result, the effect of pile shapes is routinely neglected in engineering practice and the lateral resistance of square of a square pile or H pile is considered to be equal to that of a circular pile with the same width (or diameter) and moment of inertia.

Briaud et al (1983) highlighted two major components of resistance that exist in a pile when it is vertically loaded and that are also present when it is laterally loaded. When a pile is loaded vertically, the pile derives its resistance from side friction and from the passive resistance or point bearing resistance at the toe. In the same way, when a pile is loaded laterally these two same components exist. The point bearing would be analogous to the passive resistance on the front face of the pile and the side friction would be analogous to the shear resistance on the sides of the pile. Because of differences in shape, both the passive resistance on the front face and the

shear resistance on the side of a square pile might be expected to be larger than for those on a circular pile.

Smith (1987) proposed an approach to consider shear and passive resistance components using separate shape factors for square and circular piles. Another method for accounting for this side friction was introduced by Reese and Van Impe (2001) in which the effective width of a square pile is increased to account for increased side resistance on a square pile. No shape effects have been proposed for H piles despite their widespread use. A survey performed by Filtz et al (2013), showed that 12 out of 21 Departments of Transportations (DOTs) prefer to use H piles as part of their foundation system for Integral Abutments (IABs) for bridge structures.

To improve our understanding of the influence of pile shape on resistance to lateral loading, full-scale lateral load tests were performed on four piles with three different shapes in this study. To facilitate comparative performance data, all tests piles were approximately 12” in diameter or width, one circular (12.75X3/8); two squares (HSS12X1/4); and one H pile (HP12X74). In addition, all the piles were steel to eliminate potential variations associated with different material types. The piles were located 18 ft behind a Mechanically Stabilized Earth (MSE) Wall with a granular fill compacted to approximately to 95% of the standard Proctor maximum density, which is typical for bridge abutments.

Using the test results, back analysis was performed with the computer program LPILE to observe any indication that the pile shape was influencing the lateral resistance. P-multipliers were developed to account for the shape effects based on the test results. Comparison of the lateral load vs. deflection curves measured in the testes were also made with those predicted using the methods proposed by Reese and Van Impe (2001), and Smith (1987).

The thesis is organized in the following manner. Chapter 2 provides a literature review of research related to the topic of the thesis. Chapter 3 provides a summary of the test layout. Chapter 4 covers the instrumentation used to obtain the data. Chapter 5 provides a summary of the test results. The analyses that were performed to investigate the influence of shape effects are included in Chapter 6 in addition to the comparison of existing methods against measured results; and a new p-multiplier approach is proposed and valuated. Conclusions based on the results of field testing and analyses are provided in Chapter 7.

2 LITERATURE REVIEW

Some researchers have theorized that the lateral resistance of square piles will be higher than that of circular piles. No full-scale load test result has been found in the literature. The literature review contained herein consists of the appraisal of those theorized cross-sectional shape effects on lateral resistance.

2.1 Smith (1987)

Pressuremeter methods have been increasingly recognized for improving the quality of p-y curves. Some researchers have converted the pressuremeter pressure to accommodate the theoretical normal stress and shear stress distributions to formulate a normal pressure contribution vs. displacement (Q-y) and a side shear contributions vs. displacement (F-y) curve. Figure 2-1 provides a graphical representation of Q-y and F-y contribution for the p-y curve along with expected pressure distributions for the shear and normal stress on the pile.

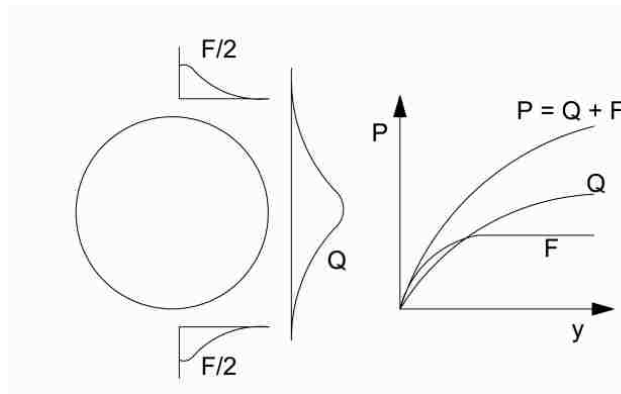


Figure 2-1: Q-y and F-y Contributions (After Smith 1987)

Based on reviews of elastic and plastic theories, full scale testing, model pile torsion testing, and existing vertical shear pressuremeter design rules, Smith (1987) provides the following summary:

1. Evidence confirms the existence of side shear on laterally loaded piles.
2. The prediction of F-y curves is of paramount importance for correct calculation of the governing p-y curves.
3. Installation disturbance and initial stresses against the pile wall must be taken into account.

Smith proposes that the cross-sectional shape of the piles has an effect on the ultimate shear reaction, hence when calculating the ultimate shear reaction shape factors are used in (2-1). See Figure 2-2 for schematic behavior of the shape of the pile on the shear reaction vs. deflection.

$$F_f = \tau_f SF 2R \tag{2-1}$$

Where,

$\tau_f =$ *calculated from existing pressuremeter design rules*

$SF = 0.79$ for circular piles

$= 1.76$ for square piles

$R =$ pile radius

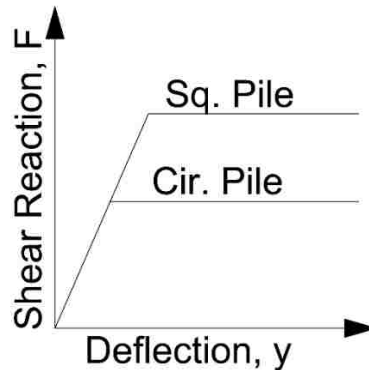


Figure 2-2: Schematic F-y (After Smith 1987)

The construction of the p-y curve can be done by the addition of the F-y and Q-y curves as shown in Figure 2-1. Following Briaud et al (1983), the prediction of Q-y curves uses the entire non-linear expansion curve from the pressuremeter. In this article Smith used the same equation (2-2) but with SQ of 0.75 for circular piles instead of 0.8 as defined in Briaud et al (1983).

2.2 Briaud et al (1983)

One of the key elements for analyzing a laterally loaded pile is the soil model. The governing differential equation relating the lateral force (p) on the soil and pile deflection (y) at any point along a pile is a fourth order equation and it requires the use of numerical methods and/or simplifying assumptions. Briaud et al (1983) describes a rational method for obtaining the p-y curve for a pile from the results from pressuremeter (PMT) pressure vs. expansion curve.

Based on the recognition that axially loaded piles derive their capacity from the passive resistance or point bearing capacity and the shear resistance or side friction along the pile, it can be said that bearing and side friction also exist when the pile is loaded laterally. The point resistance is analogous to the passive pressure on the front face of the pile and designated as the front resistance Q . The side friction is analogous to the shear resistance on the side of the pile and is designated as the side friction F .

Briaud et al (1983) evaluated Q and F resistance by comparing the predicted behavior with the actual behavior of two piles which were loaded laterally: one in soft clay and one in medium dense sand. Unfortunately, only one pile type was loaded at each site, therefore, the accuracy of the method in accounting for different pile shapes was not evaluated.

A 3 foot diameter drilled shaft with several pressure cells on the side wall was loaded laterally in a stiff clay profile as shown in Figure 2-3. At a horizontal load of 43 tons, the soil resistance due to front reaction was calculated from the pressure cell readings. For the measured pressures based on front resistance only, horizontal and moment equilibrium cannot be obtained. However, once the friction forces corresponding to the full shear strength of the stiff clay were included, the horizontal and the moment equilibrium were approximately satisfied. This exercise was intended to illustrate two points:

1. Friction resistance is an important part of the total resistance.
2. The friction resistance is fully mobilized before the front resistance.

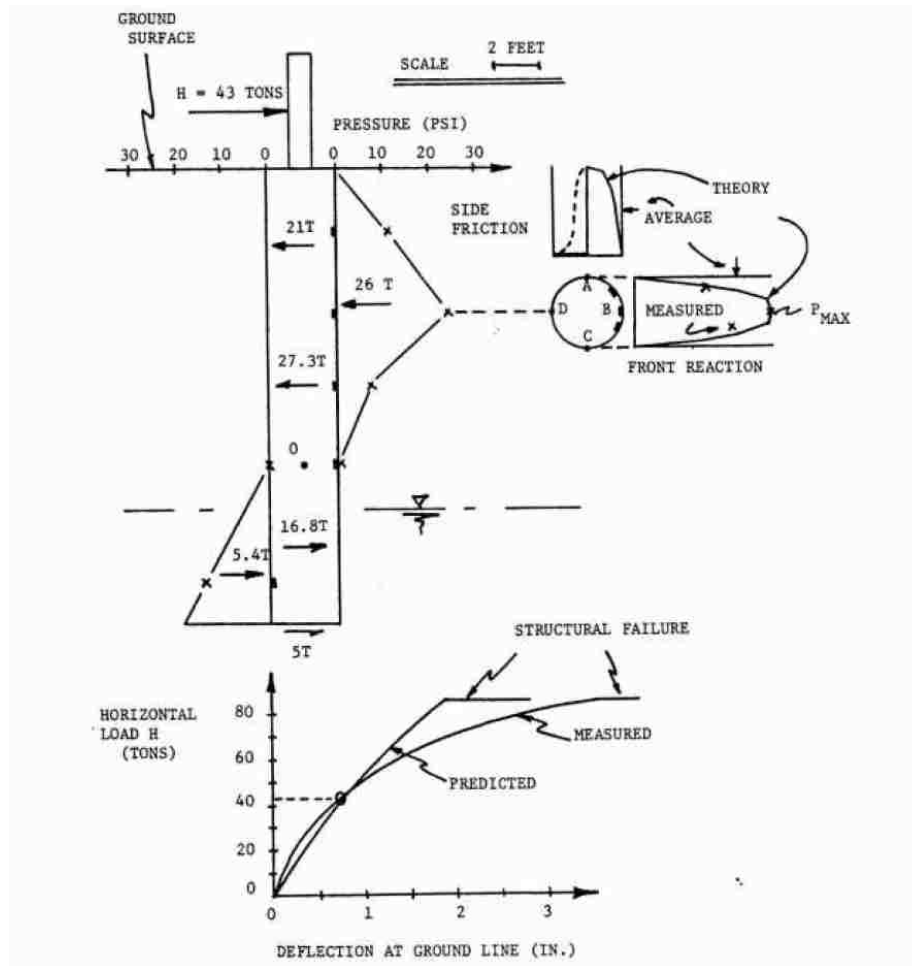


Figure 2-3: Friction and Front Resistance Forces for Texas A&M U. Drilled Shaft (Briaud et al 1983)

The proposed method by Briaud et al (1983) using the PMT relies on the analogy of loading between the PMT and the pile. The analogy is not complete; however, and the pressuremeter curve is not identical to the p-y curve. Briaud uses the pressuremeter curve to compute a Q-y curve for the pile given by (2-2) and an F-y curve for the pile given by (2-3).

$$Q(\text{front}) = p(\text{pmt})B(\text{pile})S(Q) \quad (2-2)$$

Where,

$Q(\text{front}) = \text{the soil resistance due to front reaction (force/unit length of pile),}$

$p(\text{pmt})$ = the net pressuremeter pressure,

$B(\text{pile})$ = the diameter or width of the pile,

$S(Q)$ = the shape factor = 1.0 for square piles loaded parallel to their sides, and
= 0.8 for circular piles and square piles not loaded parallel to their sides,

$$F(\text{side}) = \tau(\text{side})B(\text{pile})S(F) \quad (2-3)$$

Where,

$F(\text{side})$ = the soil resistance due to friction (force/unit length of pile),

$\tau(\text{side})$ = the soil shear stress obtained from the pressuremeter curve by the sub-tangent method,

$B(\text{pile})$ = the diameter or width,

$S(F)$ = the shape factor = 2.0 for square piles loaded parallel to their sides, and
= 1.0 for circular piles and square piles not loaded parallel to their sides

The total resistance (force/unit length of pile), P , is computed using (2-4) pressuremeter tests were performed in two additional locations in Texas where lateral load tests had been previously been performed. The first test, in Sabine, Texas, was performed in marine clay with high plasticity. The steel pile was 1.06 ft in diameter and 42 ft long. Pressuremeter readings were recorded at different depths using the commercial TEXAM pressuremeter which uses a pre-bored hole. Using (2-2), (2-3), and the total resistance using (2-4),

$$P = F(\text{side}) + Q(\text{front}) \quad (2-4)$$

p - y curves were computed for different depths. It was noted in this test that any irregularities of the p - y curve are due to the fact that F - y curve is obtained by differentiation of the pressuremeter curve and therefore any imprecision in the PMT measurements is magnified in the F - y curve.

The Mustang Island test was performed at a site with medium to dense uniform fine clean sand. The steel pile was 2 ft in diameter and 70 ft long. PMT were performed with the commercial TEXAM pressuremeter at different depths, P-y curves were generated using the same method as at the Sabine test site.

For the Sabine load test, Figure 2-4 shows the p-y curve obtained from the PMT performed at 2.5 ft. In this figure a comparison between the PMT prediction and the measured can be made. The proposed method makes it possible to distinguish between the friction model and the front resistance model. From the limited evidence shown in this article it seems that reasonable p-y curves for piles can be prepared from the PMT first or reload curves.

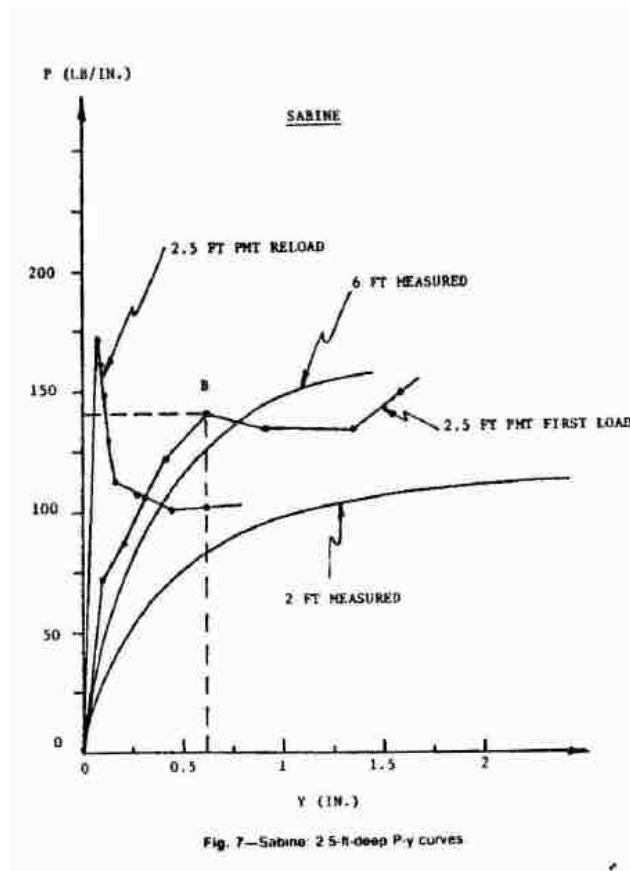


Figure 2-4: Sabine 2.5 Deep P-y Curves (Briaud et al 1983)

2.3 Reese and Van Impe (2001)

Reese and Van Impe suggest the computation of an equivalent circular diameter for piles with a noncircular cross-section when analyzing lateral load resistance. The primary experiments, and most of case studies, have been performed with piles with circular cross-section. However, piles used in engineering practice may also have different shapes and are often employed in design.

Figure 2-5 shows conceptually the stresses from the soil that would act on the pile when the pile is deflected from left to right.

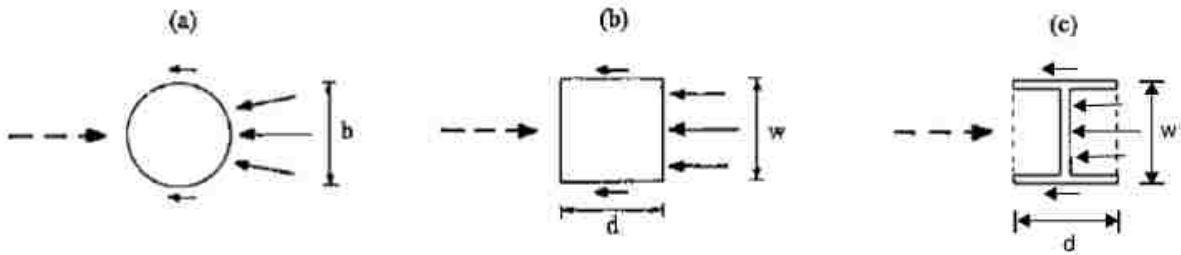


Figure 2-5: Schematic Drawing Showing Difference in Lateral Resistance Owing to Pile Shape (After Reese and Van Impe, 2001)

One of the main assumptions by Reese and Impe (2001) was that a pile with a rectangular cross-section with the same width as the diameter of a circular section and with half the depth or one radius, would provide the same lateral resistance as a pile with a circular cross-section. This assumption is based on the fact that under lateral load the back half of a circular section loses contact with the adjacent soil and cannot provide resistance. Then, if Figure 2-5(b) is considered, which has a width and depth of one pile diameter, the resistance to deflection would be greater since the shearing stresses could act along the back half of the section. With the

assumptions and concepts discussed above, (2-5) was written to compute the equivalent diameter of a circular pile, b_{eq} :

$$b_{eq} = w \left[\frac{P_{uc} + 2 \left(d - \frac{w}{2} \right) f_z}{P_{uc}} \right] \quad (2-5)$$

Where,

w = width of the section

d = depth of section

P_{uc} = ultimate resistance of a circular section with a diameter b equal to w

f_z = Shearing resistance along the sides of the rectangular shape at depth z below the ground surface

For cohesionless soils the unit side resistance, f_z , may be computed with (2-6):

$$f_z = K_z \gamma z \tan(\phi_z) \quad (2-6)$$

Where,

K_z = lateral earth pressure coefficient

γz = effective vertical soil stress at depth z

ϕ_z = Shear angle (between the soil and the wall of the pile); $\frac{2}{3}$ friction angle of the soil ($\frac{2}{3} \phi$)

If the dimensions d and w in Figure 2-5(b) are the same as the diameter, the equations above will show a somewhat larger equivalent diameter b_{eq} . The equivalent diameter using the equations above will vary with depth. It is recommended to compute b_{eq} at different depths and then average these values in making a solution.

2.4 Filz et al (2013)

One of the many objectives of this research was to determine the effects of the orientation of piles with strong and weak axis, such as H-pile. Part of the research methodology for illustrating the importance of the orientation of the H-pile was to perform a survey of different Departments of Transportation (DOTs) across the United States and Canada. A total of 45 surveys were sent and 27 responses were received.

Twenty-one agencies responded to the questions about use of different pile types in Integral Abutment Bridges (IABs). Of those responding 12 agencies used steel H-piles only; 5 agencies use steel H-piles and pipe piles; and 4 agencies use H-piles, pipe piles, and concrete piles.

Twenty-one agencies responded to the question about orientation of steel H-piles as follows: A total of 15 agencies orient steel H-piles with their weak axis perpendicular to the bridge centerline direction; 3 agencies orient steel H-piles with their strong axis perpendicular to the bridge centerline direction; and 3 agencies orient steel H-piles in either direction.

None of the agencies provided a design methodology that supports the use of a particular pile orientation. The most important concern from the agencies surveyed was thermal movement interactions and design requirements. Seismic concerns are important for Caltrans and Washington DOT.

Some agencies provided maximum lateral deflection for piles. The values range from 0.25 to 2.25 in., with the average being 1.5 in.

One of the key findings in this report was that a slight majority of the agencies use exclusively H-piles for abutment support. Most of the agencies orient the piles for weak moment resistance.

In the numerical model based on Virginia IAB as the pile size increased, shear forces also increased in the piles. Strong pile orientation (web parallel to bridge alignment) considerably increases the shear forces in the pile. The same effect is true with the moments, as the pile size increases so does the moment. And the orientation plays a significant role in the moment magnitude, strong pile orientation increases the moments in the pile. However, in their analyses the difference were directly related to the difference in the centroidal moments of inertia for the respective pile orientations for the pile rather than differences in soil resistance owing to the shape of the pile.

In the IA v3 Spreadsheet analysis 65 models were analyzed, since most agencies used weak axis orientation, 53 in piles were oriented in the weak axis and the rest strong axis. It was observed that orienting the piles with their webs parallel to the abutment alignment produced a decrease in the bending moment in the longitudinal direction and an increased in the transverse direction. See Figure 2-6 for a schematic of the pile orientation.

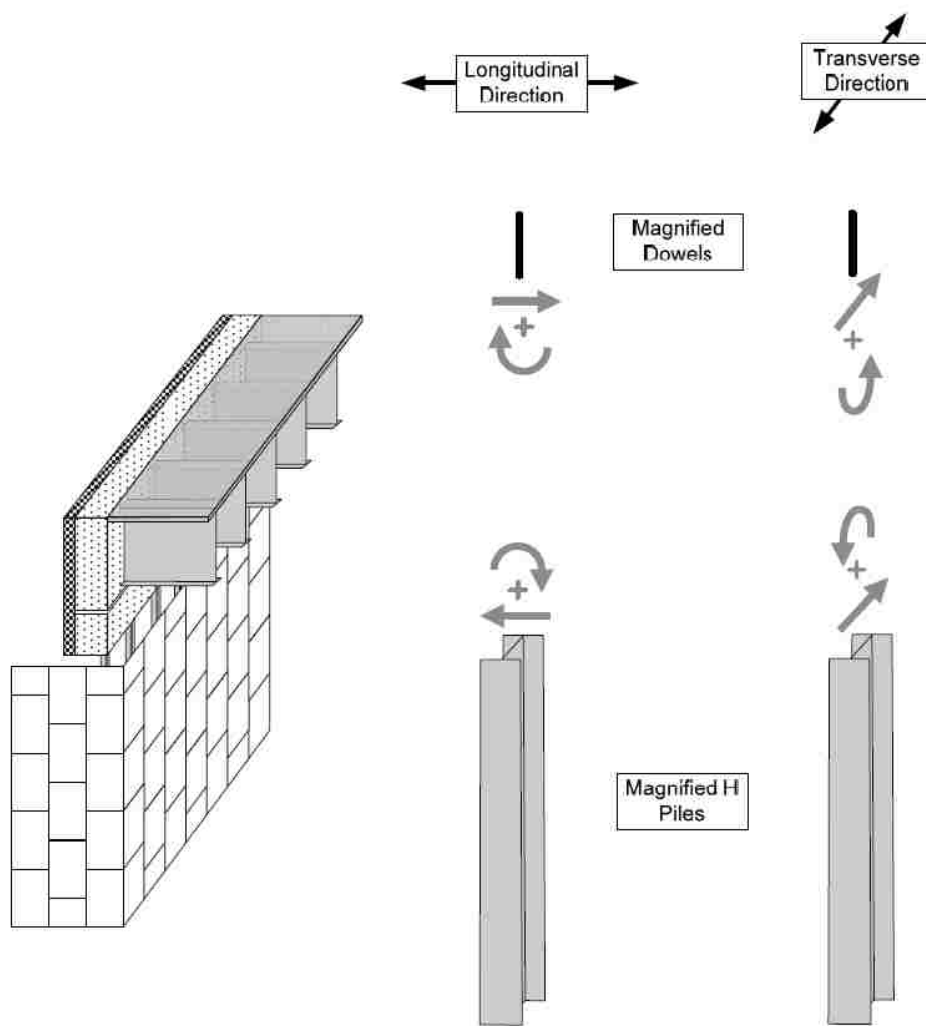


Figure 2-6: Sign Convention (Fitz et al 2013)

3 TEST LAYOUT

The lateral load tests were performed at a site provided by Geneva Rock near the Point of the Mountain between Lehi and Bluffdale, Utah as shown on the map in Figure 3-1. The coordinates for the site are $40^{\circ}27'11.3''$ N $111^{\circ}53'57''$ W. At the site full-scale Mechanically Stabilized Earth (MSE) wall was constructed to investigate the lateral resistance of bridge abutment piles near MSE wall. The test piles included circular, square, and H piles. In addition to tests of piles with the reinforced soil near the MSE wall. Additional tests were performed on piles in compacted soils outside of the reinforced zone.

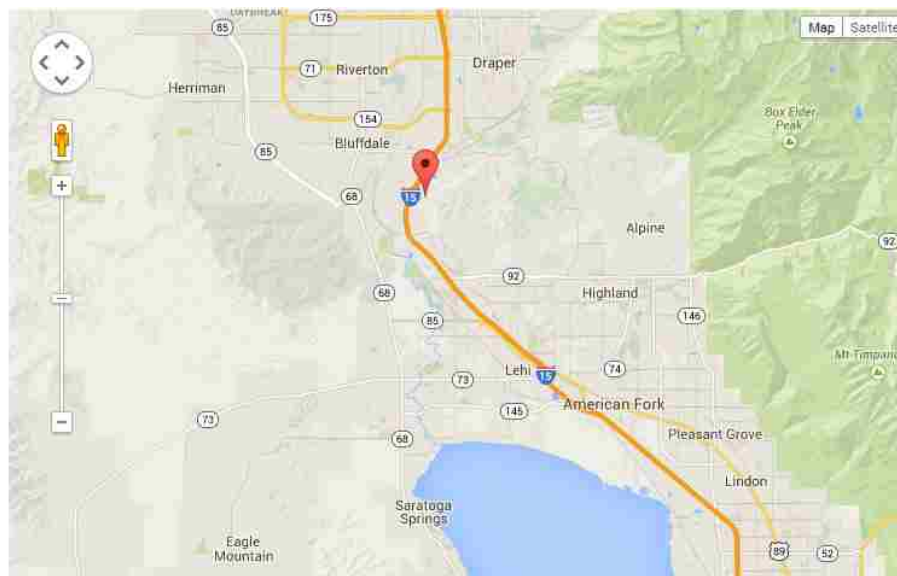


Figure 3-1: Location of Test Site

3.1 MSE Wall

The wall was a one-stage MSE wall built up to a height of 15 ft at the time of testing. The main test area dimensions were 100 ft long section with a one-stage MSE wall which eventually extended up to 20 ft high. Half of the wall was reinforced using welded wire mesh while the other half was reinforced with steel strips.

Figure 3-2 shows elevation and plan view of the wall, with the pile locations and metal reinforcement mentioned above. The triangular face shown in Figure 3-2 was constructed on each side of the test fill to bring the wall down to the native ground surface at a slope of 2H:1V.

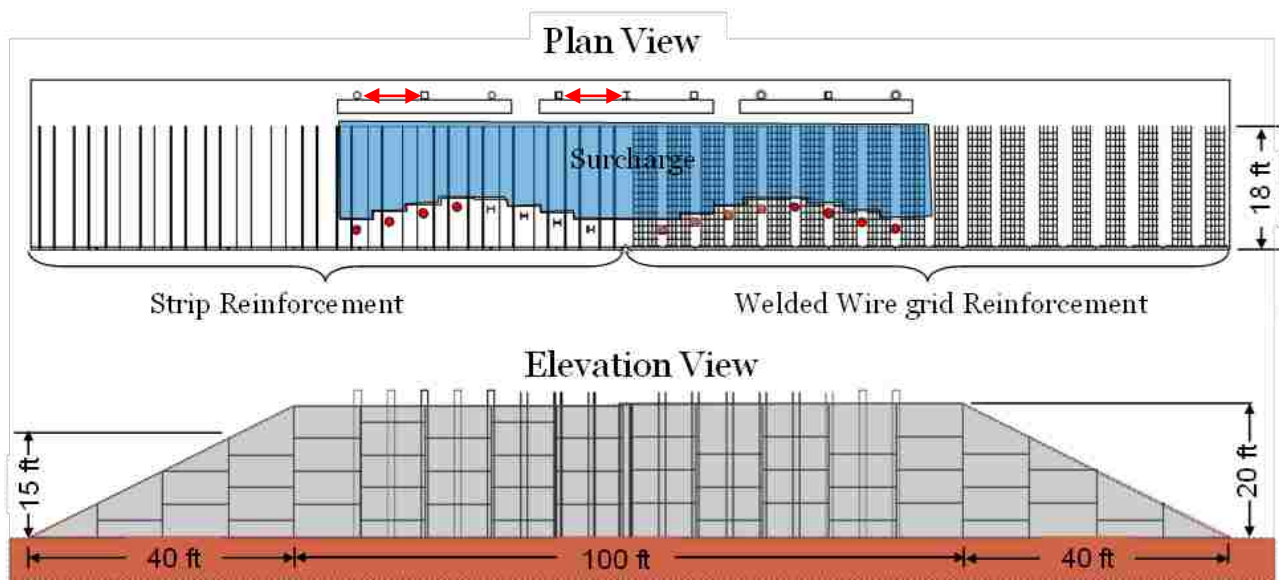


Figure 3-2: Schematic Plan & Elevation View Showing Layout of Test Piles & MSE Wall

3.1.1 Backfill

The fill used behind the wall was provided by Geneva Rock to minimized haul costs. The material was classified as gravelly sand and corresponded to an AASHTO A-1-a classification or SM according to the Unified Soil Classification System. Figure 3-3 shows the

grain-size distribution curve for the selected fill. The mean grain size (D_{50}) is 2.3 mm, the coefficient of gradation (C_c) is 1.6, the coefficient of uniformity (C_u) is 40, and the fines content is 14%. For design, the fill was assumed to have a friction angle of 34° and a moist unit weight of 124 pcf. The maximum measured density and optimum moisture content from the Standard Proctor were 128 pcf and 7.8%, respectively.

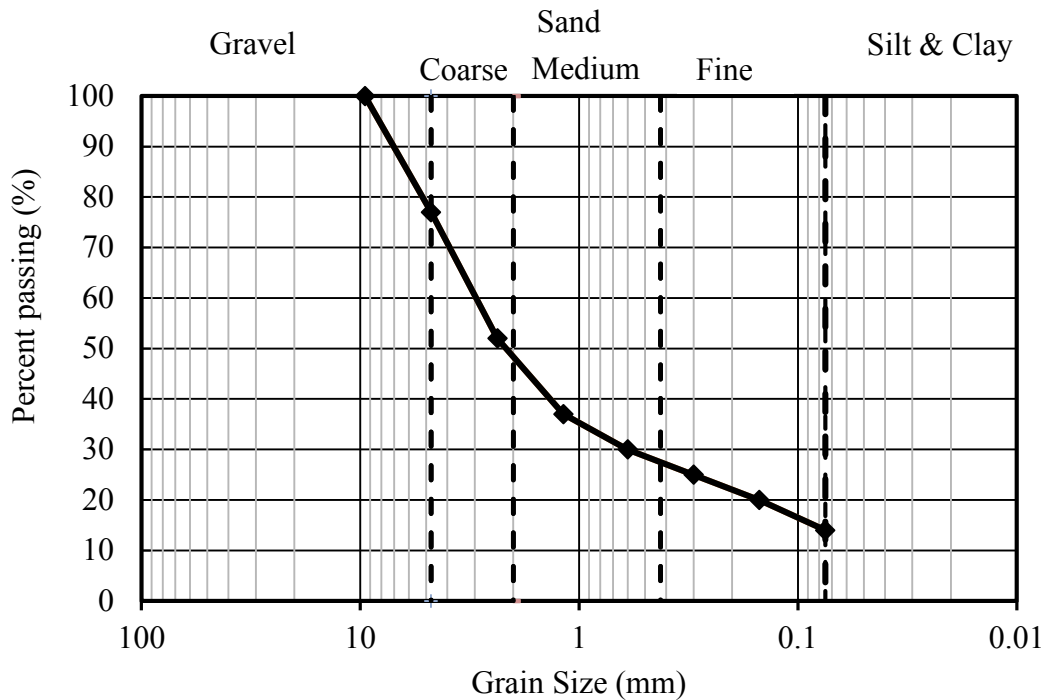


Figure 3-3: Gradation for Select Backfill

The granular fill around the pile was compacted to approximately 95% of the standard Proctor maximum density and would be typical of fill for a bridge abutment. Roller compactors were used in the areas where the roller fit with no problem (See Figure 3-4); in those areas where the space was reduced, i.e. between the wall and the piles, a vibratory plate was used for compaction (see Figure 3-5). A jumping jack type compactor was used around the reaction piles

which were used for the tests discussed in this thesis (see Figure 3-6). Nuclear density tests were performed during construction to assure compliance with the design requirements (see Figure 3-7).



Figure 3-4: Roller Compaction Between Test Piles and Reaction Piles



Figure 3-5: Plate Compaction Between MSE Wall and Piles Adjacent to The MSE Wall



Figure 3-6: Jumping Jack Type Compaction Around Test Piles Investigated in This Study



Figure 3-7: Nuclear Density Gauge Testing

3.2 Piles

The piles tested in this research study included a total of one pipe pile, one H-pile, and two square tube piles. Atlas Steel donated the pipe piles and the square tube piles, and the H-piles were donated by Spartan Steel. The dimensions of the piles were as follow: 12.75X3/8 pipe pile (A252-Grade 3), HP12X74 pile, and HSS12X1/4 square tube piles. The pile properties are summarized in Table 3-1.

Table 3-1: Pile Properties

Type	Dia. /Depth in	Flange Width in	Wall/Web Thickness in	Flange Thickness In	I [with Angle Iron] in ⁴	E ksi	F _y ksi
12.75X3/8	12.75	-	0.349	-	279 [314]	29,000	57
HSS12X1/4	12	-	0.233	-	248 [335]	29,000	57
HP12X74	12.1	12.2	0.605	0.61	186 [186]	29,000	57

The test piles were driven by Deseret Deep Foundations, Inc. prior to construction to a depth of 18 ft below the native ground surface. Figure 3-8 provides a photo of the pile driving stage prior to construction of the MSE wall and backfill. This depth was sufficient to hold the pile in place during construction. The piles were driven open-ended and left hollow during testing to eliminate non-linear behavior due to cracking in concrete and facilitate subsequent back-analysis.



Figure 3-8: Driving Pile with a Diesel Type Hammer

As indicated previously, several single piles were driven beyond the back of the reinforced soil mass approximately 22 ft behind the MSE wall, to provide controlled testing where the presence of the wall was not expected to influence the lateral pile resistance. These piles were initially loaded parallel to the MSE wall, to determine the shape influence on the resistance to lateral loading. After the lateral load testing these single piles also provided a reaction against the test piles that were loaded perpendicular to the MSE wall.

3.3 Load Apparatus

The load was applied 1 ft above the ground surface (16 ft from the bottom of the MSE wall). Different segments of steel were attached to the hydraulic jack in combination with an HSS section that reacted against another pile being tested. In that configuration two piles per test were performed. Figure 3-9 shows the lateral load test for the H pile and Square1. All of the sections of the strut were bolted together in fixed connections. The strut was also bolted to the hydraulic jack. The jack had a capacity of 300kips and a maximum stroke of 13 inches. A tie-rod load cell was placed in the socket of the jack and pinned to a clevis on the pile. The clevis was bolted to a channel that was welded onto the pile. All of the connections were fixed, except for the pinned connection between the tie-rod load cell and the clevis, to ensure safety.



Figure 3-9: Load Apparatus

4 INSTRUMENTATION

4.1 Load Cell and Pressure Transducer

During each test, the load applied to each pile was monitored by a tie-rod cell and checked with an electric pressure transducer attached to the hydraulic pump. The tie-rod cell was placed between the hydraulic jack and the pile. Figure 4-1 shows a photo of the load cell and pressure transducer during one of the tests. The pressure transducer was attached to the hydraulic jack and measured the hydraulic pressure. The pressure transducer was read during loading to verify accuracy of the load cell by comparing both readings. Based on laboratory calibrations, the load obtained from the pressure transducer was found to be much more accurate and reliable than the tie-rod load cell. Nevertheless, load from both the transducer and the tie-rod cell were recorded using the computer data acquisition system at a rate of two samples per second. The same hydraulic jack, tie-rod cell, and pressure transducer were used in all tests.

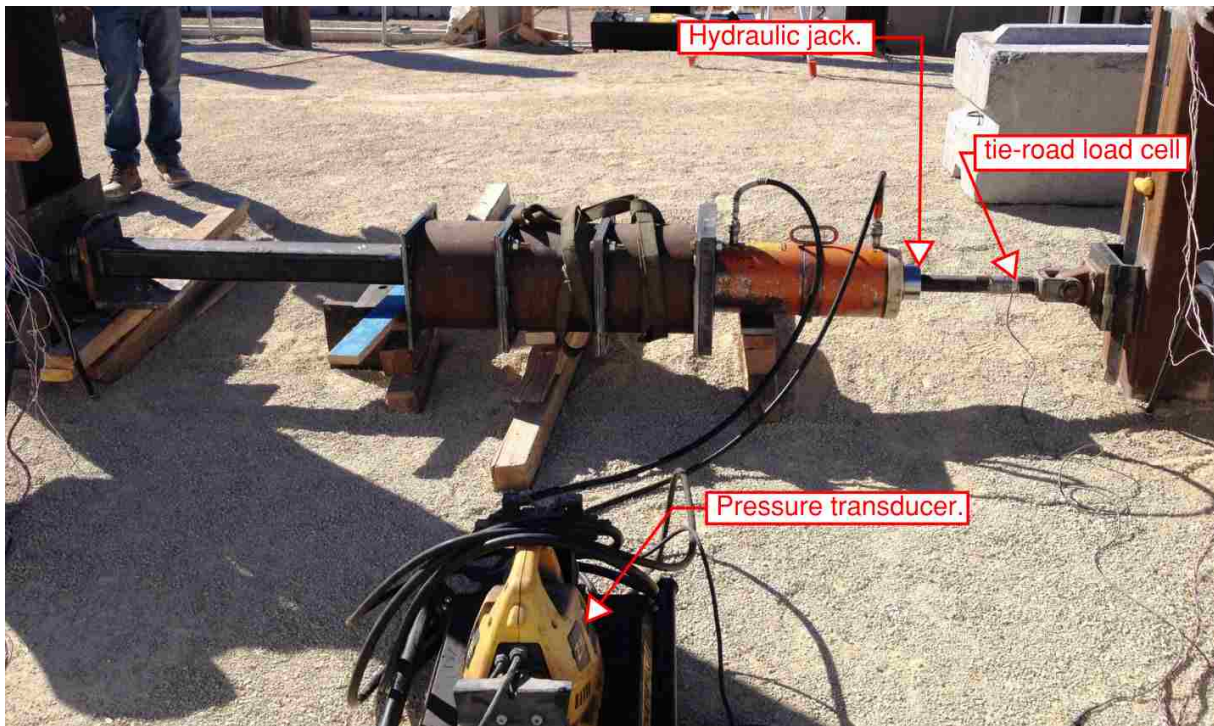


Figure 4-1: Typical Tie-Rod Cell and Pressure Transducer Layout

4.2 String Potentiometers

String potentiometers were used to measure the displacement and rotation of the pile head and displacement of the ground surface. The string potentiometers were attached to an independent reference frame. The reference frame was supported by two pre-cast concrete blocks spaced at about 8 ft on either side of the test pile. To measure the pile head displacement and rotation, the string potentiometers were attached to a magnetic clamp at the load point on the pile and three feet above the load point. To measure ground displacement in front of the pile, stakes were driven at 1 ft intervals directly in front of the pile, parallel to the loading direction. Figure 4-2 shows a typical instrumentation layout of the string potentiometer. Similar set ups

were used for the different load tests. Table 4-1 shows the string potentiometer distances from pile and string potentiometer name corresponding to those distances.

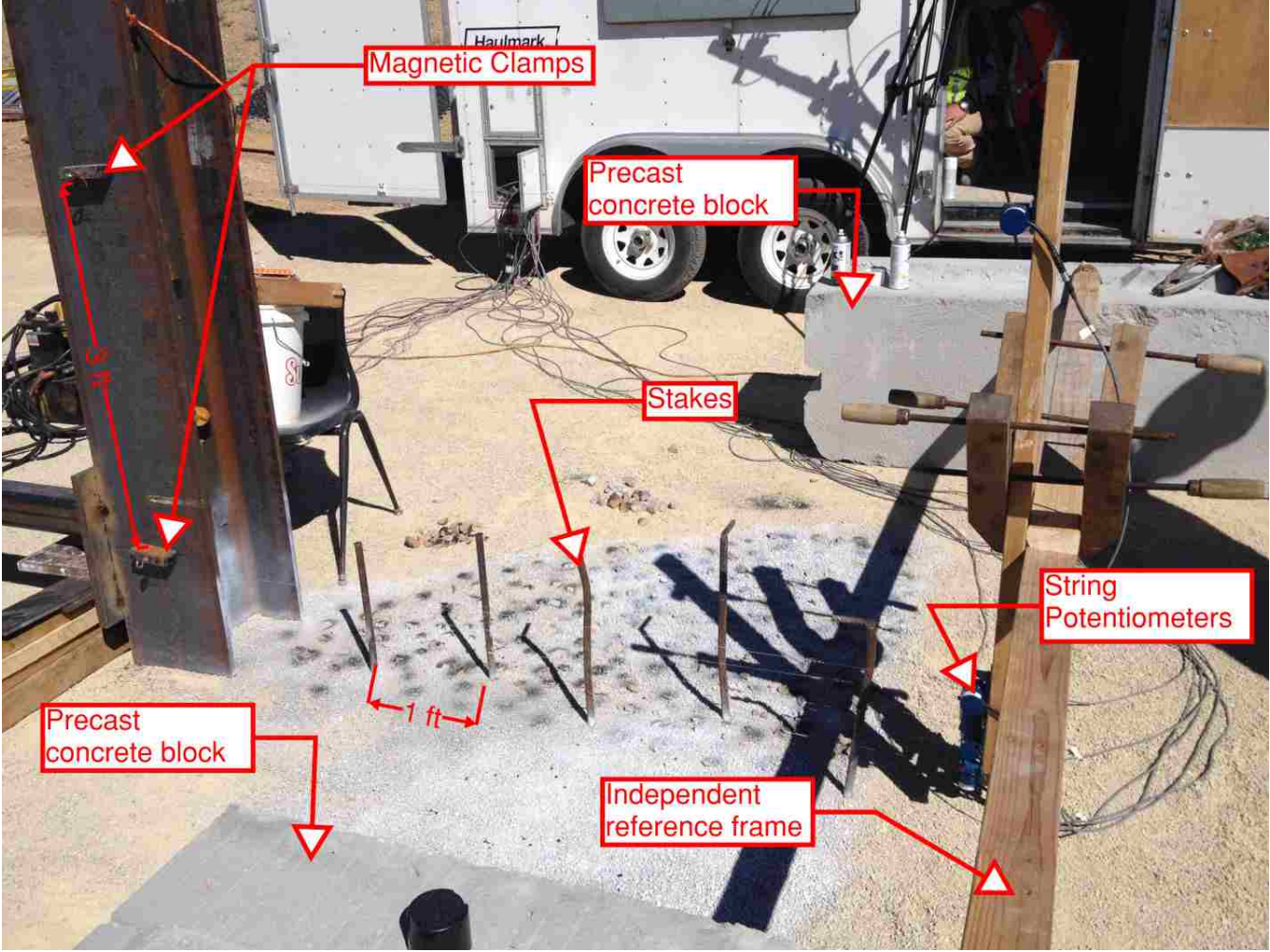


Figure 4-2: String Potentiometer Instrumentation (H-pile)

Table 4-1: String Potentiometer Distances

Test	Load Point on pile	3 ft above load point on pile	Distance from stake to the front face of pile				
			1 ft	2 ft	3 ft	4 ft	5 ft
H-Pile	SP-35	SP-36	SP-1	SP-40	SP-39	SP-37	SP-38
Square 1	SP-31	SP-32	SP-33	SP-34	-	-	-
Square 2	SP-35	SP-36	SP1	SP39	SP40	SP38	SP37
Circular	SP-32	SP-31	SP8	SP34	SP7	SP33	SP3

4.3 Strain Gauges

Waterproof electrical resistance type strain gauges were bonded to each test pile at depths of 8, 11, 14, 17 and 20 ft below the top of the pile, which correspond to 1, 4, 7, 10 and 13 ft below the ground surface when the backfill has an elevation of 15 ft. The strain gauges were bonded in pairs on opposite sides of the pile parallel to the direction of loading. To protect the strain gauges from the driving piles, an iron angle was placed on top of the strain gauges and welded onto the pile. Figure 4-3 shows typical strain gauge instrumentation on one side of the pile with the angle iron protection.



Figure 4-3: H Pile Strain Gauge Instrumentation

4.4 Digital Image Correlation (DIC) Camera System

Digital Image Correlation, known by the acronym DIC, is a method of measuring displacement based on correlation of the images from two cameras with overlapping fields of view. The system used in this study was manufactured by Dante Dynamics and employs two digital cameras that are spaced at a fixed distance apart that provide overlapping views of a specific object. The camera captures the area around the object being measured, then the software uses a correlation algorithm to define displacements in the x, y and z directions along

with corresponding strains. The software generates color contour plots of any desired displacement, deformation, and strain. The object being measured should be painted with a high contrast pattern to increase the resolution and accuracy of the results. A typical setup of the cameras can be seen in Figure 4-4.



Figure 4-4: Typical DIC Set Up

For these tests, the DIC unit was used to measure displacement and heave of the soil in front of the pile being tested. The ground was painted with white spray paint and black pebbles were spread around the painted area to give enough contrast to the capture. Figure 4-5 shows the contrast pattern used for these tests. An image was taken immediately after each load increment during the test of the pile and again after a five minute relaxation period.



Figure 4-5: Ground Contrast Pattern for DIC Capture

5 LATERAL LOAD TESTING

The lateral load tests analyzed herein were performed on July 1, 2014 and July 2, 2014. The two tests performed cover a total of four piles at fill elevation of fifteen feet. Figure 5-1 shows a plan view of the piles tested; the double arrow shows the direction of loading.

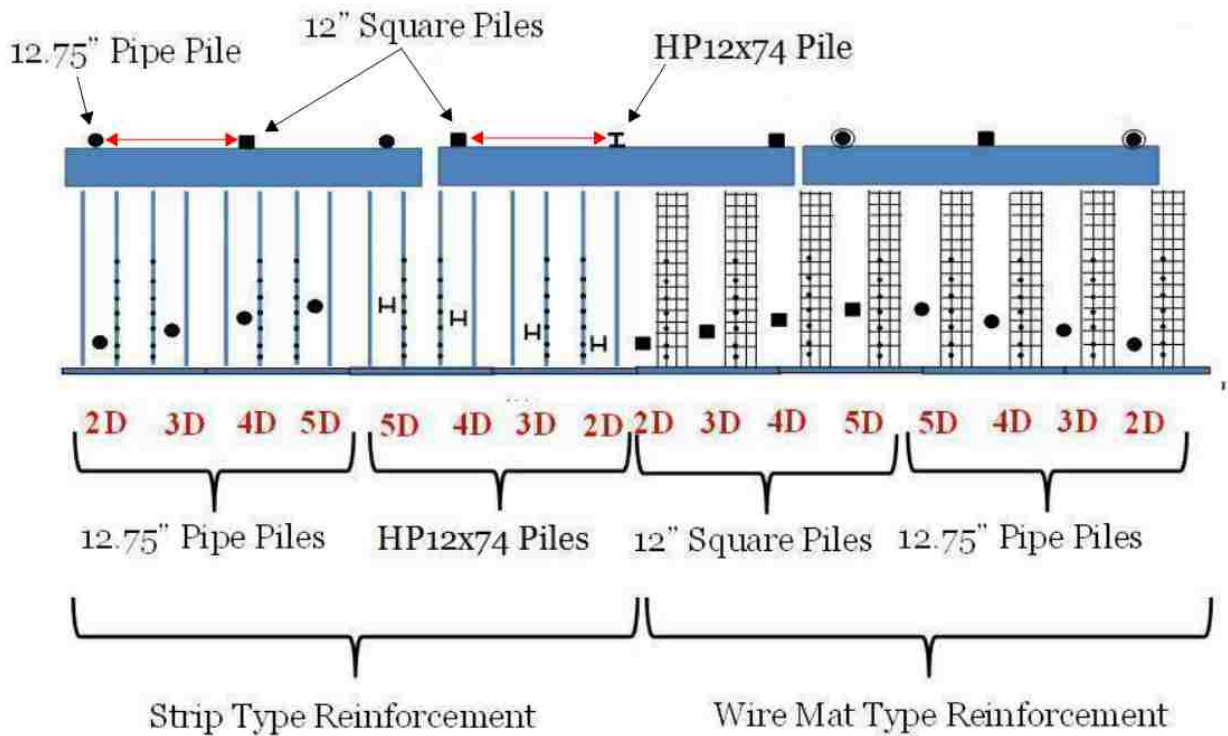


Figure 5-1: Plan View of the Lateral Load Tests

Testing was performed using displacement control approach, where load was applied to reach displacement increments of 0.25 inches up to a total head deflection of 3 inches. Once the

desired displacement was reached at each push, the fluid flow into the jack was cut off so the jack displacement remained constant for 5 minutes. Pile head load and displacement readings were taken at the peak load, 1 minute hold, and 5 minutes hold. Because the 1 minute hold and the 5 minute hold did not vary much from each other, the 1 minute hold was used as the final load. Static equilibrium and deflection is represented better with the 1 minute hold. The peak load was only maintained for a few seconds before decreasing. Although the peak load might be appropriate for rapidly applied load such as an earthquake it would overestimate the pile resistance for static loading. A megadac data logger was used to collect the data at a rate of 2 readings per second.

5.1 Load Displacement Curves

Load-displacement curves were plotted for each test performed. Figure 5-2 shows the pile head peak load vs. deflection curves for the three different cross-sections.

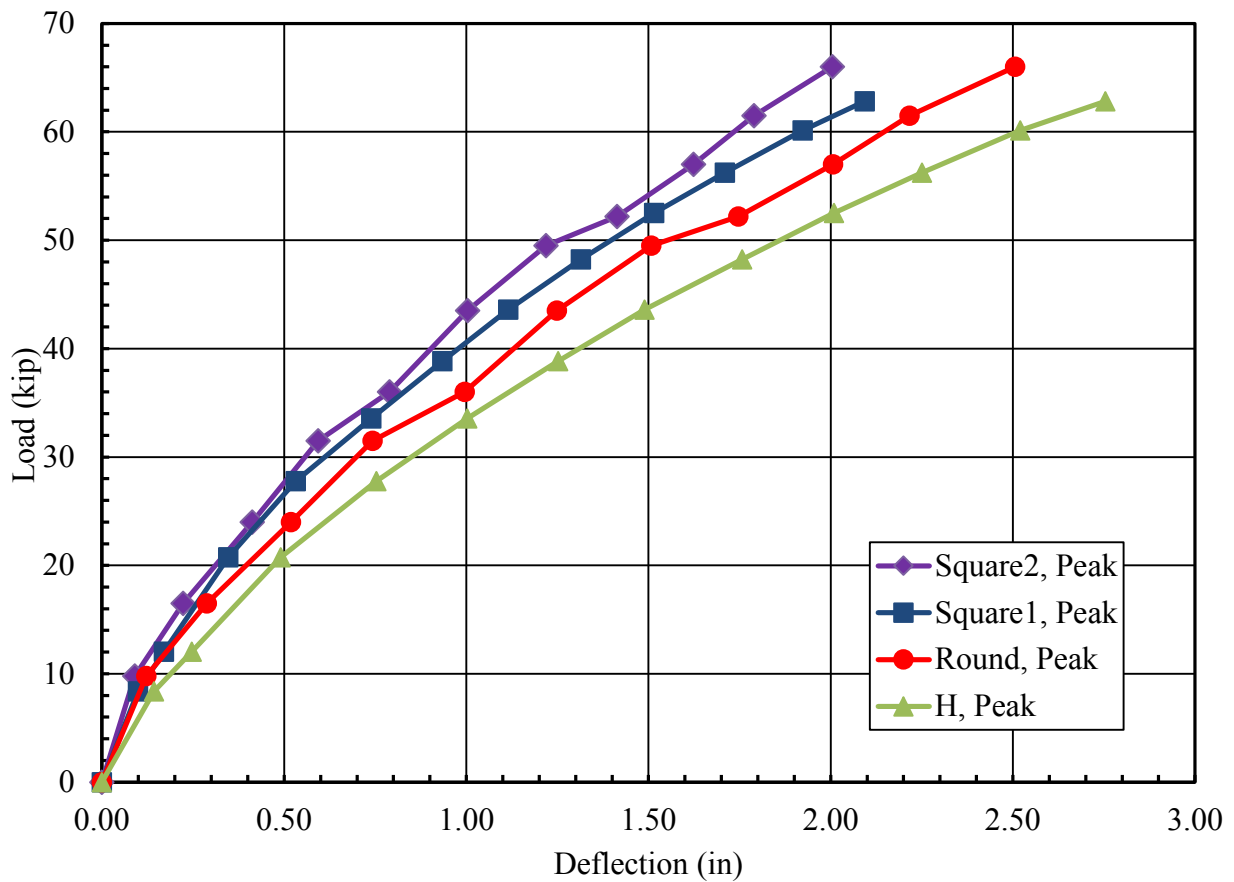


Figure 5-2: Pile Peak Head Load vs. Deflection Curves

A comparison of the load-deflection curves indicates that the resistance is lower for the H pile for a given deflection. The load was applied perpendicular to the web (weak axis) of the H pile, where the moment of inertia is significantly lower than the square pile and circular pile. Although the moment of inertia and width/diameter are very similar for the square and circular piles, the square piles show more resistance against lateral loading than the circular pile. It is possible that the front resistance is higher due to a higher pressure distribution on the front face of the square pile as well as increased resistance on the side. The resistance of the circular pile

fits between the H and the square; the pressure distribution on the circular pile could be higher at the center of the pile but reduces as it approaches the sides as shown in Figure 2-1.

Figure 5-3 shows the values from the 1 minute hold. In comparison to Figure 5-2 it can be seen that the displacement varies slightly, but the load decreases. The average decrease in lateral resistance from the peak to the 1 minute hold is about 4% and this percentage is similar for all three piles. For the given deflection the resistance is highest for the square piles and lowest for the H pile.

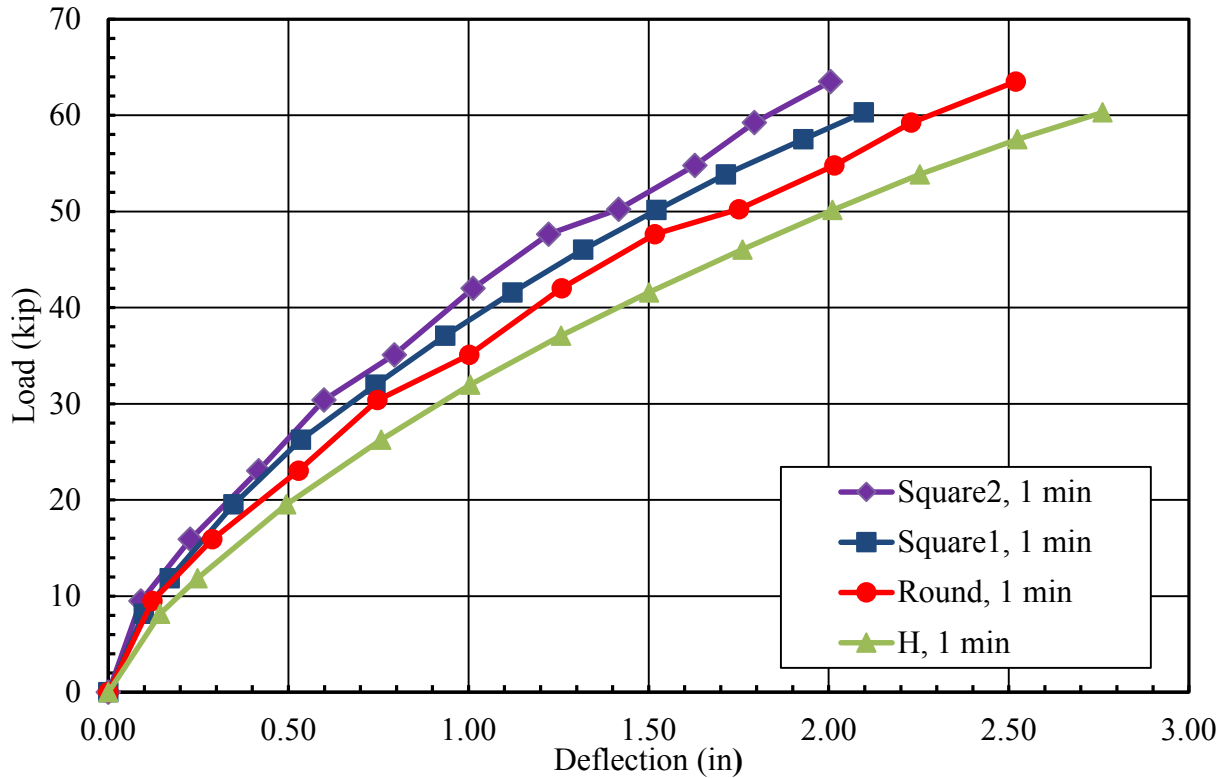


Figure 5-3: Pile 1 Minute Head Load vs. Deflection Curves

5.2 Pile Performance

The bending moment in the pile is calculated from the strain gauges reading using (5-1).

$$M_i = \frac{EI}{D_o} [(\mu\varepsilon_{ti} - \mu\varepsilon_{to}) - (\mu\varepsilon_{ci} - \mu\varepsilon_{co})] (10^{-6}) \quad (5-1)$$

Where,

M_i = the bending moment in inch-kips for the pile at the i th data point,

E = the modulus of elasticity of steel (29000 ksi),

I = the moment of inertia of the pile in in^4 ,

$\mu\varepsilon_{ti}$ = the micro strain for the i th data point on the tension (+) side of the pile,

$\mu\varepsilon_{to}$ = the micro strain for the initial data point on the tension side of the pile,

$\mu\varepsilon_{ci}$ = is the micro strain for the i th data point on the compression (-) side of the pile,

$\mu\varepsilon_{co}$ = is the micro strain for the initial data point on the compression side of the pile, and

D_o = the outside diameter of the pile or width perpendicular to the direction of loading in inches.

Figure 5-4 , Figure 5-5, and Figure 5-6 show the bending moment vs. depth curves for the Round, Square2, and H piles, respectively. It should be noted that as the load increases the bending moment also increases. The graphs also show that the maximum bending occur at a depth of 4 ft below ground level, or 5 ft below the applied load. The H pile and the circular pile almost have the same magnitude of bending moment, even though the H pile has a smaller moment of inertia when compared to the circular. Figure 5-7 includes all the tested piles at approximately 60 kip for all cases. Although the load-deflection curves for the two square piles are very close to agreement, their bending moment curves are not.

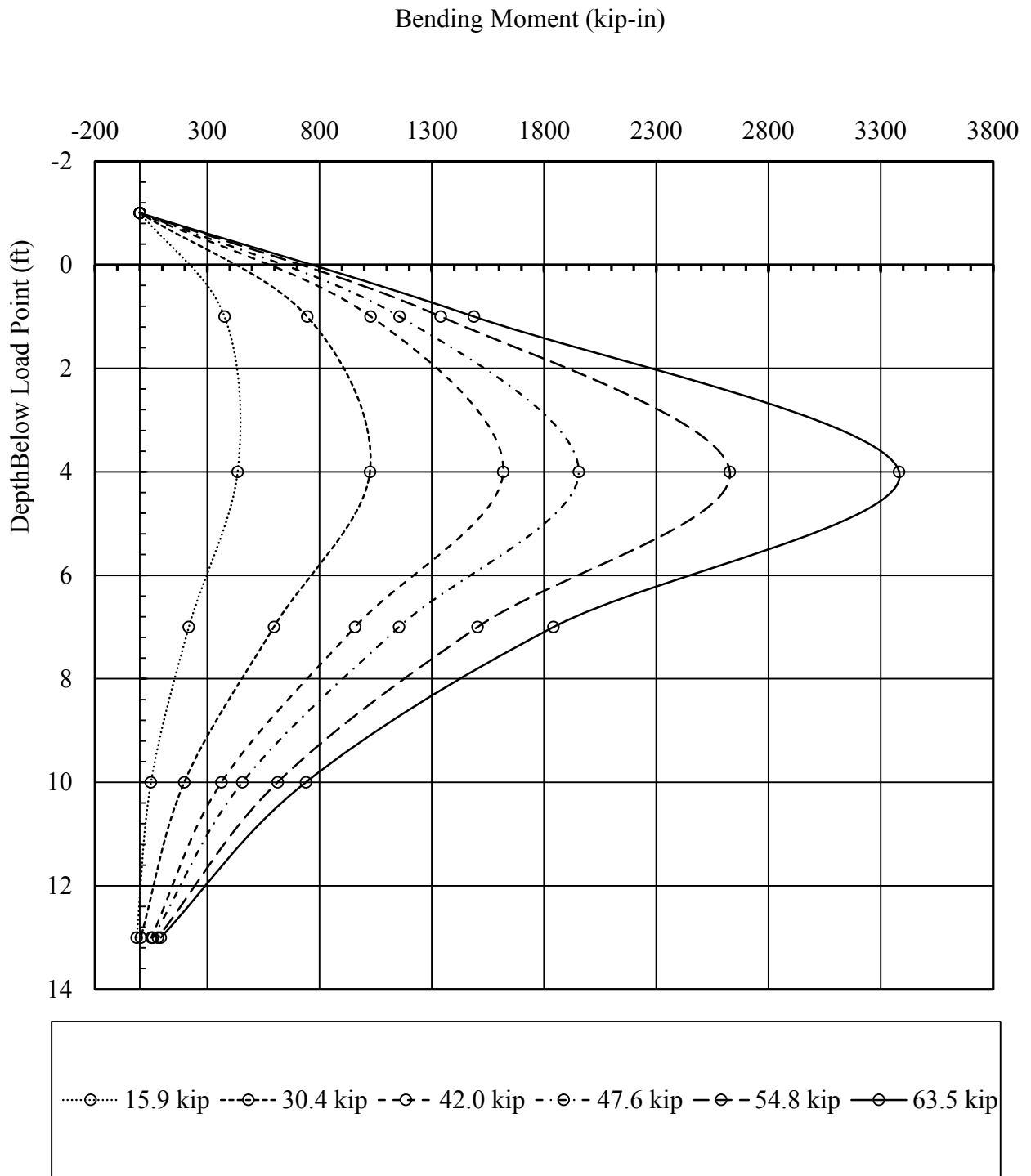


Figure 5-4: Bending Moment vs. Depth for Selected Head Loads for the Circular Pile

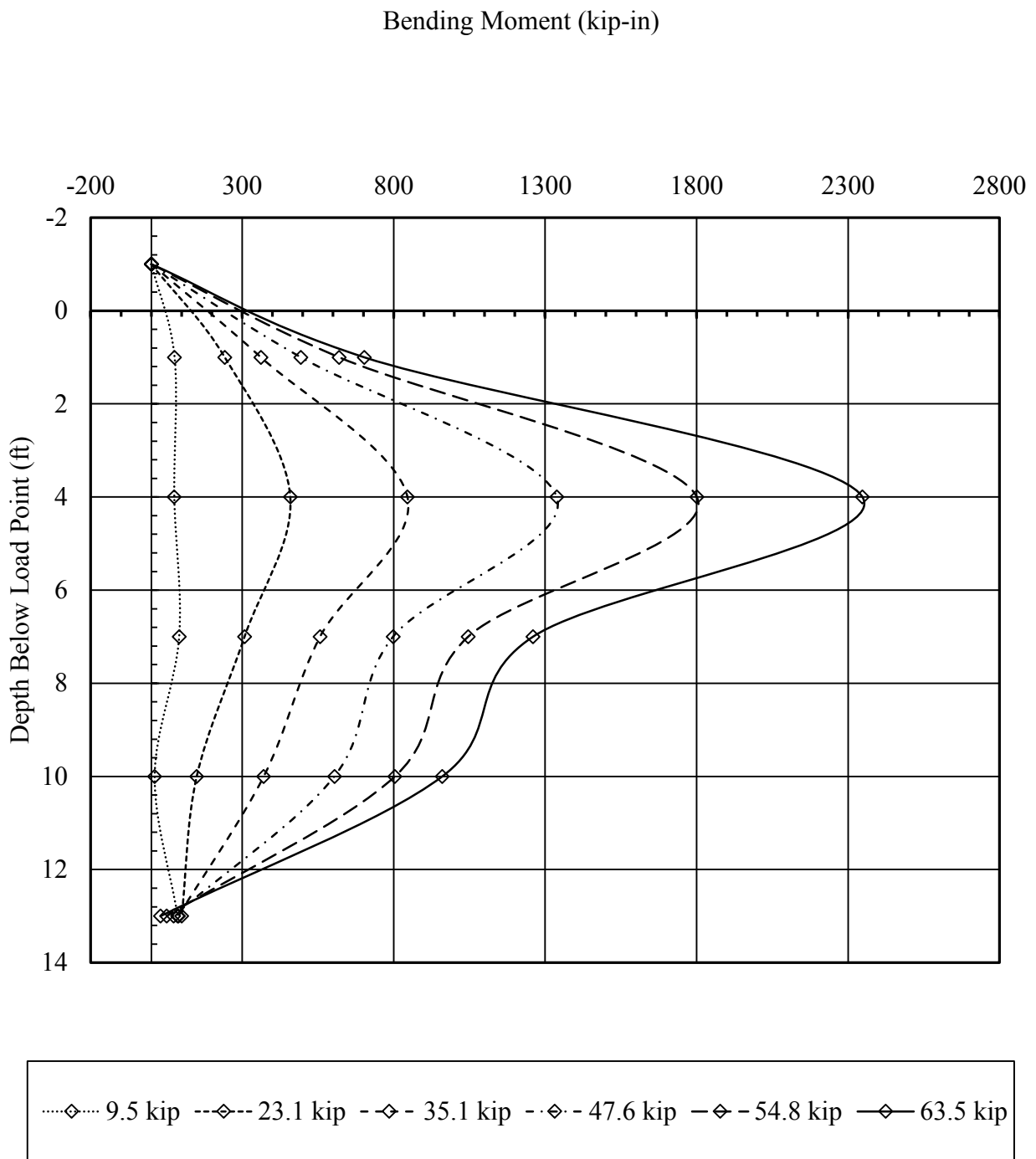


Figure 5-5: Bending Moment vs. Depth for Selected Head Loads for Square2

Bending Moment (kip-in)

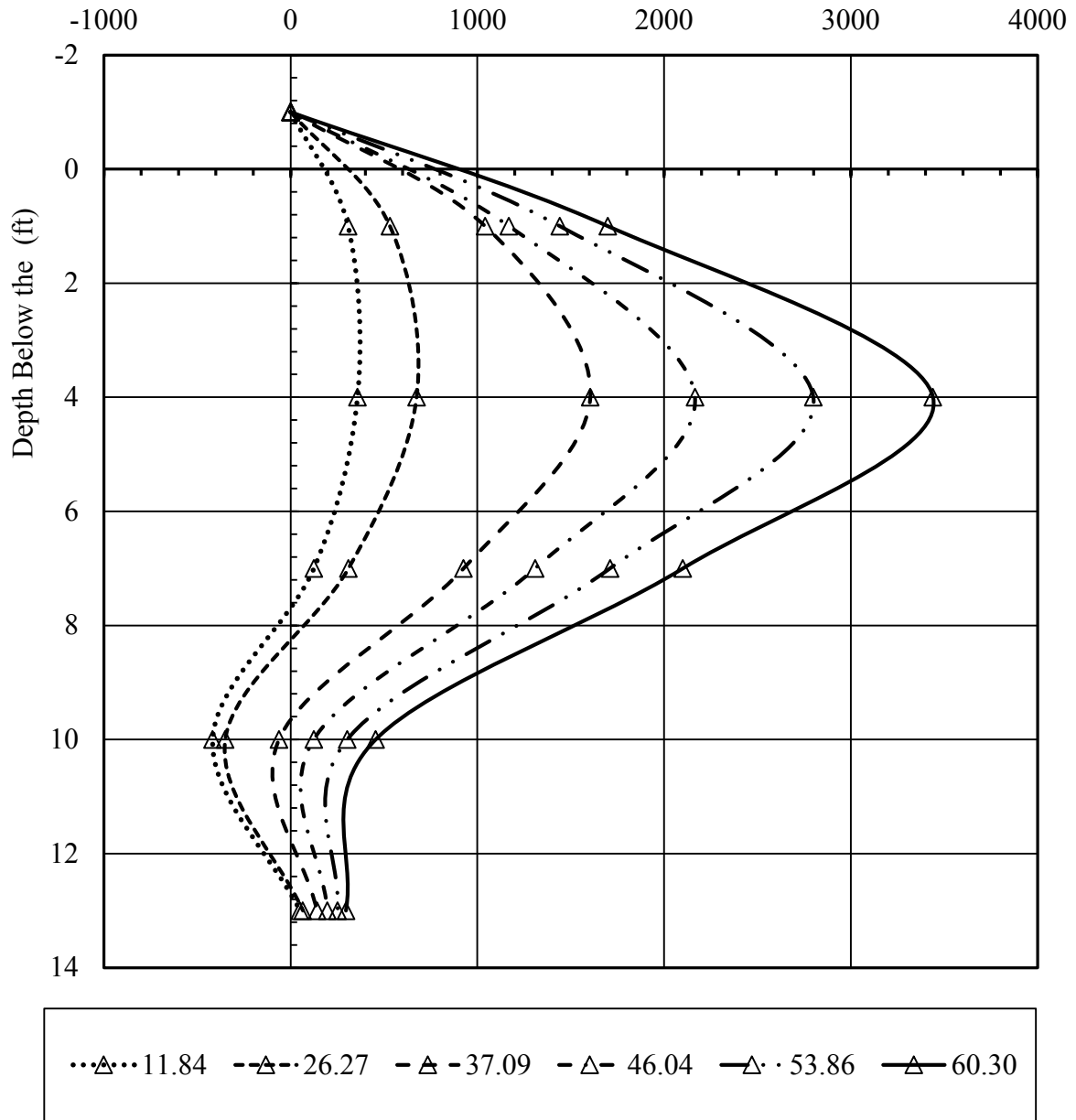


Figure 5-6: Bending Moment vs. Depth for Selected Head Loads for H Pile

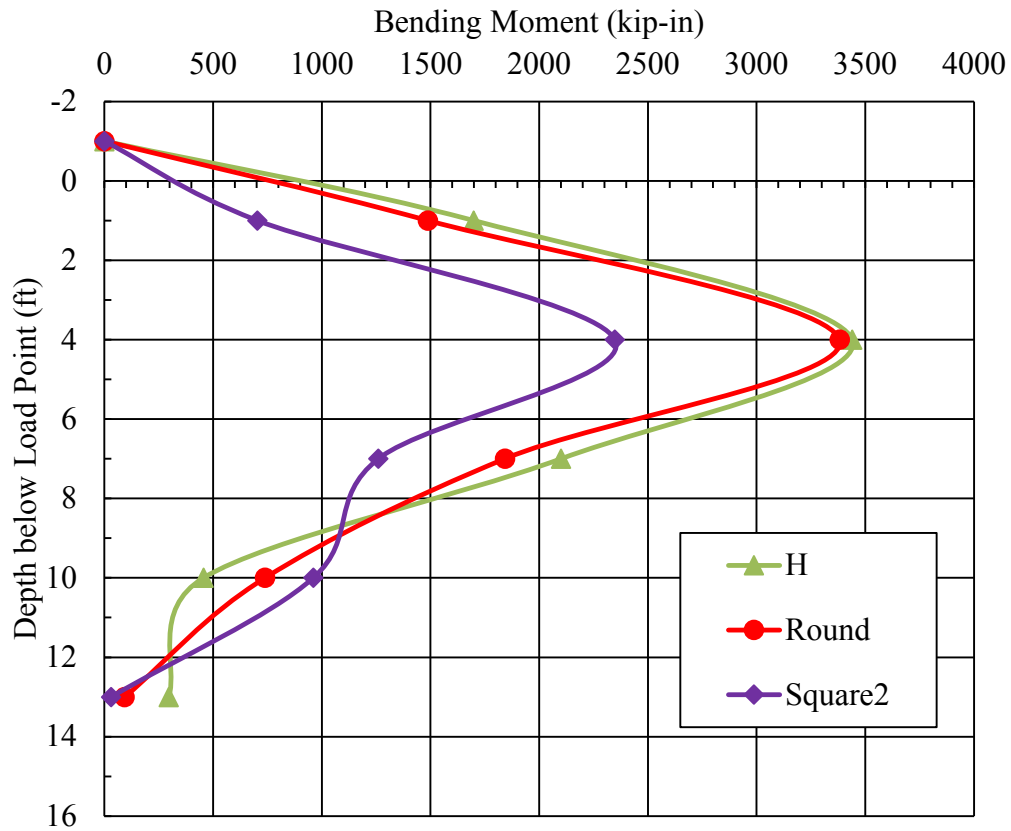


Figure 5-7: Maximum Bending Moment vs. Depth for the Three Shapes

Figure 5-8 shows the measured bending moment of inertia vs. applied load. The H pile shows the highest maximum bending moment of the four piles tested. Square1 shows the lowest bending moment of inertia. It is important to note that despite the big moment of inertia difference between the H pile and the circular pile; their maximum bending moments are really close. The measured maximum bending moment for square2 is better than square1 even though their moment of inertia is the same.

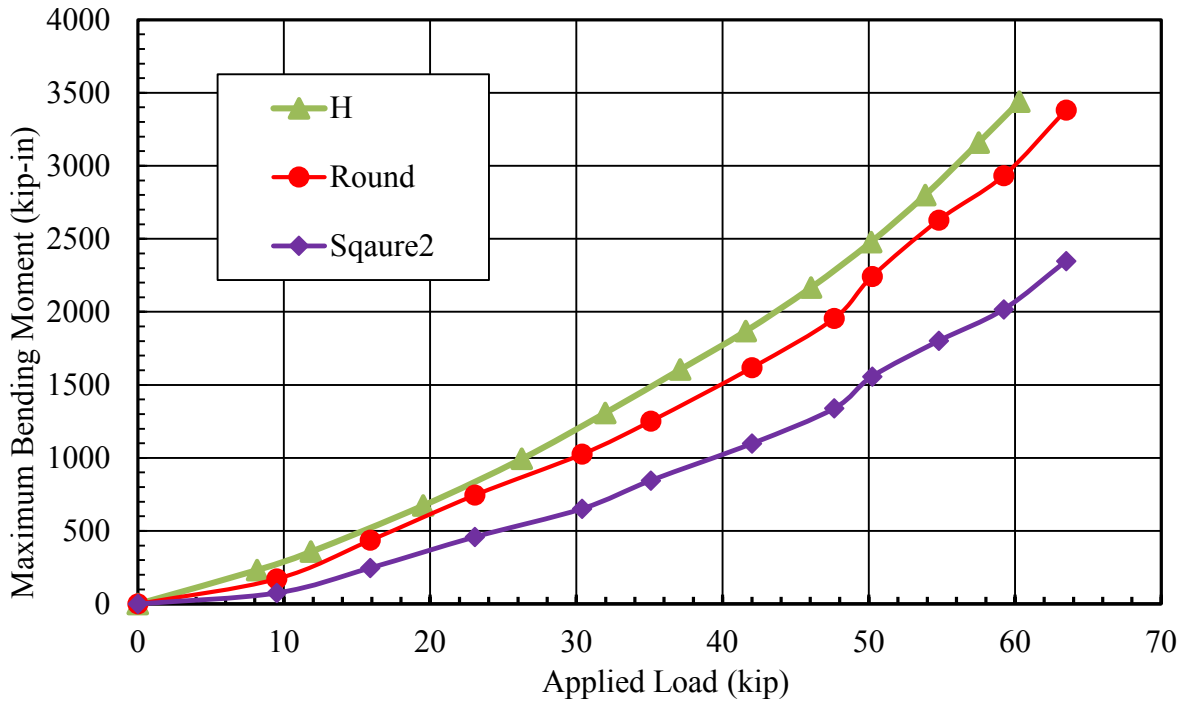


Figure 5-8: Maximum Bending Moment vs. Applied Load for the Three Shapes

5.3 Ground Displacement

The ground displacement was recorded using string potentiometers and the DIC station. The final readings of the string potentiometers were plotted vs the distance from the stakes to the face of the pile to compare how much the ground had displaced during the load test.

Figure 5-9 shows a combined plot for all the tests. Overall, the circular pile showed the most ground displacement experiencing the highest movement on the first three feet from the face of the pile. Both square piles (square1 and square2) experienced similar ground displacement, with maximum displacements of 1 inch for square1 and 0.8 for square2 at a distance of 1 ft from the face of the piles. The H pile behaved a bit different than the rest of the piles by showing its maximum ground displacement of 0.55 inches at a distance of 2 ft from the projected face between the two flanges.

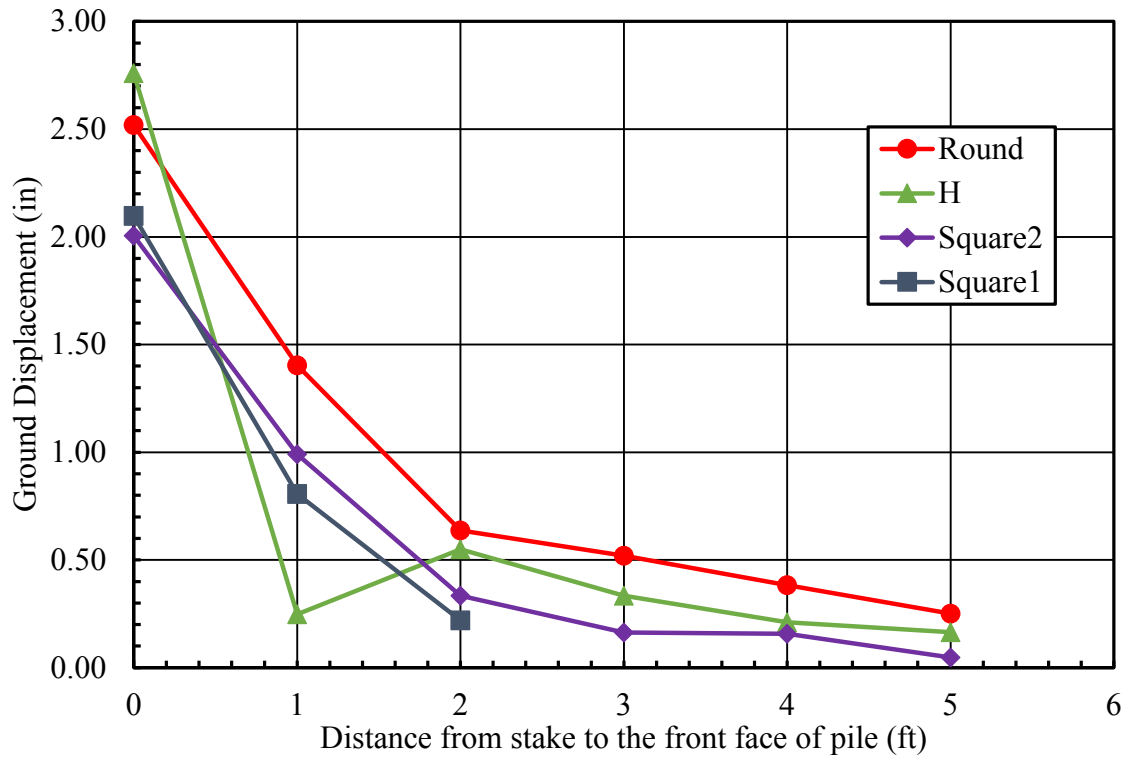


Figure 5-9: Ground Displacement vs. Distance From Pile Plot for All Piles Tested

Figure 5-10 and Figure 5-11 show the DIC final image for the circular and H pile, respectively. They both show agreement with the measured ground displacements with the string potentiometers. For the circular pile there is a difference in the maximum ground displacement measured of about 7% higher for the string potentiometer from the values obtained using the DIC. Similar difference was observed with the DIC values taken for the H pile, where the string potentiometers show somewhat higher values. The failure planes discussed in Section 5.5 can be observed in these images for both piles. No images were taken for the square piles during these tests.

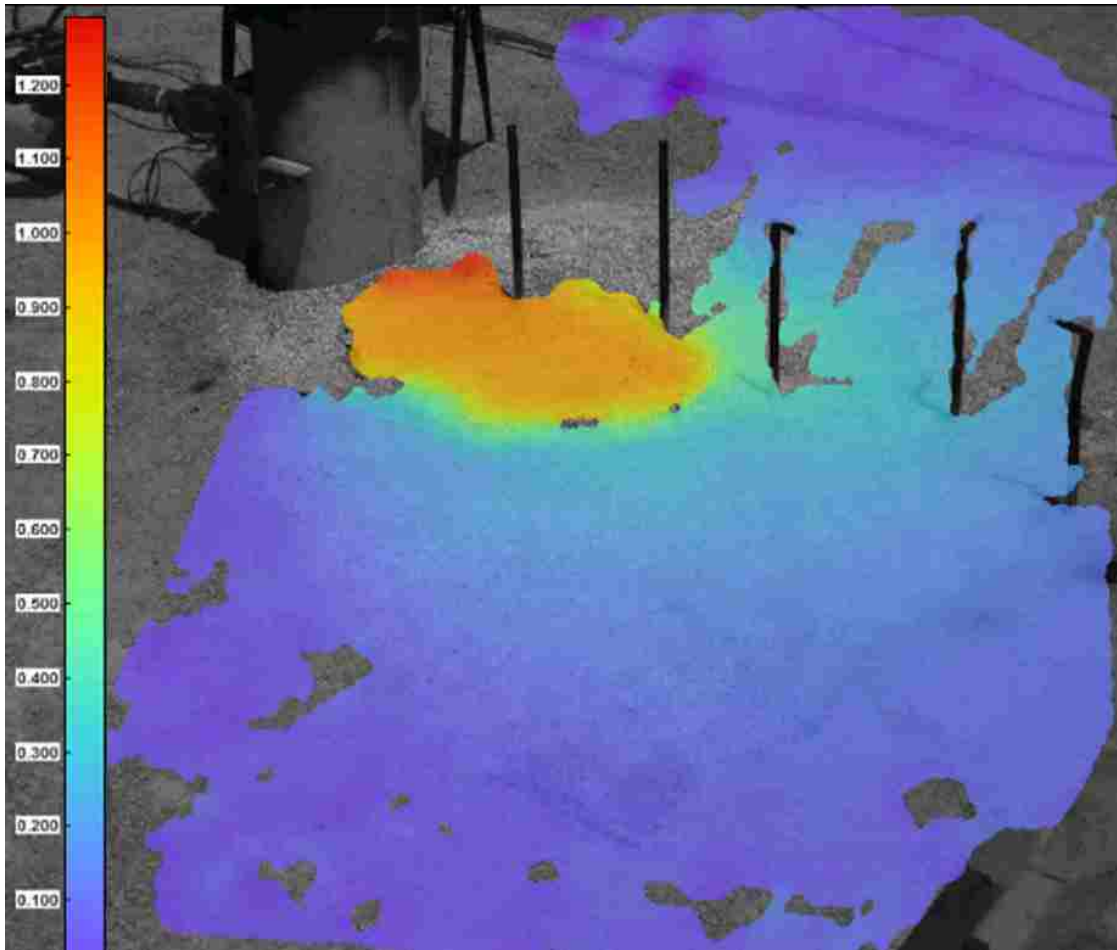


Figure 5-10: Circular Pile Ground Displacement From DIC

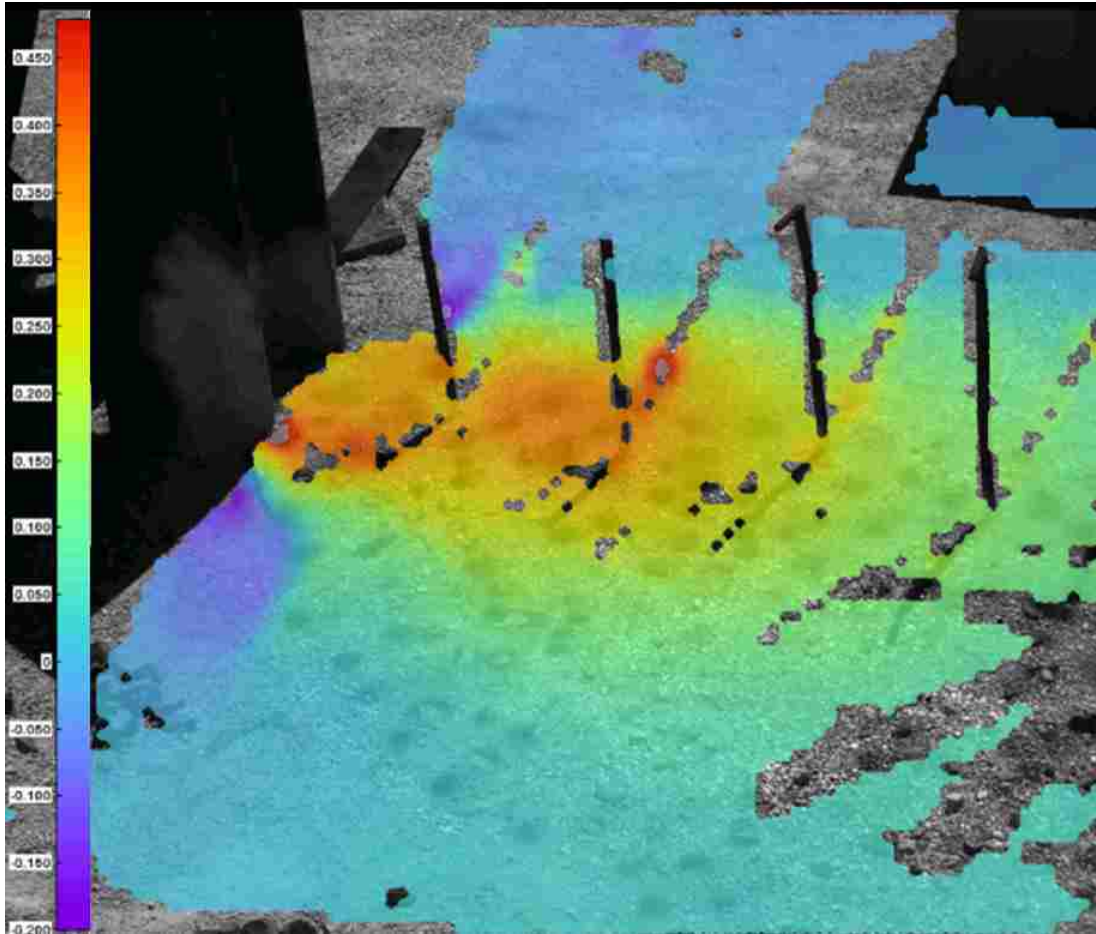


Figure 5-11: H Pile Ground Displacement From DIC

5.4 Heave

Elevation measurements were taken before and after all tests with surveying equipment. The locations of the points measured were usually in the front corners of the piles and beside the stakes where the string potentiometers were attached. Measurements were taken very carefully to avoid any reading interruption from the string potentiometers. The heave measured is close to zero at a distance of about five feet in front of the pile face as shown in Figure 5-12. The square piles heave the most at a distance of one foot away from the face of the pile. The H pile

displaced the most soil at the projected face of the pile in between flanges. The circular pile shows settlement on the face of the pile, but then the highest heave among all the piles at a distance of five feet.

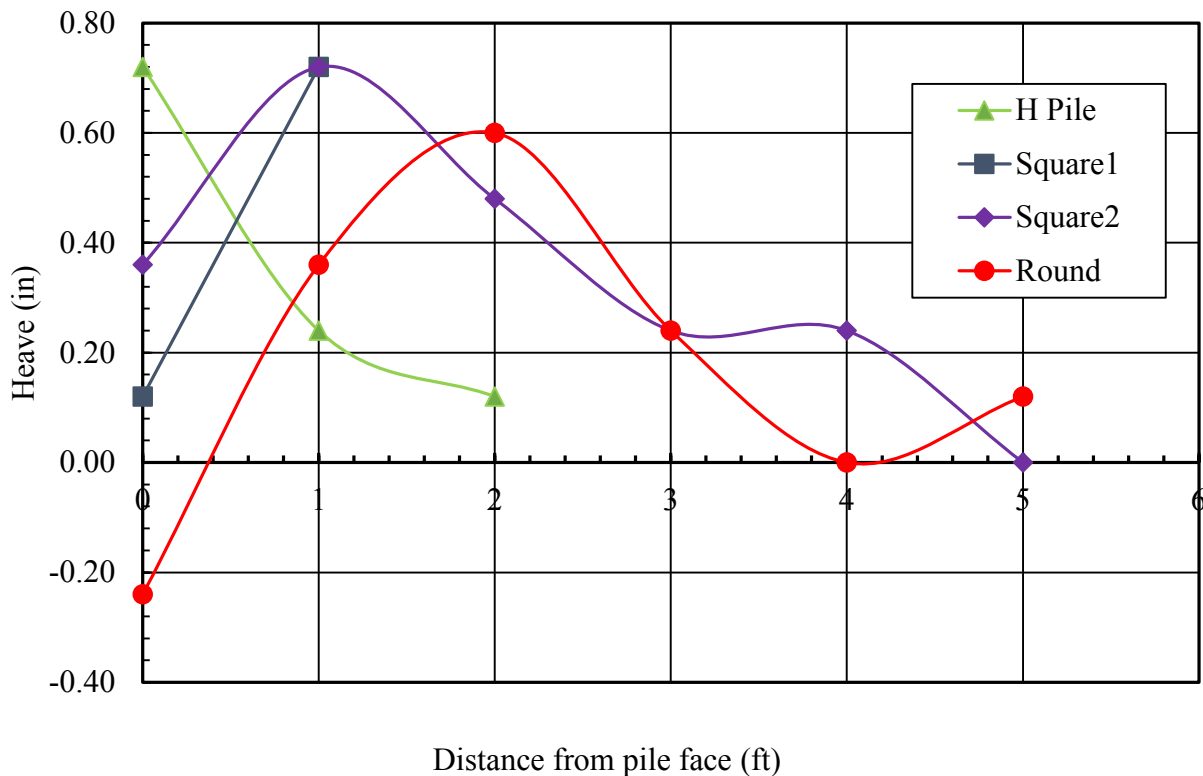


Figure 5-12: Heave vs. Distance From Pile Face

5.5 Failure Planes

After completion of each lateral load test, the cracks that developed on the ground surface in front of the pile were spray painted for better observation and recording of the failure surfaces. Measurements of the cracks and angle with respect to the edge of the pile were taken. Figure 5-13 shows comparative pictures of the failure planes for the three different pile shapes. The square and H pile developed wedge type of failure while the failure geometry for the circular pile

was more elliptical. Failure planes are very distinct and concentrated for the square and H piles, while the failure planes are more dispersed around the perimeter of the pile.



Figure 5-13: Failure Planes for the Distinct Shapes

Reese and Van Impe (2002) suggest that failure planes fan out from the edge of square shaped piles at an angle, α , between ϕ and $\phi/2$ for dense sand. The wedge angle tends to be higher for the H pile, but the cracks tend to propagate less than the square pile. The H pile appears to have a smaller projected area of soil resisting against lateral loading, while the square pile developed longer cracks and smaller wedge angles giving the impression there is more soil mass resisting against lateral loading. The cracks developed by the circular piles propagate more than the H and square, these cracks do not start on the edge but more towards the middle of the pile. By comparing the surface failure of the circular pile to Figure 2-1 it can be noticed the similarities when it comes to pressure distribution. Although the pressure distribution cannot be seen in the surface failure, where cracks developed it is where the higher pressure occurs according to Figure 2-1.

6 LATERAL LOAD ANALYSIS

The computer program LPILE was used to perform the lateral pile load analyses in this study. LPILE is the commercial version of the computer program COM624 which was originally developed by Reese and Matlock at the University of Texas in the 1970s and is one of the most widely used programs for the lateral pile load analysis. LPILE uses the finite difference method to iteratively solve for the deflection, shear force, and bending moment of the pile with depth by modeling the pile as a beam column. The analysis of the laterally loaded pile by the finite difference method has been researched extensively by Reese and Matlock since the 1960s.

The soil model in LPILE was first calibrated by matching the computed load-deflection curve to the measured test data for the round pile. This assumed that the load-deflection curve for this pile would be more accurately predicted due to the circular cross-sectional shape of the pile. Subsequently, the calibrated soil parameters were used to compute load-deflection curves for the square and H pile with the appropriate section modulus for each pile. Discrepancies between the measured and computed curves could then be attributed to differences in resistance associated with the pile shape. Finally, several approaches to account for the influence of pile shape on lateral resistance were used to determine if they could produce agreement with the measured behavior of the square and H pile.

6.1 Pile Material Properties

Because each of the pile load tests was conducted to a maximum pile head deflection of approximately 3 inches or until yield of the steel became a concern the test piles were considered to behave as a linear elastic material. For this material type, the pile diameter, wall thickness, and moment of inertia were required. In addition, the length of the pile with respect to the load point was provided. The moment of inertia for each of the test piles was different than the standard values for the corresponding shape due to the addition of the iron angles to the front and back sides of the piles. When accounting for the welded iron angles, the moment of inertia increased as summarized in Table 3-1.

At the time of the testing, the lateral loads were applied approximately 34 ft above the toe of the pile which was one foot above the ground surface. For practical purposes the pile can be considered to be hollow because the pile plugged with soil about 10 ft above the toe which is considerably below the zone where applied lateral load might have transferred load to the soil. In addition, the soil in the plug likely provided very little to the moment of inertia or composite elastic modulus of the pile. Figure 6-1 shows a typical cross-section properties input window from LPILE.

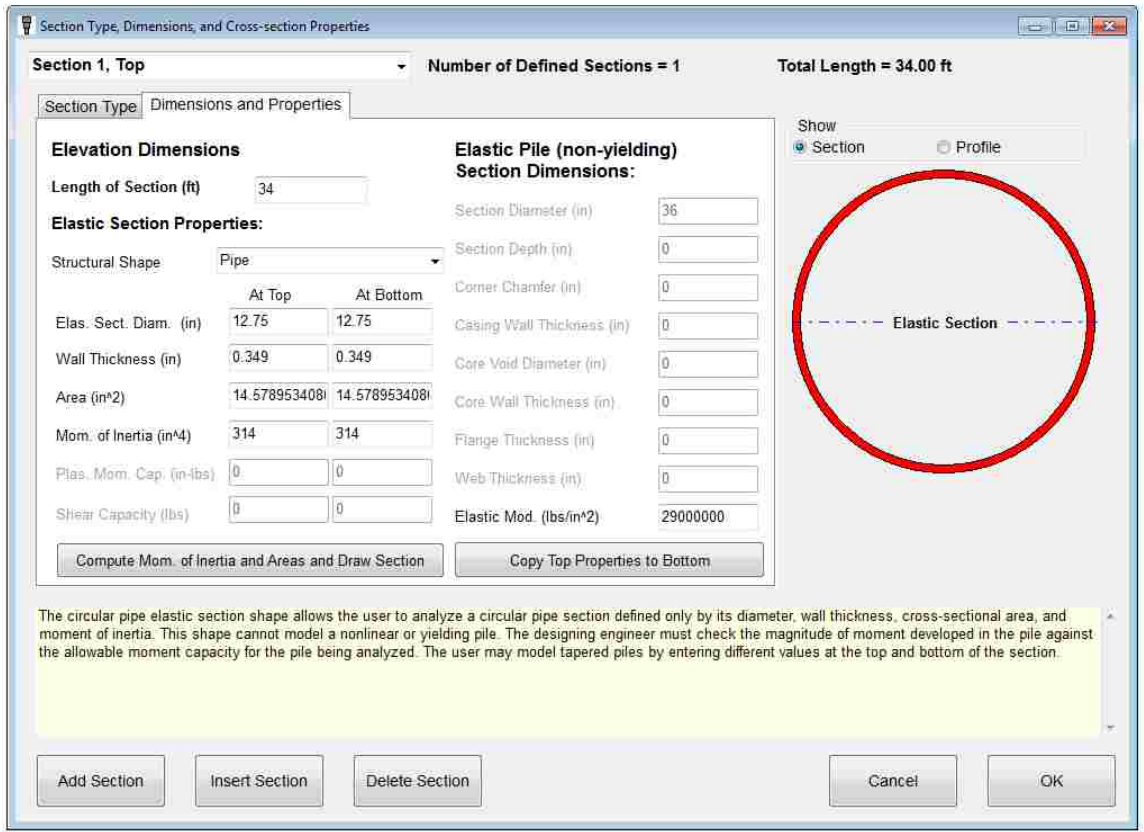


Figure 6-1: LPILE Input Property Window (Round Pile)

6.2 Pile Load Model

Loads were applied in the program using a pinned-head boundary condition to match field conditions. The lateral load was applied as a shear force and the applied moment was set to zero to satisfy the pile head boundary conditions. The applied loads were the same as the loads applied during incremental loading of each test pile.

6.3 Soil Properties Model

At the time of tests, the soil profile consisted of 15 ft of compacted granular backfill underlain by 18 ft of native silty sand to sandy silt above the toe of the pile as shown in

FIGURE. Because lateral load is typically transferred within 5 to 10 pile diameters of the ground surface, the lateral pile response was primarily controlled by the properties of the compacted granular fill. This observation was borne out in the LPILE analyses because small changes to the soil properties in underlying native soil layer had relatively little effect on the pile response.

The granular backfill and native soil layers were both modeled using the p-y curve shape for sand developed by the API (1982). In this approach, p is the horizontal soil resistance per length of pile and y is the lateral soil displacement y. According to API, the p-y curve is given by (6-1)

$$p = AP_u \tanh \left[\frac{(kx)}{(AP_u)} y \right] \quad (6-1)$$

Where,

$A = 3.0 - 0.8(z/b) > 0.9$ for static loading,

$A = 0.9$ for cyclic loading,

$x =$ the depth below the ground surface,

$b =$ pile width/diameter, and

$P_u =$ ultimate lateral resistance

The ultimate lateral resistance for sand has been found to vary from wedge type failure at the shallow depths determined by (6-2) to a flow-ground type failure at greater depths defined by (6-3). The equation giving the smallest value of P_u should be used as the ultimate resistance. The typical wedge type failure shape is illustrated in Figure 6-2. The angle β is typically assumed to be $45^\circ + \phi/2$ while the fan angle, α , is thought to be between $\phi/2$ and ϕ for dense sand around $\phi/2$ for loose sand.

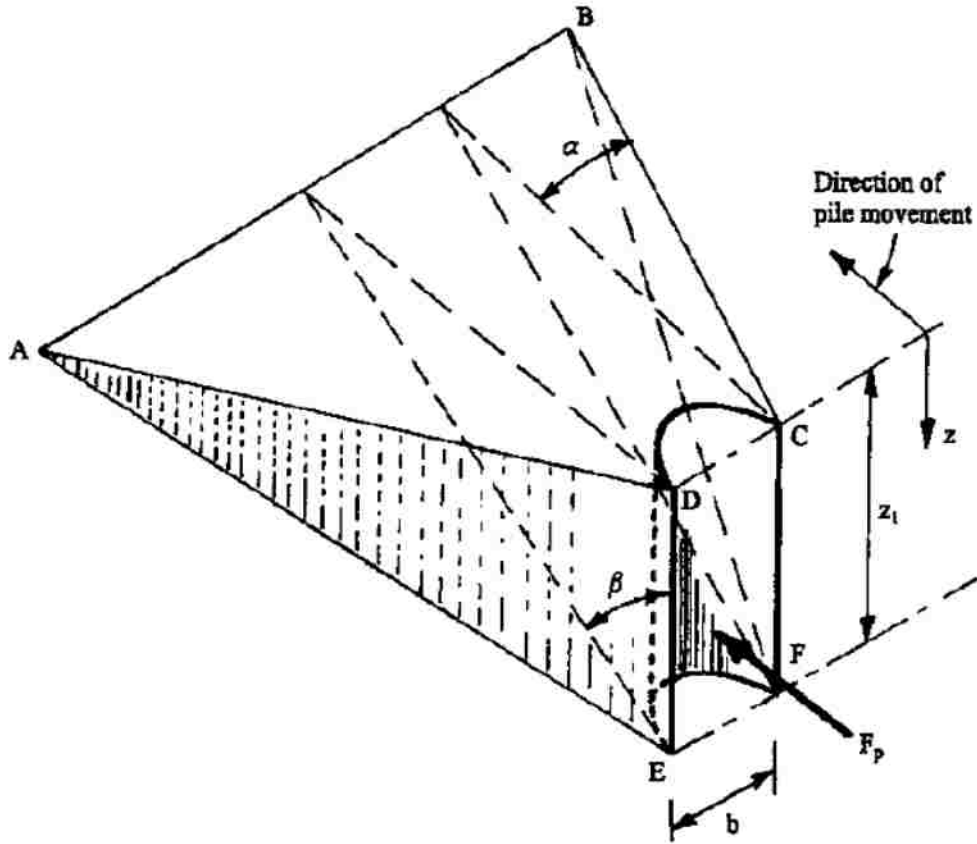


Figure 6-2: Illustration of Wedge Type Failure Adjacent to Piles at Shallow Depths During Lateral Loading

$$P_{us} = (C_1x + C_2b)\gamma'x \quad (6-2)$$

$$P_{ud} = C_3b\gamma'x \quad (6-3)$$

Where,

P_u = ultimate resistance (force/unit length), (s=shallow, d=depth),

γ' = effective soil unit weight, lb/ft³,

x = depth, in,

ϕ' = angle of internal friction of sand, degrees,

$C_1, C_2, C_3 =$ coefficient determined from Figure 6-3 as a function of the friction angle,
and

$b =$ average pile diameter from surface to depth, in

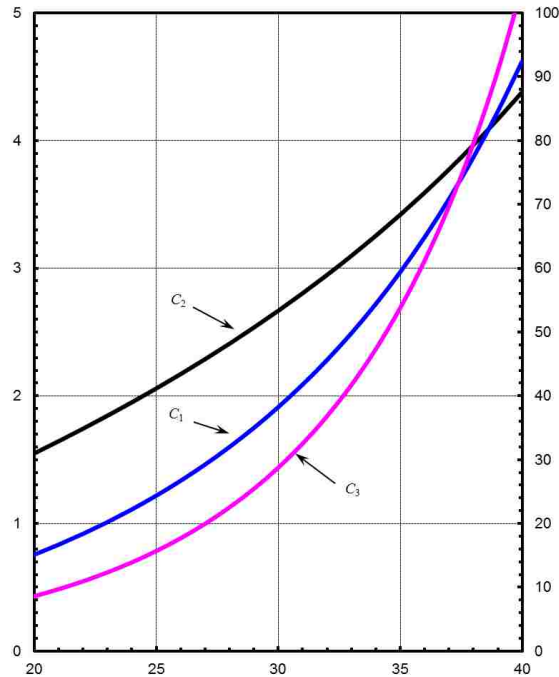


Figure 6-3: Coefficients $C_1, C_2,$ and C_3 as Function of Friction Angle

To develop the p-y curves, the model requires the user to provide data regarding the soil friction angle, ϕ ; the lateral soil stiffness, k ; and moist unit weight. The unit weight of the soil used was known from the density tests performed during construction; however, direct measurements of ϕ and k were not available. API suggest that ϕ and k can be estimated using the curves shown in Figure 6-4, but experience indicates that there can be significant variations in from these values in actual practice (Brown et al 1988, Rollins et al 2005, Rollins et al 2011). Since relatively few lateral load tests have been performed on piles in compacted gravelly sands

such as the backfill material used in this research, the soil strength and stiffness parameters are poorly calibrated. Thus, the friction angle, ϕ ; and stiffness, k ; were back-calculated from LPILE by matching the calculated the load-deflection curves with those obtained from the field tests for the round pile.

Both friction angle and soil stiffness have an effect on the computed load-displacement curves; however, k has a greater effect on the curve at small deflections while ϕ has a greater effect on the curve at large deflection near the ultimate resistance. Altering the soil stiffness for example, can have significant effects on the shape of the load-deflection curve of the pile.

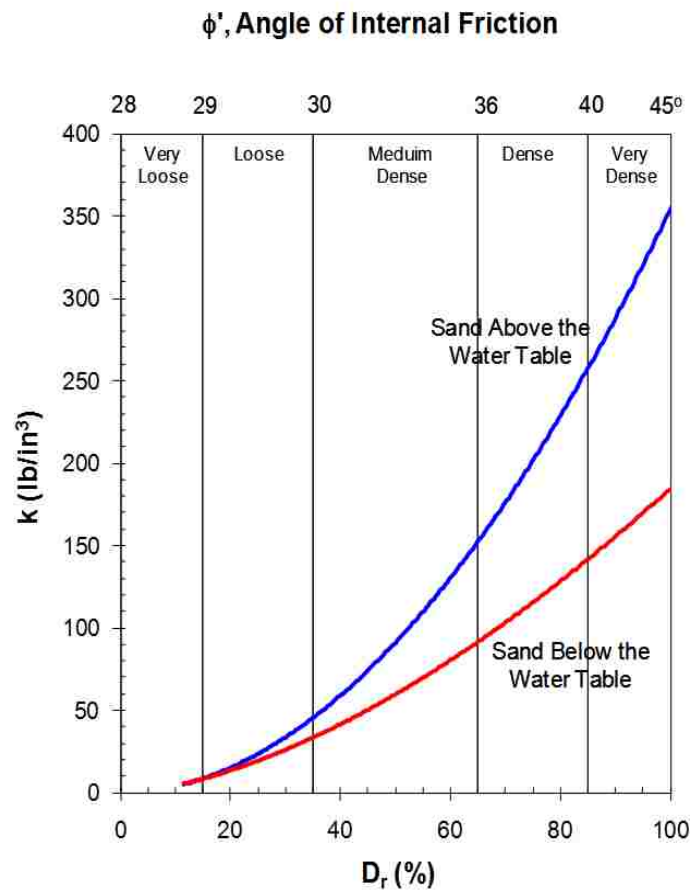


Figure 6-4: Subgrade Reaction Modulus, k Used for API Sand Criteria in p - y Analysis (API, 1982)

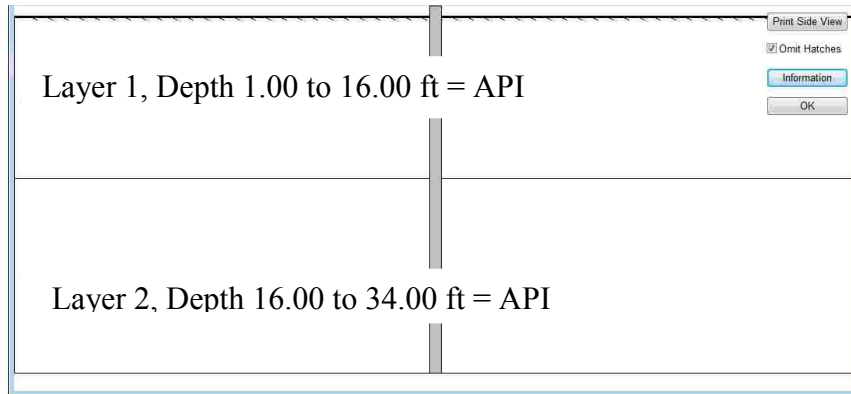


Figure 6-5: Side View of Soil Layers in LPILE (Round Pile)

Table 6-1 provides a summary of the back-calculated soil properties for the profiles used in the analyses. The friction angle and the soil stiffness shown are the values back-calculated in LPILE that have the best agreement with the test data. For soil compacted to 95% of the standard Proctor a relative density of about 50 to 60% might be expected (Lee and Singh 1971). The back-calculated friction angle and k values for the reinforced fill appear to be considerably higher than what would predicted by the API criterion would suggest. However, using the API k value produced a much softer load-deflection curve than what was measured, as shown in Figure 6-6.

Table 6-1: Soil Profile Properties Used in LPILE Analysis

Depth (ft)	Description	Soil Type (p-y model)	Effective Unit Weight, γ' (pcf)	Friction Angle, ϕ (degrees)	p-y Modulus, k (pci)
1 to 16	Reinforced Fill	API Sand (O'Neill)	129	45	250
16 to 34	Natural Soil	API Sand (O'Neill)	125	34	100

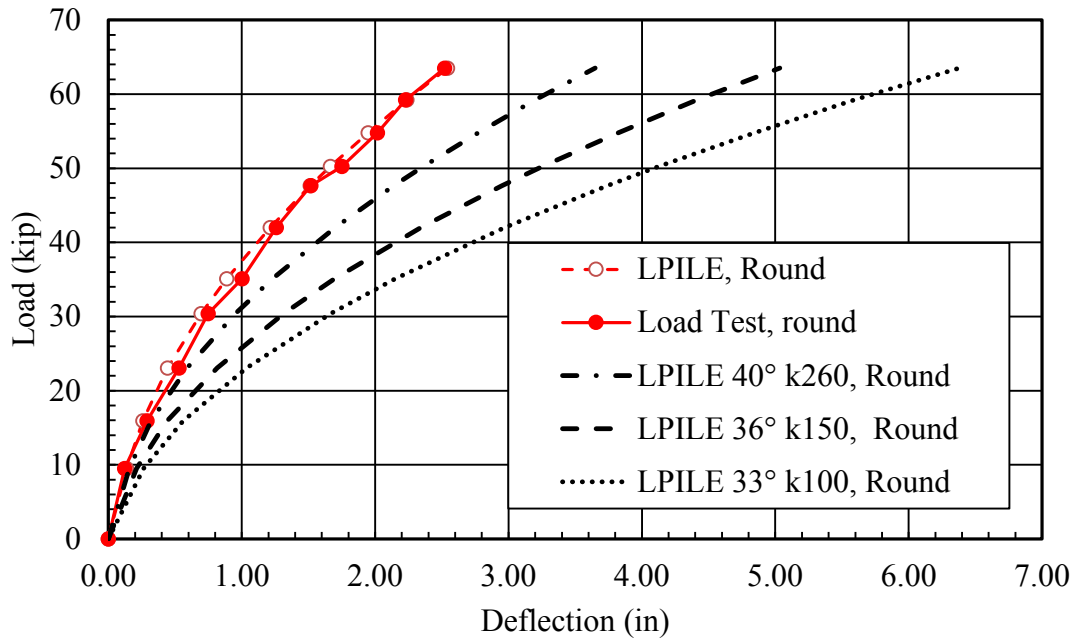


Figure 6-6: Load vs. Deflection Curve for Various ϕ and k (Round)

6.4 Results of LPILE Analysis

The LPILE model was first calibrated by matching the load-deflection curve to the test data of the round pile. This assumed that the load-deflection curve for this pile would be more accurately predicted due to the circular cross-sectional shape of the pile. Figure 6-7 shows the result of the round test data and LPILE analyses. Although the agreement is generally very good, it should be noted that the computed curve in LPILE does not exactly match the test data. Every effort was made to produce a well-calibrated model in LPILE; however, the curves seem to be shaped somewhat differently, leading to small differences in the curves within certain deflection ranges. The differences are most obvious at deflections less than 0.75 while at higher deflection the curves seem to match very well.

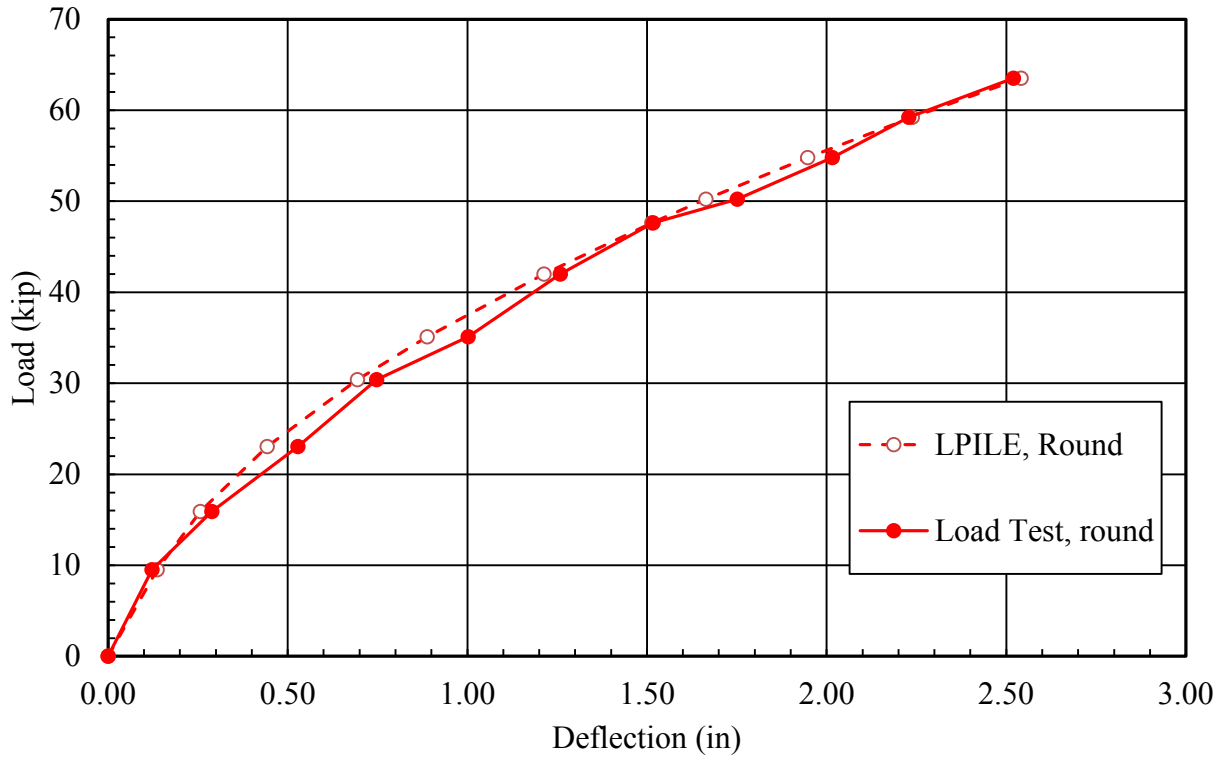


Figure 6-7: Load-Deflection Curves Comparison of Tested Values and Computed

When modeling the square and H piles, the same soil properties were used as those used for the round pile. However, the load-deflection curves computed by LPILE with these same parameters underestimate the measured stiffness of the piles from the field test. Figure 6-8 shows the computed and measured load-deflection curves for both square and H piles. Notice that the curves computed by LPILE for both the square and the H pile start in agreement with the test data, but they separate from one another as the load increases. At a load of 60 kips, the computed deflection for the square pile is about 0.30 inches greater than the measured deflection. Likewise, at a load of 60 kips the computed deflection for the H pile was up to 1.1 inches higher than the measured displacement. As noted in these examples the discrepancy is up to 40%

greater between measured and computed deflection for the H pile and a relative smaller difference for the square pile up to 17% at 60 kips.

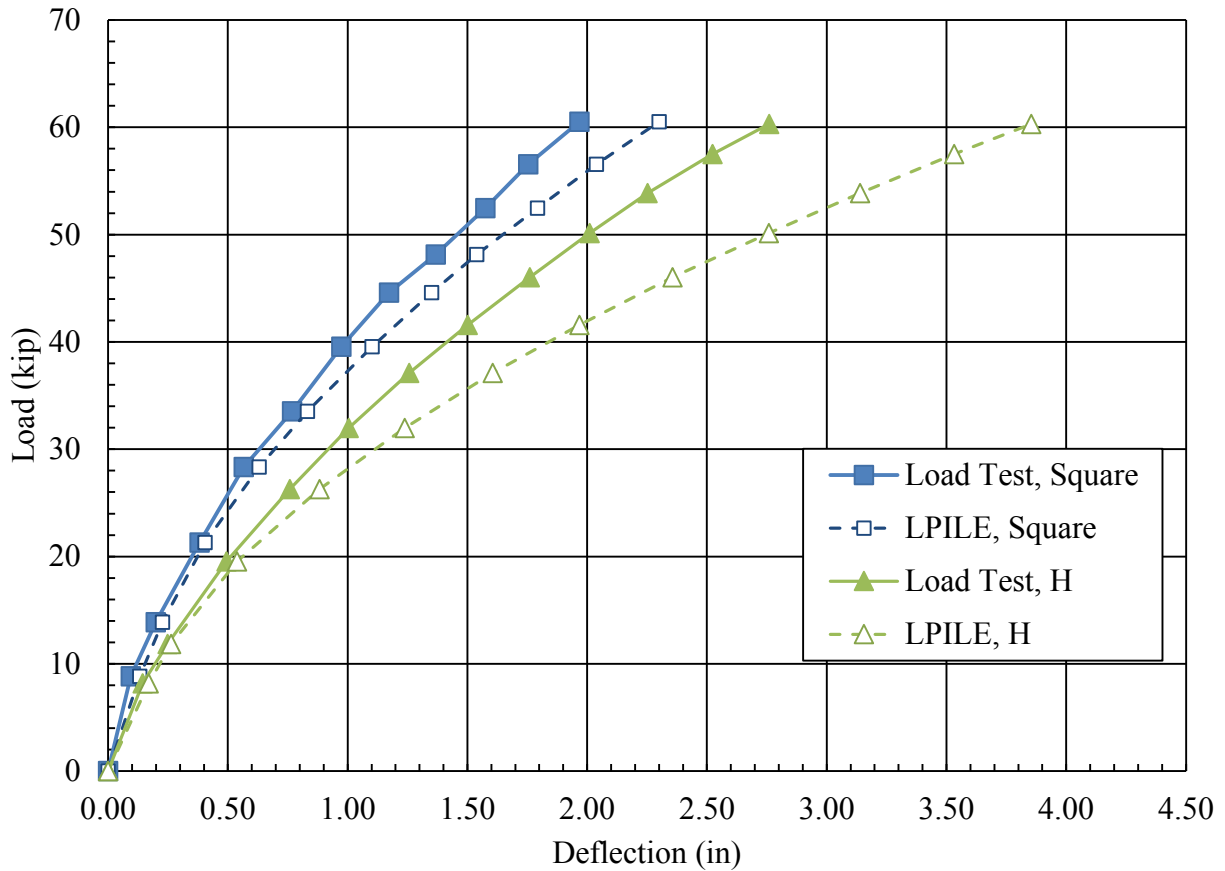


Figure 6-8: Load-Deflection Curves Comparison of Tested Values and Computed (Square & H)

The computed bending moment vs. depth curves for each of the LPILE models are shown in Figure 6-9 for the round, Figure 6-10 for the square, and Figure 6-11 for the H pile along with the bending moment vs. depth curves from the strain gauges test data.

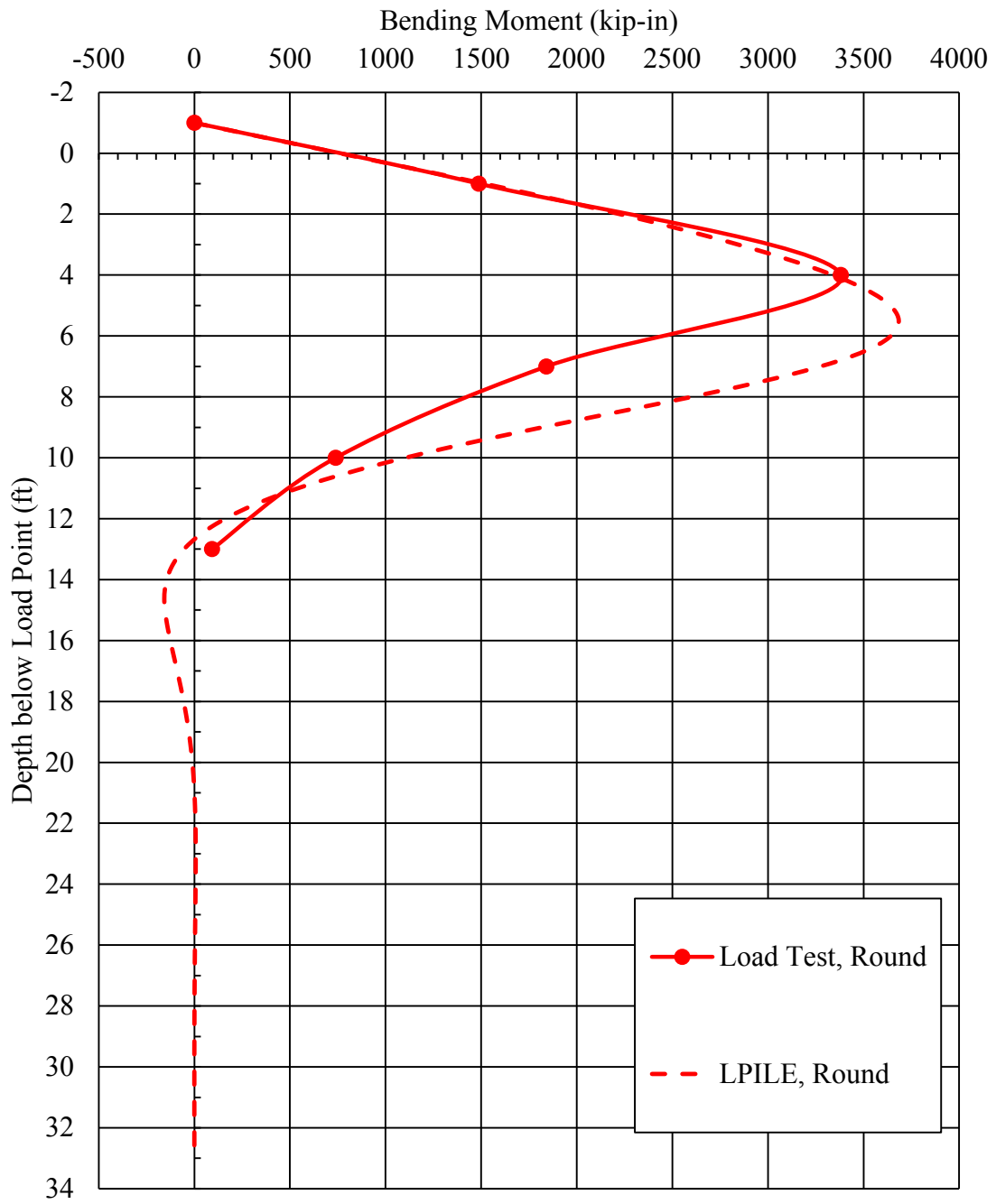


Figure 6-9: Bending Moment vs. Depth (Round Pile)

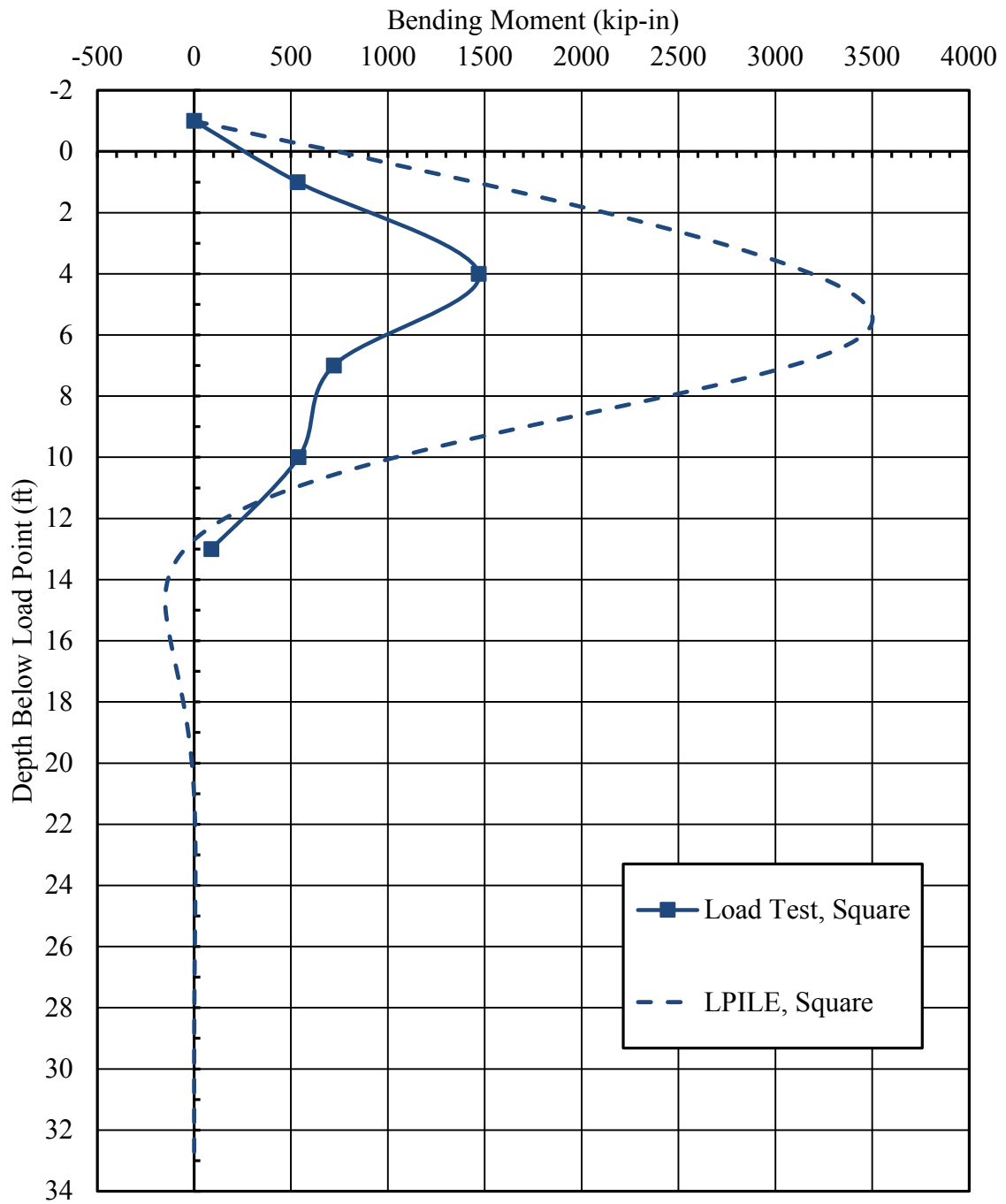


Figure 6-10: Bending Moment vs. Depth (Square Pile)

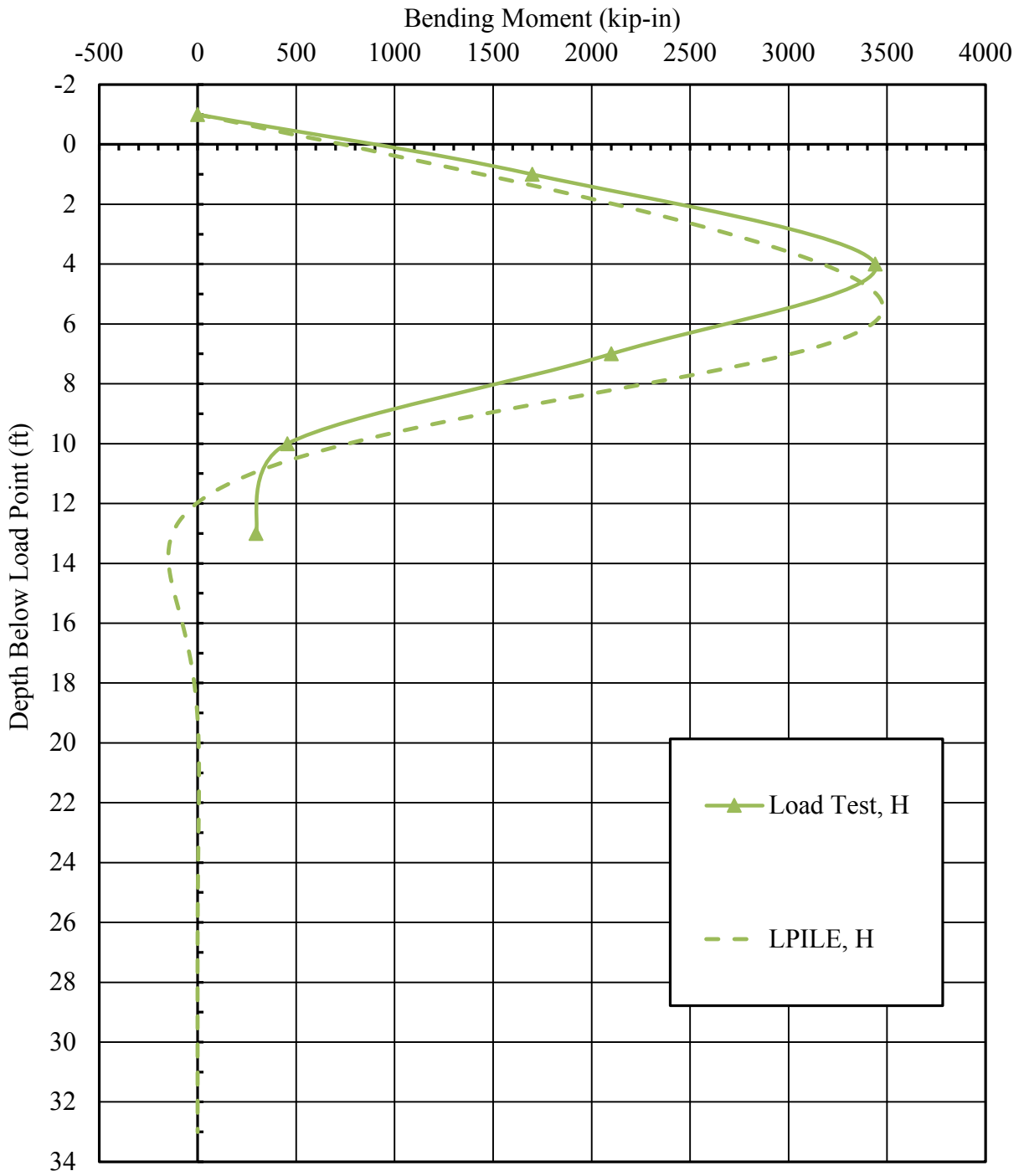


Figure 6-11: Bending Moment vs. Depth (H Pile)

From the bending moment vs. depth curves we can notice that the maximum bending moment for all types typically occurs at a depth of about 4 ft below ground level on the measured values since the strain gauge was installed at that depth. In reality, maximum value might have occurred at a greater depth if the gauges had been closer together. When LPILE computes the bending moment curve does it nearly continuously; thus, giving a more accurate maximum bending moment depth. LPILE typically shows the maximum bending moment occurring at a depth of about 5.5 ft below ground level. Apart from the maximum value, the general shape of the computed bending moment versus depth curves are in reasonably good agreement with the measured shapes.

The H pile, which had the lowest moment of inertia, experienced the highest bending moment almost overlapping with the round pile. However, the round pile had a maximum bending moment very similar to the H pile, even though it had a higher moment of inertia. The square pile on the other hand, experienced the least bending moment of the three cross-sectional shapes as can be noted in Figure 6-12 where the maximum bending moment is plotted vs. the applied load.

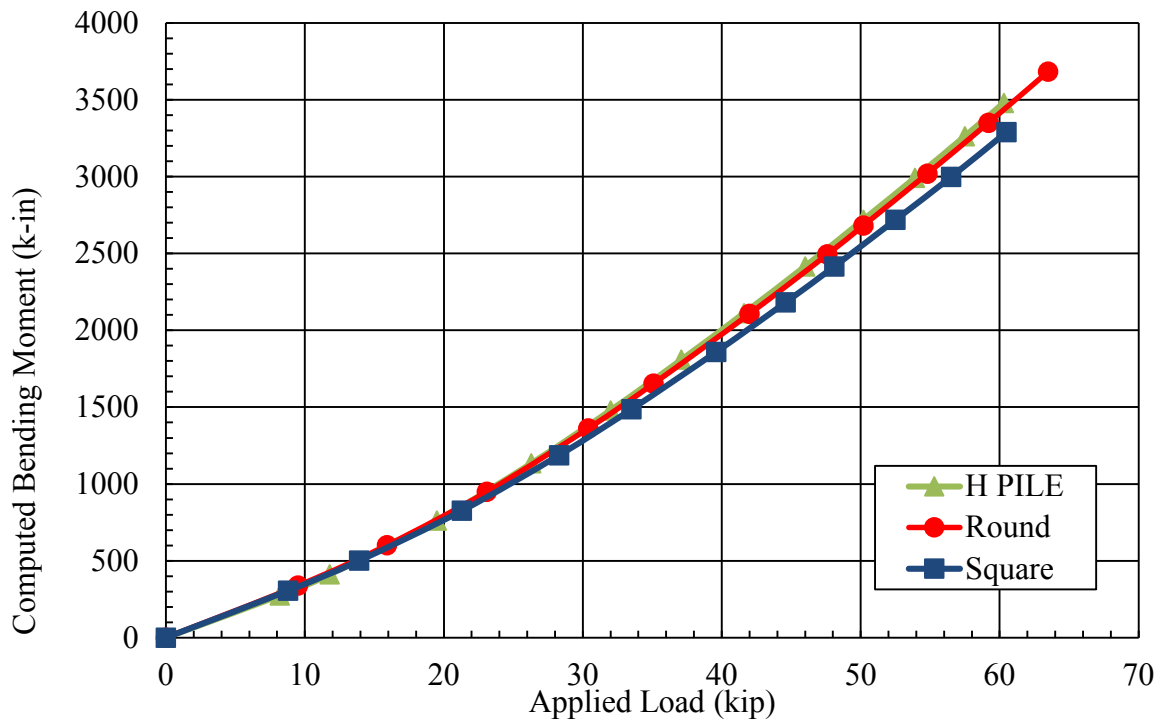


Figure 6-12: Maximum Computed Bending Moment vs. Applied Load for the Three Shapes

6.5 Reese and Van Impe Equivalent Diameter

As discussed in section 2.3, Reese and Van Impe proposed using an equivalent pile diameter to account for the side friction on piles with non-circular cross-section. To calculate the equivalent diameter using (2-5), first the ultimate resistance of a circular section with a diameter equal to the width of the non-circular cross-section needed to be computed. Following the API recommendations for computing p-y curves in sand described previously, the ultimate resistance was computed as a function of depth for each pile. Secondly, the unit side friction, f_z , was computed as a function of depth for the square and H pile sections using (2-6). In making this calculation K was assumed to be equal to 1.0 and the friction angle between the pile and sand

was made equal to two-thirds of the friction angle of the soil back-calculated using LPILE in Table 6-1.

Once the ultimate resistance, P_u and side friction, f_z were determined, (2-5) was used to compute the equivalent diameter as a function of depth for the square and H piles. The depth range used was from ground level until 15 ft below the surface, as the depth increased, b_{eq} decreased. As recommended by Reese and Van Impe, the average diameter of these values was selected. Table 6-2 shows the average equivalent diameters for the square and H piles which are only slightly higher than the physical widths of the pile themselves. In fact, the percent increase in widths was only 1.41% and 1.45% for the square and H pile, respectively. These results suggest that the increased in lateral resistance may result from an increase in both the passive and shear resistance on the pile not simply the shear resistance on the sides alone.

Table 6-2: Reese and Van Impe Equivalent Diameter (Square & H piles)

Square	H
b_{eq} in	b_{eq} In
12.2	12.3

After obtaining these equivalent diameters, the square and H piles were modeled in LPILE as a circular section with their corresponding pile properties (E and I) but with a greater effective width. No properties were changed besides the cross-sectional shape and widths. Load-deflection curves were obtained for each pile modeled and compared with the measured load-deflection curves.

For the H pile, Figure 6-13 shows the load-deflection curves for the load test, for the initial LPILE model and when using Reese and Van Impe's effective width approach. Notice that there is not much difference in the computed curves when using the effective width of 12.3 inches obtained from the Reese and Van Impe approach and the original LPILE model curve with the actual width of 12 inches. The two curves are nearly identical. The equivalent diameter would need to be significant higher to make this method work. For the H piles used in this research this method is insufficient for simulating the real behavior of the pile.

Figure 6-14 shows the same comparison load-deflection plots for the square pile as were shown previously for the H pile. Plots include the measure load-deflection curve along with the curves computed by LPILE with the original pile diameter and the increased diameter in the same graph. As with the H pile, the load-deflection curve for the square pile with the slightly larger effective width was nearly identical to the computed curve with the original width. In other words, there was not much of an increment in resistance for the equivalent diameter method. For the square pile behaved in the same way, not much of an increment for the equivalent diameter method. Just like the H pile, the equivalent diameter would need to be higher to have an impact on the load-deflection curves.

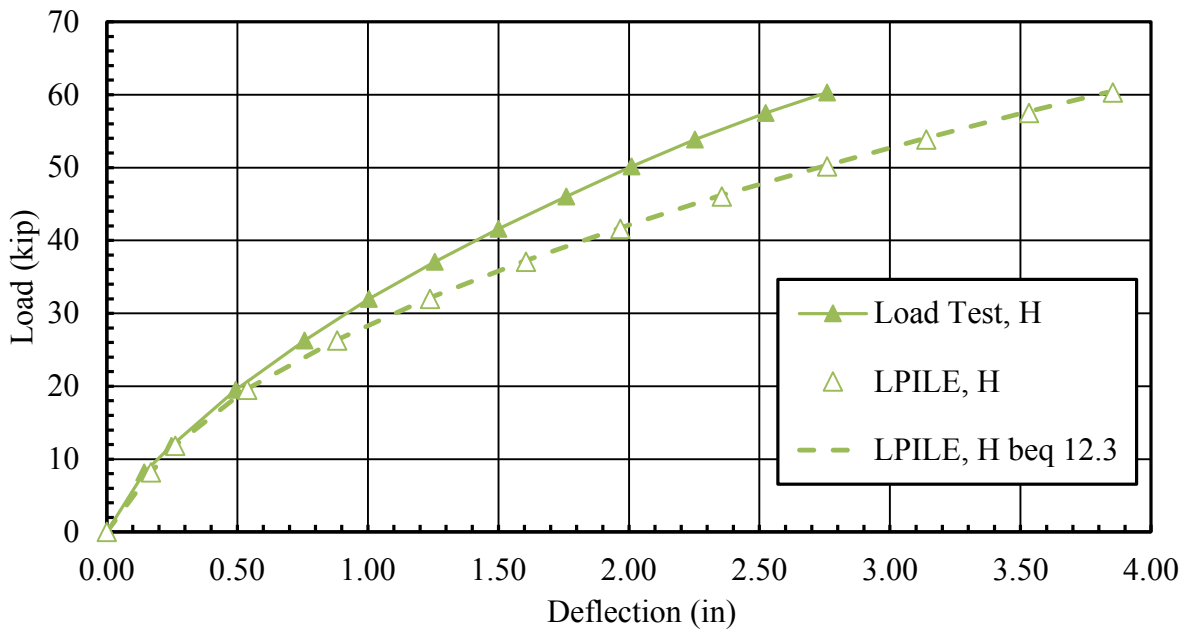


Figure 6-13: Load vs. Deflection Curves for Reese & Van Impe's Approach (H Pile)

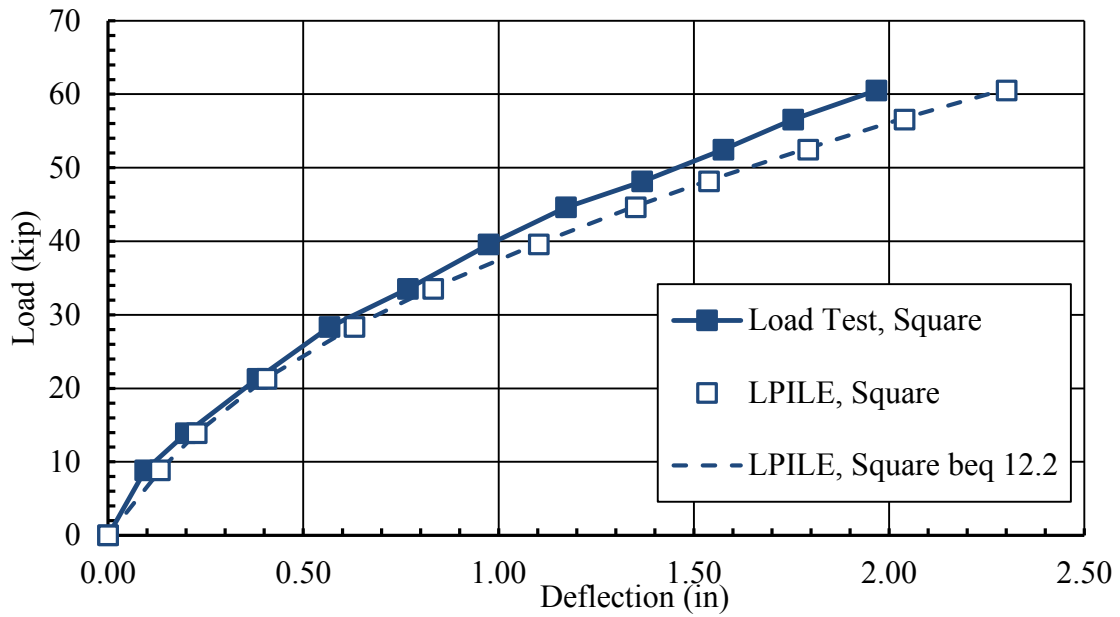


Figure 6-14: Load vs. Deflection Curves for Reese & Van Impe's Approach (Square Pile)

6.6 Briaud and Smith F-y/Q-y Mechanism

One application of the pressuremeter test (PMT) is the design of laterally loaded piles because of the analogy of loading between the PMT and the pile. However, for the laterally loaded test performed in this thesis, the PMT data was not available for use. The assumption was to have our calibrated curve, based on the performance of the round pile, be the direct correlation to research performed by Briaud et al 1983 as outline below.

At a variety of depths LPILE can compute the p-y curves for the round pile. P-y curves were computed by LPILE at depths of 1, 3, 5, 7, 9, 11, 13, and 15 ft below the ground surface based on the calibrated soil model. Figure 6-15 shows all the p-y curves for each depth and the increasing resistance as the depth increases. At those same depths F-y curves were computed for the round pile using (6-4) and it was assumed that resistance developed linearly with a displacement up to a value of 0.10 inch then remained constant at the maximum resistance. Then, to obtain the Q-y curve for the round pile the F-y curves were subtracted from the p-y curves.

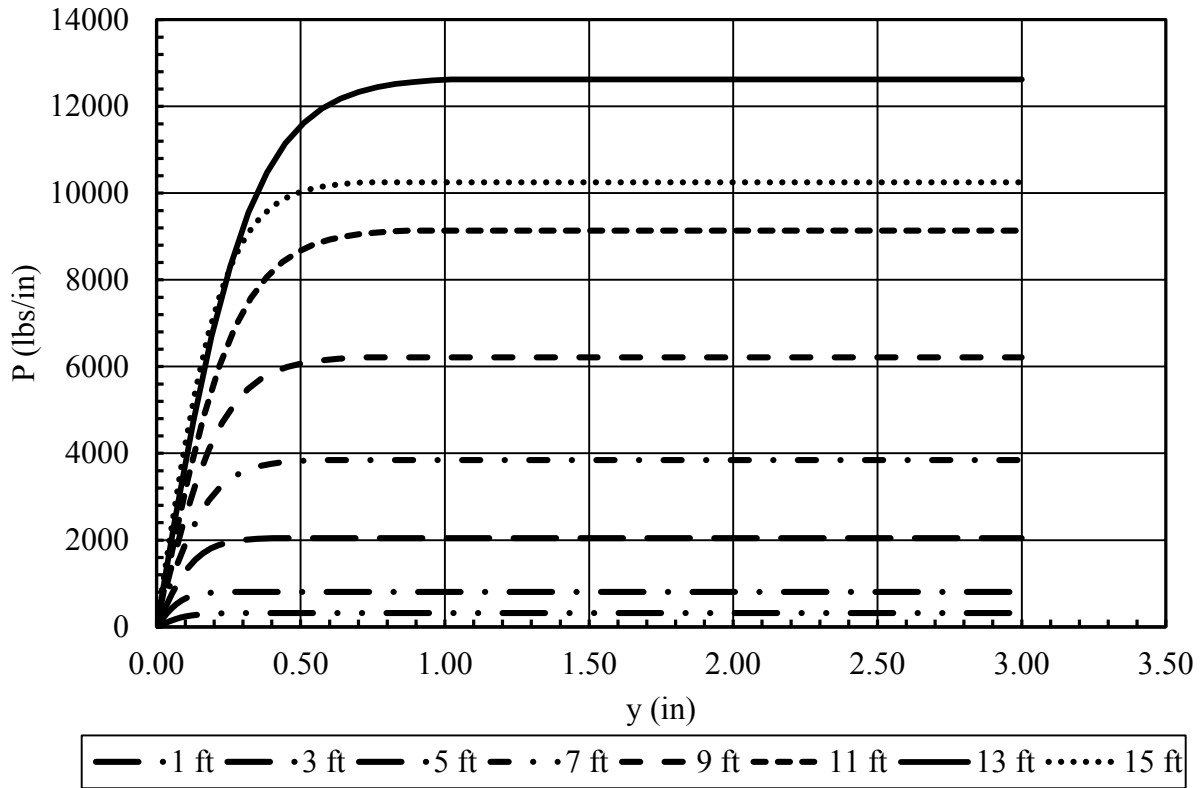


Figure 6-15: P-y Curves at Given Depth (Round pile)

$$F = k\gamma z \tan(\delta)D \tag{6-4}$$

Where,

K = lateral pressure coefficient, 1.00 for API sands,

γ = unit weight of the soil,

z = depth,

δ = shear angle between soil and wall of the pile, $\frac{2}{3}\phi$, and

D = diameter of the pile or width of the non-circular pile

Once Q-y curves were back-calculated from the original p-y curves, the shape factors given by Briaud et al 1983 in (2-2) were used as a ratio to scale up the normal stress (Q) in the

Q-y curves for the round pile to get Q-y curves for the square pile. At that same depth, the friction force (F) in the F-y curves that were computed using (6-4) were multiplied by the ratio of shape factors given in (2-1). For the square pile it was also assumed that the friction developed linearly with displacement of 0.10 inch. Figure 6-16 shows F-y curves for the round and square pile at a depth of 7 ft. It is important to observe the difference between the two, the square pile shows much more side friction than the round.

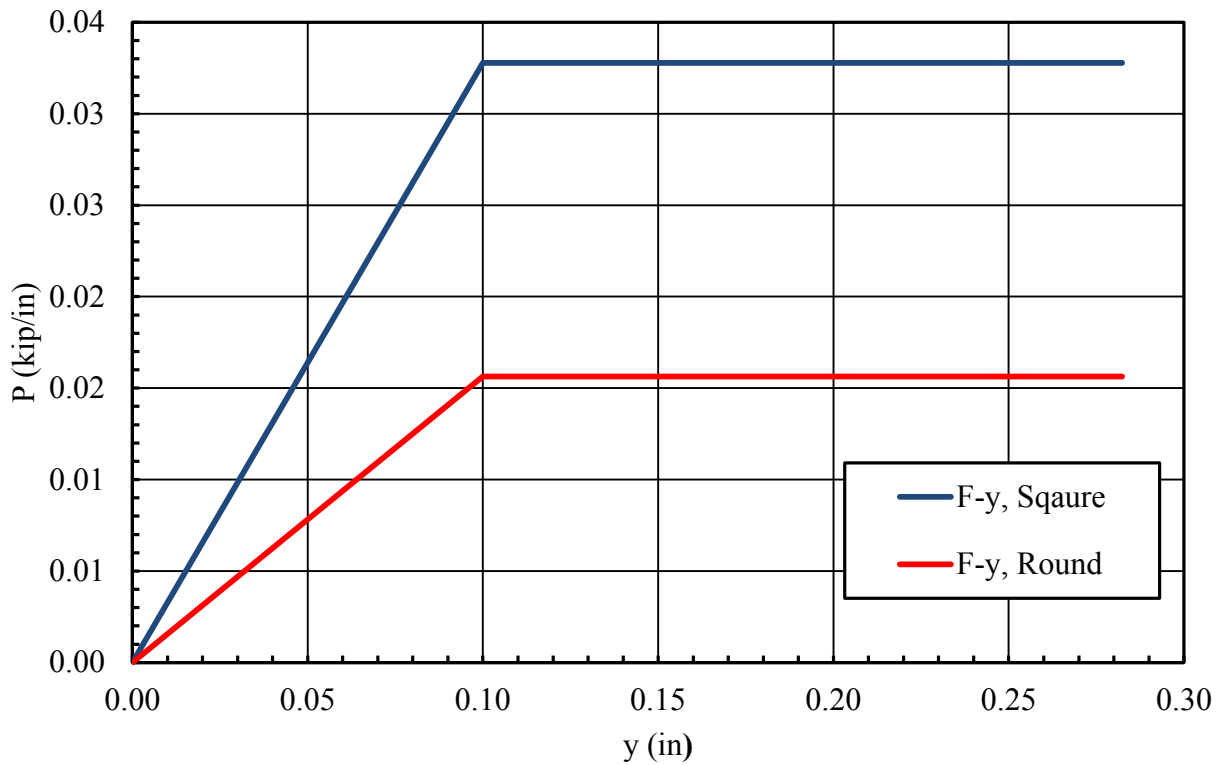


Figure 6-16: F-y Curves for Both Round and Square Piles at a Depth of 7 ft

After computing F-y curves at all given depths for the square pile, the resulting Q-y and F-y were added by following (2-4) to obtain p-y curves for the square pile. It was observed that even though the side friction of the square pile was much higher, the contribution to the overall

resistance was not significant. The normal stresses tend to contribute much more to the lateral resistance according to this analysis. Figure 6-17 intends to replicate Figure 2-1 from Smith (1987), and, by comparison, lead to the conclusion that in this case the side friction is not a major contributor to the overall pile resistance. This analysis also pointed at the fact that as the depth increases the contribution from the side friction to the overall lateral resistance becomes less and less.

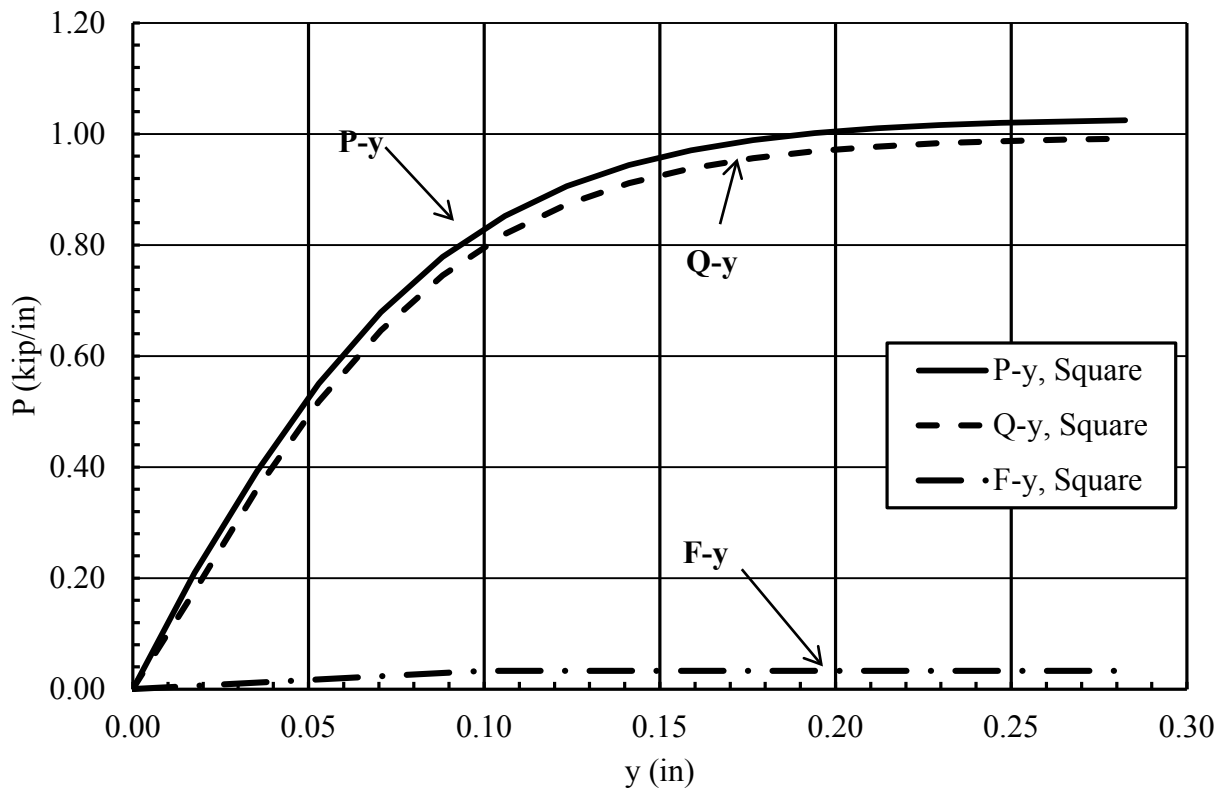


Figure 6-17: Combined $Q-y + F-y = P-y$ Curves for the Square Pile at 1 ft in Depth

Once $P-y$ curves for the square pile were obtained, these curves were then input manually into the computer program LPILE to compute load-deflection curves. It was then possible to compare these computed load-deflection curves to the measured curves from the load test to

determine if this method gave a better prediction than Reese and Van Impe 2001 and the default analysis in LPILE. Figure 6-18 provides a comparison of the measured load-deflection curve with the load-deflection curves computed using the effective width concept and the Smith Q-y + F-y concept. As before, the load-deflection curves computed by LPILE with the actual width and using Reese and Van Impe's effective width (b_{eq}) approach produced insufficient resistance to match the measured curve for the non-circular piles. In contrast, when using the F-y/Q-y mechanism, LPILE predicts a load-deflection curve with more lateral pile resistance than it ought to have relative to the measured curve. The shape factor used in (2-2) and (2-1) may be too high for the square pile, thus, providing conservative design in practice.

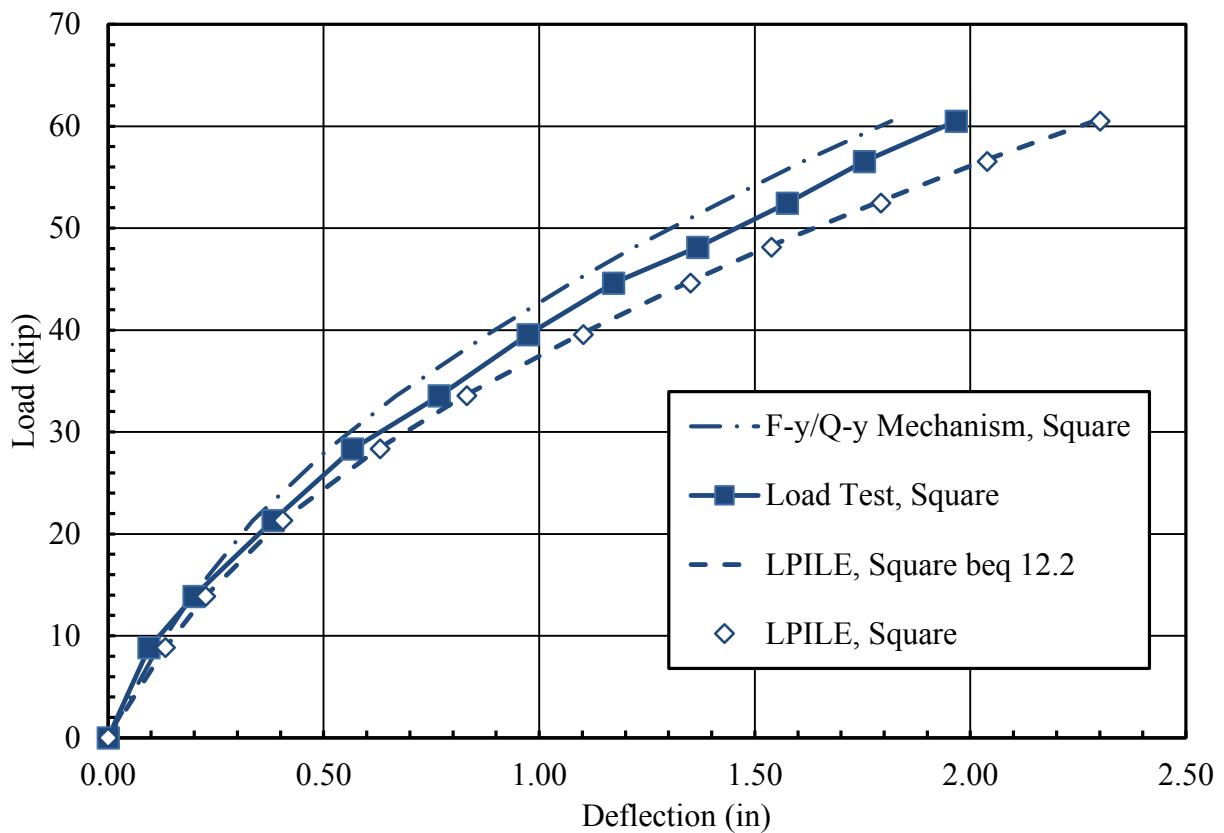


Figure 6-18: Load vs. Deflection Curves for F-y/Q-y Mechanism (Square Pile)

The same procedure was used for analyzing the H pile and comparing the results. Since shape factors for H piles were not proposed by Smith (1987) and Briaud et al (1983), the same shape factors proposed for square piles were used for the H pile. Figure 6-19 shows the predicted load-deflection curve predicted by using the F-y-Q-y mechanism. The difference between this mechanism and the lateral load test measurements was nearly 6% higher, which is better than what LPILE currently will predict for an H pile.

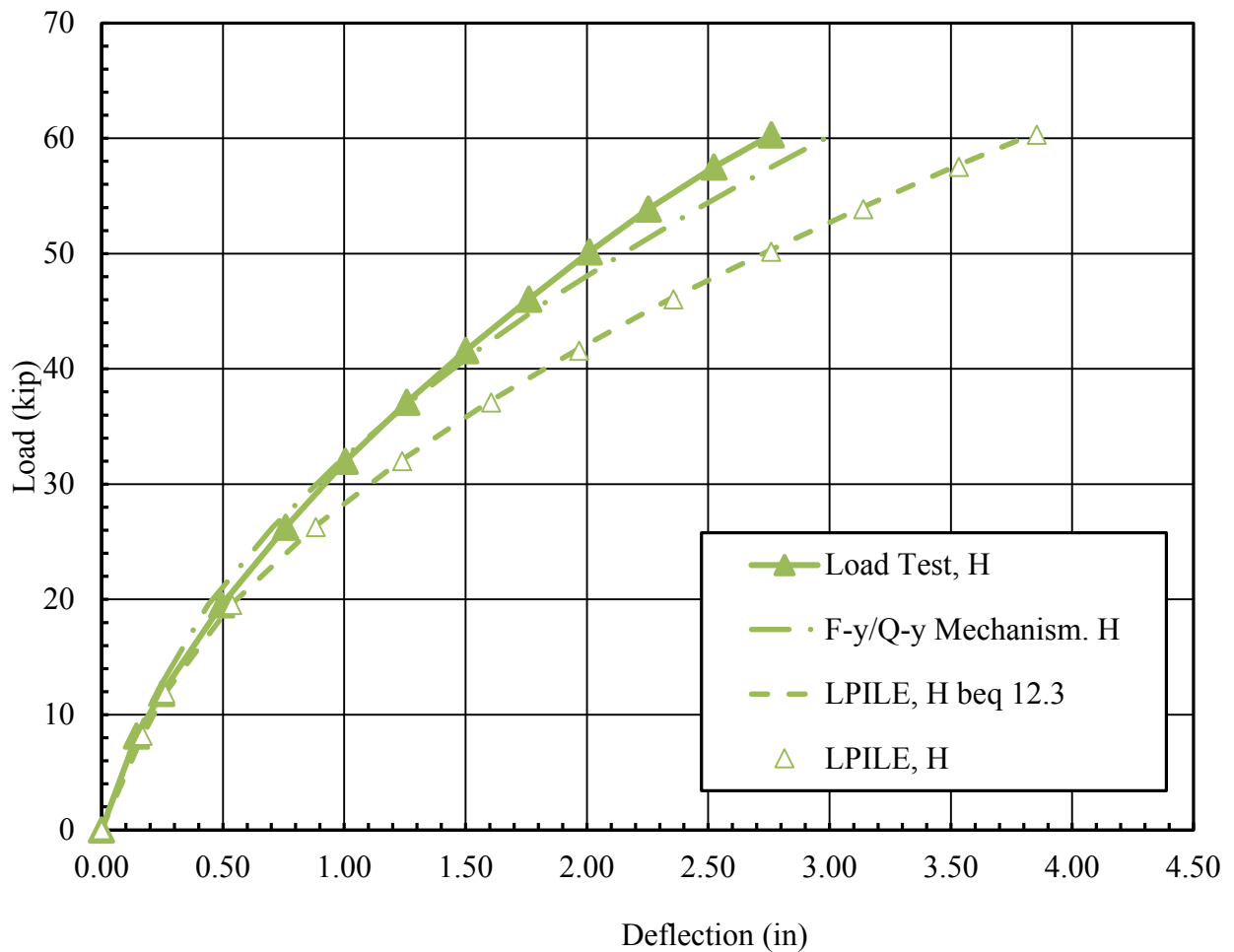


Figure 6-19: Load vs. Deflection Curves for F-y/Q-y Mechanism (H Pile)

6.7 P-multiplier Approach

Increasing the effective width to account for the shape effect as suggested by Reese and Van Impe (2001) was insufficient to account for the increased resistance. The F-y/Q-y mechanism proposed by Briaud and Smith (1983) was also inaccurate and overestimated the lateral resistance when compare to the measured curves. In an attempt to match the computed load-deflection curve to the measured curves, p-multipliers were used for non-circular cross-section piles. P-multipliers simply increased or decreased with depth, to provide a more simplified approach the sand p-multiplier was used along the entire length of the pile.

To provide agreement with the measure response, p-multipliers of 1.2 and 1.35 were required for the square and H piles, respectively. These p-multipliers were simply obtained by trial and error with the LPILE computer program. The analyses suggest that the increased resistance for the square and H pile sections was a result of the increases in both the side shear and normal stress (passive) components of resistance, where the front side was the major contributor. Using back-calculated p-multipliers provided very good agreement between the measured and computed load-deflection curves. Table 6-3 summarizes the p-multipliers used for H and square piles.

Table 6-3: P-multipliers

Pile	P-multiplier
Square	1.20
H	1.35

Figure 6-20 shows measured load-deflection curves along with curves computed using the p-multiplier approach for both square and H piles. Considering that the p-multiplier is a single constant adjustment factor for all depths and displacement levels, the load-deflection curves with the p-multiplier approach agree remarkably well with the measured curves from the test. For the square pile, the computed curve follows the same shape as the measured curve from beginning to end, with perhaps very small variances in the deflection. The p-multiplier approach produced a load-deflection curve for the H pile that agrees very well with the beginning and middle parts of the measured curve but diverges slightly at the end where the difference in deflection is about 0.1 inches for a given load.

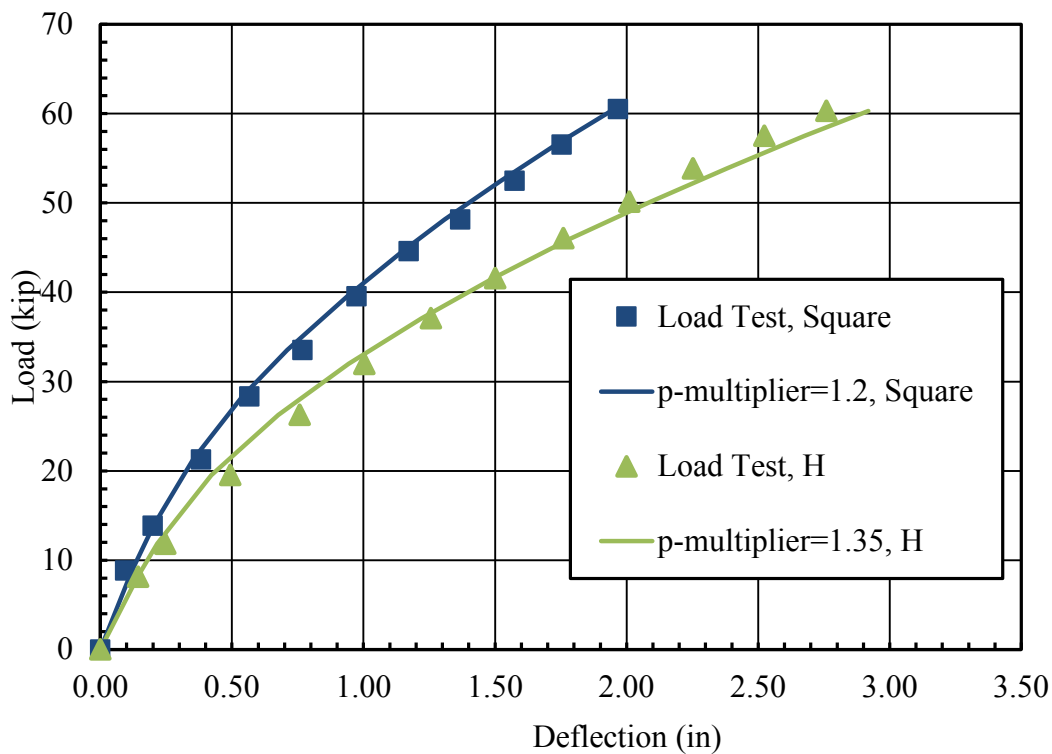


Figure 6-20: Comparison of Measured Load-Deflection Curves with Curves Computed Using P-multiplier Approach for Both Square & H piles

Figure 6-21 shows the computed load-deflection curves for all methods combined into one plot relative to the measured curve and the curve obtained. The p-multiplier approach is clearly the best approach of them all.

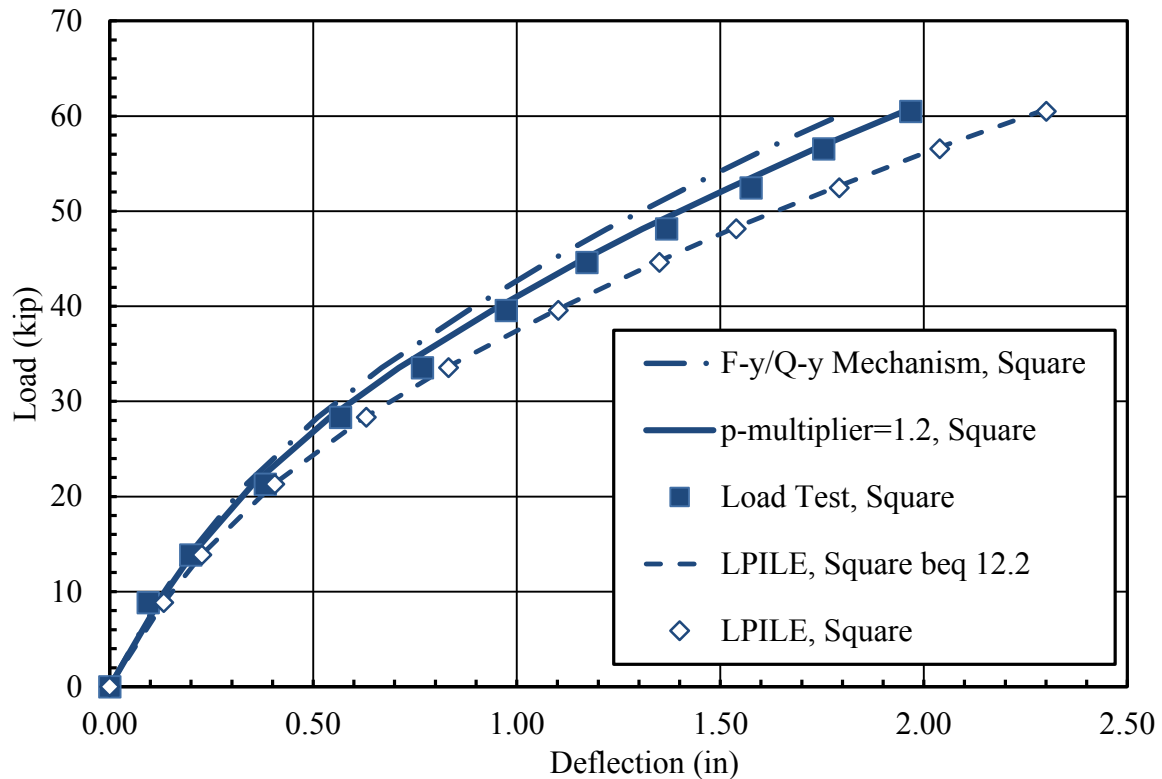


Figure 6-21: Load-Deflection Curve All Approaches Combined (Square)

Given the similarities in the shapes of the H pile and the square pile relative to the circular pile, the back-calculated p-multipliers might be expected to be a little closer to one another. For example, the projected face width and the side shear areas were nearly identical for both pile shapes. Nevertheless, the measured failure wedge for the H pile was clearly wider than for the square pile, but an explanation for this behavior is not immediately apparent.

Considering the small sample size involved in the testing, small variations in the relative compaction around each of the piles may have played some role in the differing response, although efforts were made to ensure that compaction passes were consistently applied. Because of the small set of pile load tests performed, some variations from the measured response might be observed if multiple tests had been performed for each pile type. However, it is instructive to recognize that the load-deflection curves for the two square piles were quite similar which argues for the consistency of the compaction around the test piles. Based on the limited test results at this time it seems reasonable to use a p-multiplier to account for shape effects, however, a lower-bound p-multiplier of 1.2 might be wise until additional test results can be obtained to confirm the results from this series of tests.

6.8 Bending Moment vs. Depth Curves

The computed bending moment vs. depth curves for the square and H piles are shown in Figure 6-22 and Figure 6-23, respectively. These figures include measured the bending moment vs. depth for each pile type along with the curves computed with the p-multiplier approach to be able to compare the performance of the pile using this approach. The computed bending moment curve with the p-multiplier approach shows a lower maximum bending moment relative to the original LPILE model, and the depth at which the maximum bending moment occurs is shifted upward, better matching the depth obtained from the test.

The measured bending moment vs. depth curve for the H pile agrees very nicely from 6 to 10 ft in depth with the curve computed using the P-multiplier approach. The depth of the maximum bending moment aligns better with the measured value and the maximum bending moment is reduced somewhat from the original LPILE curve with a p-multiplier of 1.0.

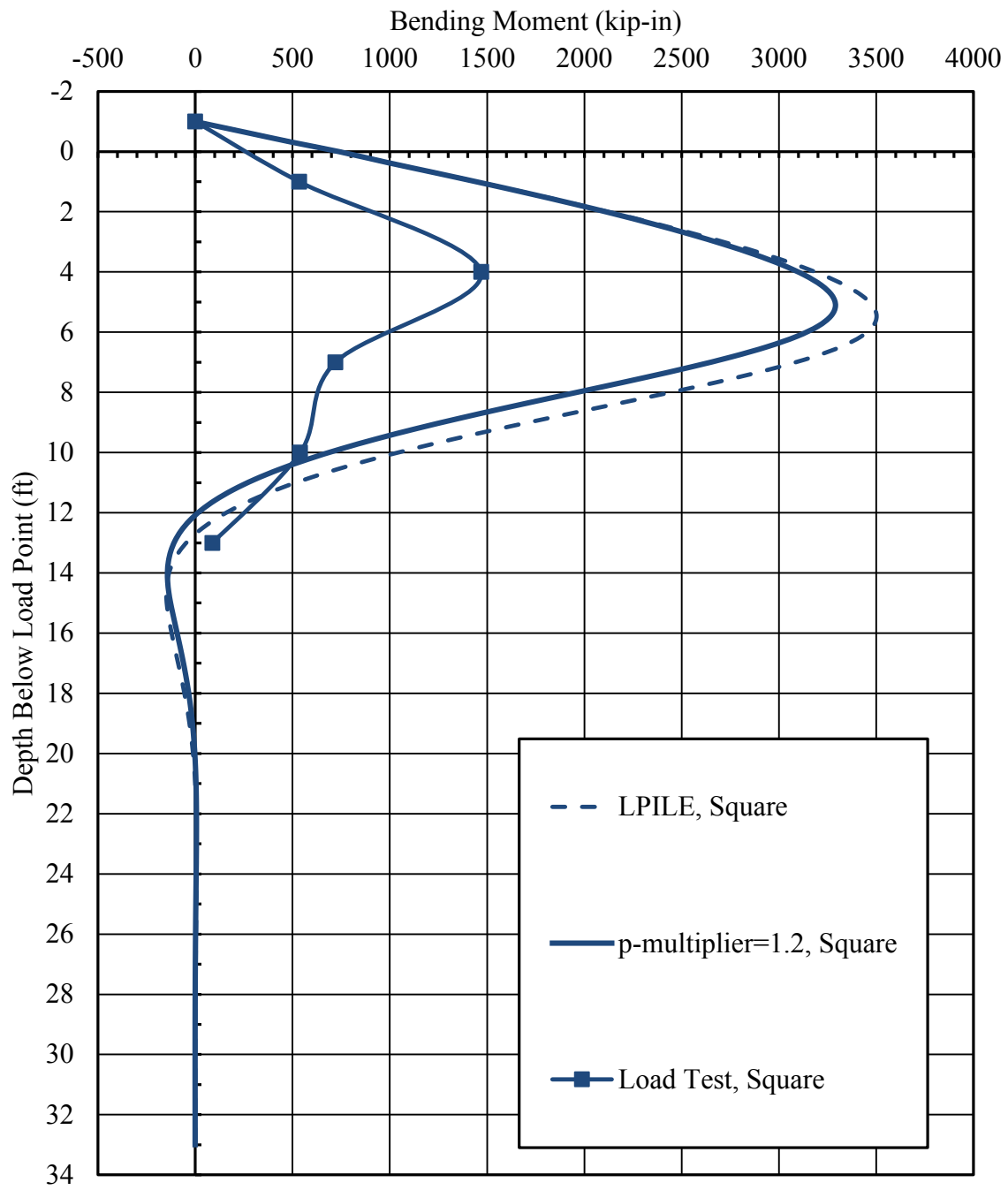


Figure 6-22: Bending Moment vs. Depth Including P-multiplier (Square)

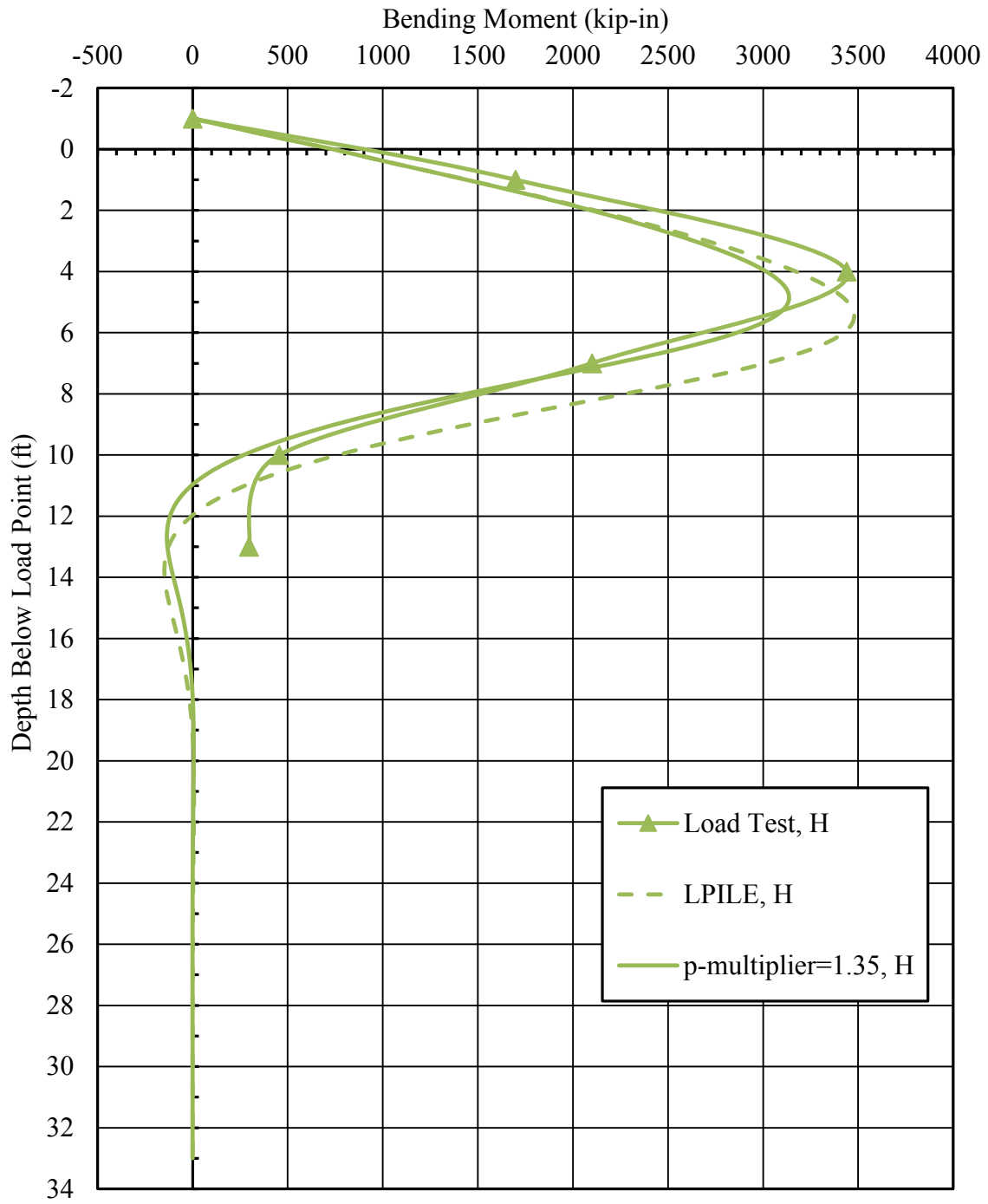


Figure 6-23: Bending Moment vs. Depth Including P-multiplier (H)

7 CONCLUSIONS

7.1 Test Results

1. As theorized by several investigators, full-scale lateral load tests demonstrated that the lateral resistance of square and H piles was greater than that for round piles after accounting for difference in widths and moments of inertia.
2. The measured maximum bending moment for all three different pile cross-sectional shapes occurred at a depth of about 4 ft below the ground level.
3. The H and round pile experienced somewhat higher bending moments relative to the square pile for a given pile head load.
4. Lateral loading of the H pile produced the greatest soil heave among the three different pile cross-sections. The major concentration of heave was in front part of the flanges. Lateral loading of the square pile produced the least heave of all the pile types.
5. Shear planes for the square and H pile sections were distinct and flared out linearly from the edges of the front face in contrast to those for the pipe pile where shear planes were more diffused.
6. The H and square pile experienced a wedge type of failure in the soil, with the H pile showing the longest cracks and wider failure angles, up to 45° . In contrast, the round pile exhibited an elliptical type of failure in the soil in front of the pile.

7.2 Lateral Load Analysis

1. Using the recommended API friction angle and the soil stiffness values produced much softer load-deflection curves than what was measured; thus, the friction angle and the soil stiffness used in the analyses were values back-calculated with LPILE that have the best agreement with the test data.
2. Increasing the effective width of the square pile to account for the shape effects as suggested by Reese and Van Impe (2001) was insufficient to account for the increased resistance. In contrast, accounting for the increased contribution of side friction and normal stress based on shape factors proposed by Briaud and Smith over-estimated the measured resistance. However, the Briaud and Smith approach produced reasonable agreement for the H pile.
3. The analyses suggest that the increased resistance for the square and H pile sections was a result of increases in both the side friction and normal stress components of resistance, not simply the side friction.
4. Even though side friction it is a contributor to the lateral resistance of the pile, it is not the major contributor. The normal stress contributes the most to the lateral resistance of the piles, which indicates a more uniform normal stress distribution on the square pile than on a circular pile.
5. P-multipliers of 1.2 and 1.35 for the square and H piles, respectively were required to provide agreement with the measured response. This simple approach was also capable of producing reasonable predictions of the measured bending moment vs. depth curves.

7.3 Recommendation For Future Research

1. To confirm the results obtained from this investigation, it would be very desirable to perform additional lateral load tests on piles with different shapes. These tests should make it possible to obtain average values of p -multipliers to account for the soil resistance around different pile shapes.
2. It will be appropriate to conduct lateral load tests on H piles loaded perpendicular to the flange (strong-axis) to determine the influence on its resistance. While the EI for the two directions of loading will be different, the soil resistance may not be substantially different because the width is about the same in each direction.

REFERENCE

- American Petroleum Institute (API) (1982) “API recommended practice for planning, designing and constructing fixed offshore platforms”, API RP 2A, 13th Edition.
- Briaud, J. L.; Smith, T. D. and Meyer, B.J. (1983). “Laterally Loaded Piles and the Pressuremeter: Comparison of Existing Methods”, *ASTM Special Technical Publication STP 835 on the Design and performance of laterally loaded piles and Pile Groups*, June.
- Briaud, J. L., Smith, T. D., and Meyer, B. J. (1983), “Using the Pressuremeter Curve to Design Laterally Loaded Piles.” *Proceedings of Annual Offshore Technology Conference*, Vol. 8, p. 495-502.
- Brown, D.A., Morrison, C., and Reese, L.C., (1988). "Lateral load behavior of a pile group in sand." *J. Geotech. Geoenviron. Eng.*, ASCE, 114(11), 1261-1276.
- Filtz, G. M., Arenas, A. E., Cousins, T. E., (2013). “Thermal Response of Integral Abutment Bridges with Mechanically Stabilized Earth Walls” *VCTIR 13-R7*.
- Lee, K. L., and Singh, A. (1971). "Relative Density and Relative Compaction." *Journal of Soil Mechanics and Foundations Design*, 97(7), 1049-1052.
- Matlock, H., and Reese, L.C. (1960). “Generalized Solutions for Laterally Loaded Piles” *Journal of the Soil Mechanics and Foundation Division*, ASCE 86(SM5)1:63-91.
- Mohamed, A., Norris, G., (2000), “Modeling Lateral Soil-Pile Response Based on Soil-Pile Interaction”, *J. Geotech. Geoenviron. Eng.*, 2000, 126(5), pp. 420–428.
- Reese, L. C., and Van Impe, W. F. (2001), “Single Piles and Pile Group under Lateral Loading”, *A. A. Balkema*, Rotterdam, Netherlands.
- Reese, L.C., Wang, S.T., Isenhower, W.M., and Arrellaga, J.A. (2004). “LPILE Plus v5.0 for Windows: A program for the analysis of piles and drilled shafts under lateral loads” Technical Manual, Ensoft, Inc, Austin, TX.

- Rollins, K.M., Lane, J.D., Gerber, T. M. (2005) "Measured and Computed Lateral Response of a Pile Group in Sand." *J. Geotechnical and Geoenvironmental Engrg.*, ASCE Vol. 131, No. 1, p. 103-114.
- Rollins, K.M., Price, J.S., and Bischoff, J. (2011). "Lateral Resistance of Piles Near Vertical MSE Abutment Walls." *Procs. GeoFrontiers 2011 Advances in Geotechnical Engineering, Geotech.* Special Pub. No. 211, ASCE, p. 3526-3535.
- Smith, T. D., (1987), "Side Friction Mobilization F-y Curves for Laterally Loaded Piles from the Pressuremeter," *Prediction and Performance in Geotechnical Engineering: Proceedings of the International Symposium*, p. 89-95, Calgary, June.
- Smith, T. D., Sylh, R. (1986), "Side Friction Mobilization Rates for Laterally Loaded Piles from the Pressuremeter," *The Pressuremeter and Its Marine Applications: Second International Symposium ASTM*, STP 950, J.L. Briaud and J.M.E. Audibert, Eds., American Society for Testing and Materials.

APPENDIX A. REESE AND VAN IMPE

γ' 7.5E-05 *k/in³*
 ϕ 45 *deg*
 0.7ϕ 31.5 *deg*
K 1.00 *API*
C₁ 7.3
C₂ 5.7
C₃ 211.4

			Square				H				
x	x	f_z	P_{us}	P_{ud}	P_{uc}	b_{eq}	P_{us}	P_{ud}	P_{uc}	b_{eq}	
ft	in	k/in ²	k/in	k/in	k/in	in	k/in	k/in	k/in	in	
1	12	0.001	0.14	2.27	0.14	12.6	0.14	2.29	0.14	12.7	
2	24	0.001	0.43	4.55	0.43	12.4	0.44	4.58	0.44	12.5	
3	36	0.002	0.89	6.82	0.89	12.3	0.89	6.87	0.89	12.4	
4	48	0.002	1.50	9.09	1.50	12.2	1.50	9.17	1.50	12.3	
5	60	0.003	2.26	11.36	2.26	12.2	2.26	11.46	2.26	12.3	
6	72	0.003	3.18	13.64	3.18	12.1	3.19	13.75	3.19	12.3	
7	84	0.004	4.26	15.91	4.26	12.1	4.27	16.04	4.27	12.2	
8	96	0.004	5.50	18.18	5.50	12.1	5.50	18.33	5.50	12.2	
9	108	0.005	6.89	20.45	6.89	12.1	6.90	20.62	6.90	12.2	
10	120	0.005	8.44	22.73	8.44	12.1	8.45	22.92	8.45	12.2	
11	132	0.006	10.15	25.00	10.15	12.1	10.15	25.21	10.15	12.2	
12	144	0.007	12.01	27.27	12.01	12.1	12.01	27.50	12.01	12.2	
13	156	0.007	14.03	29.54	14.03	12.1	14.03	29.79	14.03	12.2	
14	168	0.008	16.20	31.82	16.20	12.1	16.21	32.08	16.21	12.2	
15	180	0.008	18.54	34.09	18.54	12.1	18.54	34.37	18.54	12.2	
Avg =						12.2	Avg =				12.3

APPENDIX B. F-Y/Q-Y MECHANISM

γ 7.5E-05 *k/in³*
 ϕ 45 *deg*
 0.7ϕ 30 *deg*
 K 1.00 *API*

Shape Factor	
Briaud & Smith	1.33
Square	

Depth 1 ft <--- Drop Down Menu for Depth

P kip/in	y in	z in	z in	F _f kip/in	Q kip/in	F _f kip/in	Q kip/in	P kip/in
0.00	0.00	12.00	1.00	0.01	0.00	0.01	0.00	0.00
0.06	0.02	24.00	2.00	0.01	0.06	0.02	0.07	0.08
0.12	0.04	36.00	3.00	0.02	0.11	0.03	0.14	0.16
0.17	0.06	48.00	4.00	0.02	0.16	0.04	0.21	0.22
0.21	0.08	60.00	5.00	0.03	0.21	0.05	0.26	0.27
0.24	0.11	72.00	6.00	0.03	0.24	0.07	0.30	0.31
0.27	0.13	84.00	7.00	0.04	0.26	0.08	0.33	0.34
0.28	0.15	96.00	8.00	0.04	0.28	0.09	0.35	0.36
0.29	0.17	108.00	9.00	0.05	0.29	0.10	0.36	0.37
0.30	0.19	120.00	10.00	0.05	0.30	0.11	0.37	0.38
0.31	0.21	132.00	11.00	0.06	0.30	0.12	0.38	0.39
0.31	0.23	144.00	12.00	0.06	0.31	0.13	0.39	0.40
0.32	0.25	156.00	13.00	0.07	0.31	0.14	0.39	0.40
0.32	0.27	168.00	14.00	0.07	0.31	0.15	0.39	0.40
0.32	0.29	180.00	15.00	0.08	0.31	0.16	0.39	0.40
0.32	0.32	192.00	16.00	0.08	0.31	0.17	0.39	0.41
0.32	0.34	204.00	17.00	0.09	0.31	0.19	0.40	0.41

γ 7.5E-05 k/in³
 ϕ 45 deg
 0.7ϕ 30 deg
 K 1.00 API

Shape Factor	
Briaud & Smith	1.33
H	

Depth 1 ft <--- Drop Down Menu for Depth

P kip/in	y in	z in	z in	F _f kip/in	Q kip/in	F _f kip/in	Q kip/in	P kip/in
0.00	0.00	12.00	1.00	0.00	0.00	0.01	0.00	0.00
0.06	0.02	24.00	2.00	0.01	0.06	0.02	0.08	0.09
0.12	0.04	36.00	3.00	0.02	0.12	0.03	0.15	0.16
0.17	0.06	48.00	4.00	0.02	0.17	0.04	0.22	0.23
0.21	0.08	60.00	5.00	0.03	0.21	0.06	0.27	0.28
0.24	0.11	72.00	6.00	0.03	0.24	0.07	0.31	0.32
0.27	0.13	84.00	7.00	0.04	0.27	0.08	0.34	0.35
0.28	0.15	96.00	8.00	0.04	0.28	0.09	0.36	0.37
0.29	0.17	108.00	9.00	0.05	0.29	0.10	0.37	0.38
0.30	0.19	120.00	10.00	0.05	0.30	0.11	0.38	0.39
0.31	0.21	132.00	11.00	0.06	0.31	0.12	0.39	0.40
0.31	0.23	144.00	12.00	0.06	0.31	0.13	0.40	0.41
0.32	0.25	156.00	13.00	0.07	0.32	0.14	0.40	0.41
0.32	0.27	168.00	14.00	0.07	0.32	0.15	0.40	0.41
0.32	0.29	180.00	15.00	0.08	0.32	0.17	0.40	0.41
0.32	0.32	192.00	16.00	0.08	0.32	0.18	0.40	0.42
0.32	0.34	204.00	17.00	0.09	0.32	0.19	0.40	0.42

APPENDIX C. LPILE – ROUND PILE

The analyses performed in LPILE for each pile tested is available upon request. They have not been included in the appendix to avoid excessive information.

```
=====
LPILE Plus for windows, Version 2013-07.007
Analysis of Individual Piles and Drilled Shafts
Subjected to Lateral Loading Using the p-y Method
© 1985-2013 by Ensoft, Inc.
All Rights Reserved
=====
```

This copy of LPILE is used by:

Guillermo Bustamante
BYU

Serial Number of Security Device: 291911493
This copy of LPILE is licensed for exclusive use by: BYU, Provo, UT

Use of this program by any entity other than BYU, Provo, UT
is forbidden by the software license agreement.

```
-----
Files Used for Analysis
-----
```

```
Path to file locations: \\fs-caedm.et.byu.edu\homes\caedm\My Documents\LPILE
Analysis\TEST 2 - Round vs Square\Round\
Name of input data file: Pile Round - 1 min f45 k250 (USCS units).lp7d
Name of output report file: Pile Round - 1 min f45 k250 (USCS units).lp7o
Name of plot output file: Pile Round - 1 min f45 k250 (USCS units).lp7p
Name of runtime message file: Pile Round - 1 min f45 k250 (USCS units).lp7r
```

```
-----
Date and Time of Analysis
-----
```

Date: November 15, 2014 Time: 16:07:07

```
-----
Problem Title
-----
```

Project Name:
Job Number:
Client:
Engineer:
Description:

```
-----
Program Options and Settings
-----
```

Engineering Units of Input Data and Computations:

- Engineering units are US Customary Units (pounds, feet, inches)

Analysis Control Options:

- Maximum number of iterations allowed = 500
- Deflection tolerance for convergence = 1.0000E-05 in
- Maximum allowable deflection = 100.0000 in
- Number of pile increments = 100

Loading Type and Number of Cycles of Loading:

- Static loading specified

Computational Options:

- Use unfactored loads in computations (conventional analysis)
- Compute pile response under loading and nonlinear bending properties of pile (only if nonlinear pile properties are input)
- Use of p-y modification factors for p-y curves not selected
- Loading by lateral soil movements acting on pile not selected
- Input of shear resistance at the pile tip not selected
- Computation of pile-head foundation stiffness matrix not selected
- Push-over analysis of pile not selected
- Buckling analysis of pile not selected

Output Options:

- No p-y curves to be computed and reported for user-specified depths
- Values of pile-head deflection, bending moment, shear force, and soil reaction are printed for full length of pile.
- Printing increment (nodal spacing of output points) = 1

Pile Structural Properties and Geometry

Total number of pile sections = 1
Total length of pile = 34.00 ft
Depth of ground surface below top of pile = 1.00 ft

Pile diameter values used for p-y curve computations are defined using 2 points.

p-y curves are computed using pile diameter values interpolated with depth over the length of the pile.

Point	Depth X ft	Pile Diameter in
1	0.00000	12.7500000
2	34.000000	12.7500000

Input Structural Properties:

Pile Section No. 1:

Section Type = Elastic Pile
Cross-sectional Shape = Circular Pipe
Section Length = 34.00000 ft
Top Width = 12.75000 in
Bottom Width = 12.75000 in
Wall Thickness at Top = 0.34900 in
Wall Thickness at Bottom = 0.34900 in
Top Area = 14.57895 Sq. in
Bottom Area = 14.57895 Sq. in
Moment of Inertia at Top = 314.00000 in⁴
Moment of Inertia at Bottom = 314.00000 in⁴
Elastic Modulus = 29000000. lbs/in²

Ground Slope and Pile Batter Angles

Ground Slope Angle = 0.000 degrees
= 0.000 radians

Pile Batter Angle = 0.000 degrees
 = 0.000 radians

 Soil and Rock Layering Information

The soil profile is modelled using 2 layers

Layer 1 is sand, p-y criteria by API RP-2A, 1987

Distance from top of pile to top of layer = 1.00000 ft
 Distance from top of pile to bottom of layer = 16.00000 ft
 Effective unit weight at top of layer = 129.00000 pcf
 Effective unit weight at bottom of layer = 129.00000 pcf
 Friction angle at top of layer = 45.00000 deg.
 Friction angle at bottom of layer = 45.00000 deg.
 Subgrade k at top of layer = 250.00000 pci
 Subgrade k at bottom of layer = 250.00000 pci

Layer 2 is sand, p-y criteria by API RP-2A, 1987

Distance from top of pile to top of layer = 16.00000 ft
 Distance from top of pile to bottom of layer = 34.00000 ft
 Effective unit weight at top of layer = 125.00000 pcf
 Effective unit weight at bottom of layer = 125.00000 pcf
 Friction angle at top of layer = 34.00000 deg.
 Friction angle at bottom of layer = 34.00000 deg.
 Subgrade k at top of layer = 100.00000 pci
 Subgrade k at bottom of layer = 100.00000 pci

(Depth of lowest soil layer extends 0.00 ft below pile tip)

 Summary of Soil Properties

Layer Num.	Layer Soil Type (p-y Curve Criteria)	Layer Depth ft	Effective Unit Wt. pcf	Angle of Friction deg.	kpy pci
1	API Sand	1.000	129.000	45.000	250.000
		16.000	129.000	45.000	250.000
2	API Sand	16.000	125.000	34.000	100.000
		34.000	125.000	34.000	100.000

 Loading Type

Static loading criteria were used when computing p-y curves for all analyses.

 Pile-head Loading and Pile-head Fixity Conditions

Number of loads specified = 11

Load No.	Load Type	Condition 1	Condition 2	Axial Thrust Force, lbs	Compute Top y vs. Pile
1	1	V = 9500.00000 lbs	M = 0.0000 in-lbs	0.0000000	No
2	1	V = 15900. lbs	M = 0.0000 in-lbs	0.0000000	No
3	1	V = 23100. lbs	M = 0.0000 in-lbs	0.0000000	No
4	1	V = 30400. lbs	M = 0.0000 in-lbs	0.0000000	No
5	1	V = 35100. lbs	M = 0.0000 in-lbs	0.0000000	No
6	1	V = 42000. lbs	M = 0.0000 in-lbs	0.0000000	No

7	1	V =	47600. lbs	M =	0.0000 in-lbs	0.0000000	NO
8	1	V =	50200. lbs	M =	0.0000 in-lbs	0.0000000	NO
9	1	V =	54800. lbs	M =	0.0000 in-lbs	0.0000000	NO
10	1	V =	59200. lbs	M =	0.0000 in-lbs	0.0000000	NO
11	1	V =	63500. lbs	M =	0.0000 in-lbs	0.0000000	NO

V = perpendicular shear force applied to pile head
M = bending moment applied to pile head
y = lateral deflection relative to pile axis
S = pile slope relative to original pile batter angle
R = rotational stiffness applied to pile head
Axial thrust is assumed to be acting axially for all pile batter angles.

Computation of Nominal Moment Capacity and Nonlinear Bending Stiffness

Axial thrust force values were determined from pile-head loading conditions

Number of Pile Sections Analyzed = 1

Pile Section No. 1:

Moment-curvature properties were derived from elastic section properties

Computed Values of Pile Loading and Deflection
for Lateral Loading for Load Case Number 1

Pile-head conditions are Shear and Moment (Loading Type 1)

Shear force at pile head = 9500.0 lbs
Applied moment at pile head = 0.0 in-lbs
Axial thrust load on pile head = 0.0 lbs

Depth Distrib.	Deflect. y	Bending Moment	Shear Force	Slope S	Total Stress	Bending Stiffness	Soil Res. p	Soil Spr. Es*h
X Lat. Load feet lb/inch	inches	in-lbs	lbs	radians	psi*	lb-in ²	lb/in	lb/inch
0.000	0.000	-6.073E-08	9500.0000	-0.002703	1.233E-09	9.106E+09	0.000	
0.000	0.340	38760.	9500.0000	-0.002694	786.9268	9.106E+09	0.000	
0.000	0.680	77520.	9500.0000	-0.002668	1573.8535	9.106E+09	0.000	
131.0923	1.020	116280.	9492.4037	-0.002624	2360.7803	9.106E+09	-3.7237	
2994.3051	1.360	154978.	9327.1704	-0.002564	3146.4485	9.106E+09	-77.2730	
6629.1556	1.700	192390.	8854.7374	-0.002486	3906.0013	9.106E+09	-154.3118	
10620.	2.040	227233.	8088.5546	-0.002392	4613.4022	9.106E+09	-221.2681	
14756.	2.380	258392.	7080.4377	-0.002283	5246.0223	9.106E+09	-272.9069	
18934.	2.720	285009.	5895.3098	-0.002161	5786.4097	9.106E+09	-308.0382	
23093.	3.060	306498.	4599.2872	-0.002029	6222.6912	9.106E+09	-327.2670	
27183.	3.400	322539.	3254.5106	-0.001888	6548.3681	9.106E+09	-331.9372	
31122.	3.740	333055.	1917.3490	-0.001741	6761.8620	9.106E+09	-323.5342	
35914.	4.080	338185.	617.7877	-0.001591	6866.0130	9.106E+09	-313.5057	
40687.	4.420	338096.	-620.5818	-0.001439	6864.2102	9.106E+09	-293.5382	
45284.	4.760	333121.	-1759.9322	-0.001289	6763.2019	9.106E+09	-264.9668	

5.100	0.0189	323735.	-2771.0115	-0.001142	6572.6443	9.106E+09	-230.6603
49742.	0.000						
5.440	0.0146	310509.	-3635.3226	-0.000999	6304.1318	9.106E+09	-193.0216
54096.	0.000						
5.780	0.0108	294071.	-4343.2691	-0.000864	5970.3848	9.106E+09	-154.0110
58377.	0.000						
6.120	0.007507	275068.	-4892.4640	-0.000737	5584.5876	9.106E+09	-115.2022
62609.	0.000						
6.460	0.004754	254148.	-5286.2680	-0.000618	5159.8562	9.106E+09	-77.8389
66807.	0.000						
6.800	0.002465	231932.	-5532.5379	-0.000509	4708.8180	9.106E+09	-42.8816
70986.	0.000						
7.140	0.000600	209003.	-5642.5474	-0.000410	4243.2874	9.106E+09	-11.0447
75153.	0.000						
7.480	-0.000883	185889.	-5630.0460	-0.000322	3774.0240	9.106E+09	17.1728
79314.	0.000						
7.820	-0.002027	163062.	-5510.4318	-0.000244	3310.5645	9.106E+09	41.4615
83473.	0.000						
8.160	-0.002872	140924.	-5300.0273	-0.000176	2861.1175	9.106E+09	61.6779
87632.	0.000						
8.500	-0.003459	119813.	-5015.4481	-0.000117	2432.5154	9.106E+09	77.8217
91790.	0.000						
8.840	-0.003828	99998.	-4673.0652	-6.790E-05	2030.2142	9.106E+09	90.0131
95950.	0.000						
9.180	-0.004013	81681.	-4288.5569	-2.720E-05	1658.3343	9.106E+09	98.4714
100111.	0.000						
9.520	-0.004049	65003.	-3876.5493	5.662E-06	1319.7342	9.106E+09	103.4931
104273.	0.000						
9.860	-0.003967	50048.	-3450.3434	3.144E-05	1016.1111	9.106E+09	105.4314
108435.	0.000						
10.200	-0.003793	36849.	-3021.7231	5.090E-05	748.1200	9.106E+09	104.6767
112598.	0.000						
10.540	-0.003552	25391.	-2600.8384	6.485E-05	515.5059	9.106E+09	101.6393
116761.	0.000						
10.880	-0.003264	15626.	-2196.1574	7.404E-05	317.2422	9.106E+09	96.7337
120924.	0.000						
11.220	-0.002947	7470.5466	-1814.4760	7.921E-05	151.6711	9.106E+09	90.3650
125087.	0.000						
11.560	-0.002617	819.6106	-1460.9787	8.107E-05	16.6402	9.106E+09	82.9180
129250.	0.000						
11.900	-0.002286	-4451.0394	-1139.3392	8.025E-05	90.3674	9.106E+09	74.7484
133413.	0.000						
12.240	-0.001963	-8477.3971	-851.8519	7.736E-05	172.1128	9.106E+09	66.1767
137575.	0.000						
12.580	-0.001655	-11402.	-599.5850	7.290E-05	231.4927	9.106E+09	57.4835
141738.	0.000						
12.920	-0.001368	-13370.	-382.5476	6.735E-05	271.4453	9.106E+09	48.9074
145900.	0.000						
13.260	-0.001105	-14524.	-199.8615	6.111E-05	294.8689	9.106E+09	40.6446
150062.	0.000						
13.600	-0.000869	-15001.	-49.9330	5.449E-05	304.5561	9.106E+09	32.8497
154224.	0.000						
13.940	-0.000660	-14931.	69.3814	4.779E-05	303.1413	9.106E+09	25.6378
158385.	0.000						
14.280	-0.000479	-14435.	160.6213	4.121E-05	293.0618	9.106E+09	19.0877
162547.	0.000						
14.620	-0.000324	-13621.	226.5817	3.492E-05	276.5313	9.106E+09	13.2459
166709.	0.000						
14.960	-0.000194	-12586.	270.1902	2.905E-05	255.5242	9.106E+09	8.1308
170870.	0.000						
15.300	-8.712E-05	-11416.	294.4014	2.367E-05	231.7692	9.106E+09	3.7375
175032.	0.000						
15.640	-9.652E-07	-10184.	302.1124	1.884E-05	206.7511	9.106E+09	0.0424
179194.	0.000						
15.980	6.657E-05	-8950.5344	296.0955	1.455E-05	181.7187	9.106E+09	-2.9918
183355.	0.000						
16.320	0.000118	-7767.3664	283.7075	1.080E-05	157.6973	9.106E+09	-3.0807
106744.	0.000						
16.660	0.000155	-6635.4809	269.0359	7.577E-06	134.7172	9.106E+09	-4.1113
108409.	0.000						
17.000	0.000180	-5572.0333	250.7656	4.842E-06	113.1265	9.106E+09	-4.8448
110073.	0.000						
17.340	0.000194	-4589.2336	230.0304	2.565E-06	93.1731	9.106E+09	-5.3196
111738.	0.000						
17.680	0.000201	-3694.9854	207.8092	7.095E-07	75.0176	9.106E+09	-5.5732
113403.	0.000						
18.020	0.000200	-2893.5101	184.9317	-7.665E-07	58.7456	9.106E+09	-5.6414
115067.	0.000						

18.360	0.000194	-2185.9431	162.0853	-1.904E-06	44.3802	9.106E+09	-5.5578
116732.	0.000						
18.700	0.000184	-1570.8939	139.8260	-2.746E-06	31.8931	9.106E+09	-5.3536
118396.	0.000						
19.040	0.000172	-1044.9632	118.5884	-3.332E-06	21.2154	9.106E+09	-5.0570
120061.	0.000						
19.380	0.000157	-603.2126	98.6985	-3.701E-06	12.2468	9.106E+09	-4.6930
121726.	0.000						
19.720	0.000142	-239.5831	80.3860	-3.890E-06	4.8641	9.106E+09	-4.2838
123390.	0.000						
20.060	0.000126	52.7371	63.7964	-3.932E-06	1.0707	9.106E+09	-3.8484
125055.	0.000						
20.400	0.000110	280.9958	49.0040	-3.857E-06	5.7049	9.106E+09	-3.4028
126720.	0.000						
20.740	9.408E-05	452.6096	36.0230	-3.693E-06	9.1891	9.106E+09	-2.9604
128384.	0.000						
21.080	7.943E-05	574.9432	24.8190	-3.463E-06	11.6728	9.106E+09	-2.5317
130049.	0.000						
21.420	6.583E-05	655.1326	15.3192	-3.187E-06	13.3009	9.106E+09	-2.1250
131714.	0.000						
21.760	5.342E-05	699.9480	7.4216	-2.884E-06	14.2107	9.106E+09	-1.7464
133378.	0.000						
22.100	4.230E-05	715.6928	1.0031	-2.566E-06	14.5304	9.106E+09	-1.3999
135043.	0.000						
22.440	3.248E-05	708.1336	-4.0728	-2.247E-06	14.3769	9.106E+09	-1.0883
136708.	0.000						
22.780	2.396E-05	682.4586	-7.9504	-1.936E-06	13.8556	9.106E+09	-0.8125
138372.	0.000						
23.120	1.668E-05	643.2585	-10.7760	-1.639E-06	13.0598	9.106E+09	-0.5726
140037.	0.000						
23.460	1.058E-05	594.5268	-12.6939	-1.362E-06	12.0704	9.106E+09	-0.3676
141701.	0.000						
23.800	5.572E-06	539.6761	-13.8432	-1.107E-06	10.9568	9.106E+09	-0.1958
143366.	0.000						
24.140	1.547E-06	481.5660	-14.3548	-8.787E-07	9.7770	9.106E+09	-0.0550
145031.	0.000						
24.480	-1.598E-06	422.5406	-14.3498	-6.761E-07	8.5787	9.106E+09	0.0575
146695.	0.000						
24.820	-3.970E-06	364.4716	-13.9381	-4.998E-07	7.3997	9.106E+09	0.1444
148360.	0.000						
25.160	-5.677E-06	308.8059	-13.2177	-3.490E-07	6.2695	9.106E+09	0.2087
150025.	0.000						
25.500	-6.818E-06	256.6148	-12.2748	-2.223E-07	5.2099	9.106E+09	0.2535
151689.	0.000						
25.840	-7.491E-06	208.6435	-11.1833	-1.181E-07	4.2360	9.106E+09	0.2816
153354.	0.000						
26.180	-7.782E-06	165.3589	-10.0058	-3.431E-08	3.3572	9.106E+09	0.2957
155019.	0.000						
26.520	-7.771E-06	126.9962	-8.7939	3.119E-08	2.5783	9.106E+09	0.2984
156683.	0.000						
26.860	-7.527E-06	93.6010	-7.5891	8.061E-08	1.9003	9.106E+09	0.2921
158348.	0.000						
27.200	-7.113E-06	65.0689	-6.4241	1.162E-07	1.3211	9.106E+09	0.2790
160013.	0.000						
27.540	-6.579E-06	41.1804	-5.3231	1.400E-07	0.8361	9.106E+09	0.2607
161677.	0.000						
27.880	-5.971E-06	21.6321	-4.3036	1.540E-07	0.4392	9.106E+09	0.2390
163342.	0.000						
28.220	-5.323E-06	6.0629	-3.3768	1.602E-07	0.1231	9.106E+09	0.2153
165006.	0.000						
28.560	-4.663E-06	-5.9229	-2.5491	1.603E-07	0.1203	9.106E+09	0.1905
166671.	0.000						
28.900	-4.015E-06	-14.7376	-1.8225	1.556E-07	0.2992	9.106E+09	0.1656
168336.	0.000						
29.240	-3.393E-06	-20.7949	-1.1962	1.477E-07	0.4222	9.106E+09	0.1414
170000.	0.000						
29.580	-2.810E-06	-24.4986	-0.6666	1.375E-07	0.4974	9.106E+09	0.1182
171665.	0.000						
29.920	-2.271E-06	-26.2343	-0.2286	1.262E-07	0.5326	9.106E+09	0.0965
173330.	0.000						
30.260	-1.780E-06	-26.3639	0.1240	1.144E-07	0.5353	9.106E+09	0.0764
174994.	0.000						
30.600	-1.338E-06	-25.2225	0.3979	1.028E-07	0.5121	9.106E+09	0.0579
176659.	0.000						
30.940	-9.413E-07	-23.1168	0.6000	9.199E-08	0.4693	9.106E+09	0.0411
178324.	0.000						
31.280	-5.870E-07	-20.3264	0.7368	8.226E-08	0.4127	9.106E+09	0.0259
179988.	0.000						

31.620	-2.700E-07	-17.1048	0.8141	7.388E-08	0.3473	9.106E+09	0.0120
181653.	0.000						
31.960	1.579E-08	-13.6832	0.8372	6.698E-08	0.2778	9.106E+09	-0.000709
183317.	0.000						
32.300	2.766E-07	-10.2733	0.8102	6.161E-08	0.2086	9.106E+09	-0.0125
184982.	0.000						
32.640	5.185E-07	-7.0722	0.7362	5.773E-08	0.1436	9.106E+09	-0.0237
186647.	0.000						
32.980	7.476E-07	-4.2660	0.6174	5.519E-08	0.0866	9.106E+09	-0.0345
188311.	0.000						
33.320	9.689E-07	-2.0341	0.4550	5.377E-08	0.0413	9.106E+09	-0.0451
189976.	0.000						
33.660	1.186E-06	-0.5532	0.2493	5.320E-08	0.0112	9.106E+09	-0.0557
191641.	0.000						
34.000	1.403E-06	0.000	0.000	5.307E-08	0.000	9.106E+09	-0.0665
96653.	0.000						

* The above values of total stress are combined axial and bending stresses.

Output Summary for Load Case No. 1:

Pile-head deflection	=	0.1486885 inches
Computed slope at pile head	=	-0.0027026 radians
Maximum bending moment	=	338185. inch-lbs
Maximum shear force	=	9500.000000 lbs
Depth of maximum bending moment	=	4.0800000 feet below pile head
Depth of maximum shear force	=	0.0000000 feet below pile head
Number of iterations	=	6
Number of zero deflection points	=	4

 Computed Values of Pile Loading and Deflection
 for Lateral Loading for Load Case Number 2

Pile-head conditions are Shear and Moment (Loading Type 1)

Shear force at pile head	=	15900.0 lbs
Applied moment at pile head	=	0.0 in-lbs
Axial thrust load on pile head	=	0.0 lbs

Depth Distrib. X Lat. Load lb/inch	Deflect. y inches	Bending Moment in-lbs	Shear Force lbs	Slope S radians	Total Stress psi*	Bending Stiffness lb-in^2	Soil Res. p lb/in	Soil Spr. Es*h lb/inch
0.000	0.000	-1.215E-07	15900.	-0.004867	2.466E-09	9.106E+09	0.000	
0.000	0.000	64872.	15900.	-0.004853	1317.0669	9.106E+09	0.000	
0.000	0.000	129744.	15900.	-0.004809	2634.1338	9.106E+09	0.000	
74.3752	0.000	194616.	15892.	-0.004736	3951.2006	9.106E+09	-3.9397	
1853.4335	0.000	259422.	15701.	-0.004635	5266.9360	9.106E+09	-89.4799	
4484.9005	0.000	322739.	15119.	-0.004504	6552.4304	9.106E+09	-195.9960	
7738.2287	0.000	382794.	14099.	-0.004346	7771.6852	9.106E+09	-303.8749	
11381.	0.000	437789.	12667.	-0.004162	8888.2410	9.106E+09	-398.4315	
15219.	0.000	486153.	10893.	-0.003955	9870.1413	9.106E+09	-470.9412	
19091.	0.000	526677.	8876.9780	-0.003729	10693.	9.106E+09	-517.3316	
22835.	0.000	558589.	6727.4918	-0.003485	11341.	9.106E+09	-536.3381	
26213.	0.000	581573.	4557.0829	-0.003230	11807.	9.106E+09	-527.5879	
31837.	0.000	595775.	2374.9200	-0.002966	12096.	9.106E+09	-542.0998	

4.420	0.0579	600952.	176.9000	-0.002698	12201.	9.106E+09	-535.3610
37715.	0.000						
4.760	0.0475	597218.	-1941.7161	-0.002430	12125.	9.106E+09	-503.1763
43260.	0.000						
5.100	0.0381	585108.	-3890.8455	-0.002165	11879.	9.106E+09	-452.2793
48447.	0.000						
5.440	0.0298	565469.	-5607.7167	-0.001907	11480.	9.106E+09	-389.3242
53319.	0.000						
5.780	0.0225	539349.	-7054.5951	-0.001660	10950.	9.106E+09	-319.9299
57943.	0.000						
6.120	0.0162	507903.	-8214.1389	-0.001425	10312.	9.106E+09	-248.4739
62388.	0.000						
6.460	0.0109	472322.	-9084.5976	-0.001205	9589.3339	9.106E+09	-178.2215
66709.	0.000						
6.800	0.006414	433773.	-9675.7203	-0.001002	8806.7005	9.106E+09	-111.5445
70952.	0.000						
7.140	0.002721	393368.	-10006.	-0.000817	7986.3690	9.106E+09	-50.1207
75147.	0.000						
7.480	-0.000253	352128.	-10098.	-0.000650	7149.0986	9.106E+09	4.9113
79315.	0.000						
7.820	-0.002583	310970.	-9979.9302	-0.000501	6313.4880	9.106E+09	52.8407
83471.	0.000						
8.160	-0.004345	270692.	-9681.7966	-0.000371	5495.7356	9.106E+09	93.3033
87623.	0.000						
8.500	-0.005611	231967.	-9233.9674	-0.000259	4709.5164	9.106E+09	126.2209
91775.	0.000						
8.840	-0.006454	195343.	-8666.9051	-0.000163	3965.9554	9.106E+09	151.7509
95929.	0.000						
9.180	-0.006940	161245.	-8010.0378	-8.292E-05	3273.6808	9.106E+09	170.2429
100087.	0.000						
9.520	-0.007131	129981.	-7291.0567	-1.768E-05	2638.9421	9.106E+09	182.1988
104248.	0.000						
9.860	-0.007084	101750.	-6535.3725	3.424E-05	2065.7802	9.106E+09	188.2346
108411.	0.000						
10.200	-0.006851	76652.	-5765.7205	7.420E-05	1556.2349	9.106E+09	189.0457
112576.	0.000						
10.540	-0.006479	54702.	-5001.9046	0.000104	1110.5803	9.106E+09	185.3738
116742.	0.000						
10.880	-0.006006	35837.	-4260.6673	0.000124	727.5754	9.106E+09	177.9778
120908.	0.000						
11.220	-0.005467	19934.	-3555.6728	0.000136	404.7207	9.106E+09	167.6077
125074.	0.000						
11.560	-0.004893	6822.3651	-2897.5868	0.000142	138.5114	9.106E+09	154.9835
129240.	0.000						
11.900	-0.004305	-3709.8302	-2294.2348	0.000143	75.3190	9.106E+09	140.7772
133405.	0.000						
12.240	-0.003725	-11899.	-1750.8251	0.000140	241.5717	9.106E+09	125.6001
137570.	0.000						
12.580	-0.003166	-17997.	-1270.2148	0.000133	365.3761	9.106E+09	109.9932
141734.	0.000						
12.920	-0.002641	-22264.	-853.2080	0.000124	452.0067	9.106E+09	94.4219
145897.	0.000						
13.260	-0.002155	-24959.	-498.8680	0.000113	506.7260	9.106E+09	79.2742
150060.	0.000						
13.600	-0.001716	-26334.	-204.8320	0.000102	534.6535	9.106E+09	64.8611
154222.	0.000						
13.940	-0.001325	-26630.	32.3812	8.995E-05	540.6603	9.106E+09	51.4199
158385.	0.000						
14.280	-0.000982	-26070.	217.0822	7.814E-05	529.2890	9.106E+09	39.1198
162547.	0.000						
14.620	-0.000687	-24859.	354.1447	6.673E-05	504.6965	9.106E+09	28.0678
166709.	0.000						
14.960	-0.000437	-23180.	448.7699	5.597E-05	470.6182	9.106E+09	18.3171
170870.	0.000						
15.300	-0.000230	-21197.	506.2823	4.603E-05	430.3494	9.106E+09	9.8752
175032.	0.000						
15.640	-6.176E-05	-19049.	531.9614	3.701E-05	386.7431	9.106E+09	2.7126
179194.	0.000						
15.980	7.185E-05	-16856.	530.9085	2.897E-05	342.2200	9.106E+09	-3.2287
183355.	0.000						
16.320	0.000175	-14717.	515.0011	2.190E-05	298.7881	9.106E+09	-4.5690
106744.	0.000						
16.660	0.000251	-12654.	492.1005	1.577E-05	256.9004	9.106E+09	-6.6567
108409.	0.000						
17.000	0.000303	-10701.	461.8289	1.053E-05	217.2624	9.106E+09	-8.1823
110073.	0.000						
17.340	0.000336	-8885.0791	426.3380	6.146E-06	180.3897	9.106E+09	-9.2152
111738.	0.000						

17.680	0.000353	-7222.3197	387.4988	2.537E-06	146.6315	9.106E+09	-9.8237
113403.	0.000						
18.020	0.000357	-5723.0891	346.9083	-3.629E-07	116.1933	9.106E+09	-10.0736
115067.	0.000						
18.360	0.000350	-4391.5483	305.9022	-2.629E-06	89.1596	9.106E+09	-10.0273
116732.	0.000						
18.700	0.000336	-3226.9267	265.5716	-4.336E-06	65.5148	9.106E+09	-9.7426
118396.	0.000						
19.040	0.000315	-2224.4844	226.7813	-5.557E-06	45.1627	9.106E+09	-9.2722
120061.	0.000						
19.380	0.000290	-1376.3916	190.1919	-6.364E-06	27.9443	9.106E+09	-8.6637
121726.	0.000						
19.720	0.000263	-672.5187	156.2816	-6.823E-06	13.6538	9.106E+09	-7.9590
123390.	0.000						
20.060	0.000235	-101.1337	125.3690	-6.996E-06	2.0533	9.106E+09	-7.1943
125055.	0.000						
20.400	0.000206	350.4925	97.6354	-6.940E-06	7.1159	9.106E+09	-6.4006
126720.	0.000						
20.740	0.000178	695.5710	73.1463	-6.706E-06	14.1219	9.106E+09	-5.6038
128384.	0.000						
21.080	0.000151	947.3661	51.8722	-6.338E-06	19.2339	9.106E+09	-4.8247
130049.	0.000						
21.420	0.000126	1118.8478	33.7074	-5.875E-06	22.7155	9.106E+09	-4.0796
131714.	0.000						
21.760	0.000103	1222.4186	18.4877	-5.350E-06	24.8182	9.106E+09	-3.3810
133378.	0.000						
22.100	8.271E-05	1269.7071	6.0054	-4.792E-06	25.7783	9.106E+09	-2.7377
135043.	0.000						
22.440	6.432E-05	1271.4227	-3.9762	-4.223E-06	25.8131	9.106E+09	-2.1552
136708.	0.000						
22.780	4.826E-05	1237.2612	-11.7116	-3.661E-06	25.1196	9.106E+09	-1.6366
138372.	0.000						
23.120	3.445E-05	1175.8563	-17.4625	-3.120E-06	23.8729	9.106E+09	-1.1825
140037.	0.000						
23.460	2.280E-05	1094.7673	-21.4899	-2.611E-06	22.2266	9.106E+09	-0.7917
141701.	0.000						
23.800	1.314E-05	1000.4986	-24.0472	-2.142E-06	20.3127	9.106E+09	-0.4618
143366.	0.000						
24.140	5.318E-06	898.5422	-25.3750	-1.717E-06	18.2427	9.106E+09	-0.1890
145031.	0.000						
24.480	-8.640E-07	793.4389	-25.6972	-1.337E-06	16.1088	9.106E+09	0.0311
146695.	0.000						
24.820	-5.596E-06	688.8528	-25.2188	-1.005E-06	13.9855	9.106E+09	0.2035
148360.	0.000						
25.160	-9.068E-06	587.6538	-24.1235	-7.194E-07	11.9309	9.106E+09	0.3334
150025.	0.000						
25.500	-1.147E-05	492.0054	-22.5736	-4.776E-07	9.9890	9.106E+09	0.4263
151689.	0.000						
25.840	-1.297E-05	403.4534	-20.7098	-2.770E-07	8.1911	9.106E+09	0.4873
153354.	0.000						
26.180	-1.373E-05	323.0134	-18.6518	-1.142E-07	6.5580	9.106E+09	0.5215
155019.	0.000						
26.520	-1.390E-05	251.2549	-16.4992	1.445E-08	5.1011	9.106E+09	0.5337
156683.	0.000						
26.860	-1.361E-05	188.3803	-14.3330	1.129E-07	3.8246	9.106E+09	0.5281
158348.	0.000						
27.200	-1.298E-05	134.2974	-12.2175	1.852E-07	2.7266	9.106E+09	0.5089
160013.	0.000						
27.540	-1.210E-05	88.6856	-10.2015	2.352E-07	1.8005	9.106E+09	0.4794
161677.	0.000						
27.880	-1.106E-05	51.0533	-8.3206	2.665E-07	1.0365	9.106E+09	0.4426
163342.	0.000						
28.220	-9.922E-06	20.7894	-6.5990	2.826E-07	0.4221	9.106E+09	0.4013
165006.	0.000						
28.560	-8.750E-06	-2.7946	-5.0512	2.866E-07	0.0567	9.106E+09	0.3575
166671.	0.000						
28.900	-7.584E-06	-20.4282	-3.6837	2.814E-07	0.4147	9.106E+09	0.3129
168336.	0.000						
29.240	-6.454E-06	-32.8533	-2.4968	2.695E-07	0.6670	9.106E+09	0.2689
170000.	0.000						
29.580	-5.385E-06	-40.8019	-1.4860	2.530E-07	0.8284	9.106E+09	0.2266
171665.	0.000						
29.920	-4.390E-06	-44.9791	-0.6434	2.338E-07	0.9132	9.106E+09	0.1865
173330.	0.000						
30.260	-3.477E-06	-46.0519	0.0413	2.134E-07	0.9350	9.106E+09	0.1491
174994.	0.000						
30.600	-2.649E-06	-44.6421	0.5795	1.930E-07	0.9063	9.106E+09	0.1147
176659.	0.000						

30.940	-1.902E-06	-41.3232	0.9830	1.738E-07	0.8390	9.106E+09	0.0831
178324.	0.000						
31.280	-1.231E-06	-36.6205	1.2634	1.563E-07	0.7435	9.106E+09	0.0543
179988.	0.000						
31.620	-6.263E-07	-31.0140	1.4310	1.412E-07	0.6297	9.106E+09	0.0279
181653.	0.000						
31.960	-7.868E-08	-24.9434	1.4951	1.286E-07	0.5064	9.106E+09	0.003535
183317.	0.000						
32.300	4.234E-07	-18.8139	1.4632	1.188E-07	0.3820	9.106E+09	-0.0192
184982.	0.000						
32.640	8.910E-07	-13.0039	1.3409	1.117E-07	0.2640	9.106E+09	-0.0408
186647.	0.000						
32.980	1.335E-06	-7.8725	1.1320	1.070E-07	0.1598	9.106E+09	-0.0616
188311.	0.000						
33.320	1.764E-06	-3.7666	0.8387	1.044E-07	0.0765	9.106E+09	-0.0822
189976.	0.000						
33.660	2.187E-06	-1.0283	0.4616	1.033E-07	0.0209	9.106E+09	-0.1027
191641.	0.000						
34.000	2.608E-06	0.000	0.000	1.031E-07	0.000	9.106E+09	-0.1235
96653.	0.000						

* The above values of total stress are combined axial and bending stresses.

Output Summary for Load Case No. 2:

Pile-head deflection	=	0.2752212 inches
Computed slope at pile head	=	-0.0048672 radians
Maximum bending moment	=	600952. inch-lbs
Maximum shear force	=	15900. lbs
Depth of maximum bending moment	=	4.4200000 feet below pile head
Depth of maximum shear force	=	0.3400000 feet below pile head
Number of iterations	=	9
Number of zero deflection points	=	4

 Computed Values of Pile Loading and Deflection
 for Lateral Loading for Load Case Number 3

Pile-head conditions are Shear and Moment (Loading Type 1)

Shear force at pile head	=	23100.0 lbs
Applied moment at pile head	=	0.0 in-lbs
Axial thrust load on pile head	=	0.0 lbs

Depth Distrib. X	Deflect. y	Bending Moment	Shear Force	Slope S	Total Stress	Bending Stiffness	Soil Res. p	Soil Spr. Es*h
Lat. Load feet lb/inch	inches	in-lbs	lbs	radians	psi*	lb-in ²	lb/in	lb/inch
0.000	0.000	0.000	23100.	-0.007883	0.000	9.106E+09	0.000	
0.000	0.340	94248.	23100.	-0.007862	1913.4745	9.106E+09	0.000	
0.000	0.680	188496.	23100.	-0.007798	3826.9490	9.106E+09	0.000	
0.000	1.020	282744.	23092.	-0.007693	5740.4236	9.106E+09	-3.9507	
43.5945	1.360	376926.	22898.	-0.007545	7652.5629	9.106E+09	-91.1193	
1097.8948	1.700	469592.	22292.	-0.007355	9533.9071	9.106E+09	-205.9734	
2726.8967	2.040	558828.	21193.	-0.007125	11346.	9.106E+09	-332.9532	
4876.0189	2.380	642523.	19582.	-0.006856	13045.	9.106E+09	-456.3524	
7446.5125	2.720	718620.	17505.	-0.006551	14590.	9.106E+09	-562.0531	
10299.	3.060	785362.	15055.	-0.006214	15945.	9.106E+09	-638.6859	
13256.	3.400	841471.	12370.	-0.005850	17084.	9.106E+09	-677.5595	
16077.	0.000							

18396.	3.740	0.1489	886302.	9618.7494	-0.005462	17994.	9.106E+09	-671.1612
23974.	4.080	0.000	919960.	6722.7294	-0.005058	18678.	9.106E+09	-748.4564
30766.	4.420	0.1076	941159.	3541.0033	-0.004641	19108.	9.106E+09	-811.2132
37720.	4.760	0.0895	948855.	198.0757	-0.004217	19264.	9.106E+09	-827.4768
44418.	5.100	0.0732	942776.	-3114.9123	-0.003794	19141.	9.106E+09	-796.5370
50622.	5.440	0.0585	923437.	-6221.7805	-0.003376	18748.	9.106E+09	-726.4377
56274.	5.780	0.0456	892006.	-8987.3611	-0.002969	18110.	9.106E+09	-629.2391
61437.	6.120	0.0343	850100.	-11325.	-0.002579	17259.	9.106E+09	-516.8486
66220.	6.460	0.0246	799591.	-13194.	-0.002209	16234.	9.106E+09	-398.9406
70734.	6.800	0.0163	742441.	-14584.	-0.001864	15073.	9.106E+09	-282.5526
75072.	7.140	0.009373	680587.	-15512.	-0.001545	13818.	9.106E+09	-172.4678
79303.	7.480	0.003693	615862.	-16010.	-0.001254	12504.	9.106E+09	-71.7775
83476.	7.820	-0.000862	549942.	-16121.	-0.000993	11165.	9.106E+09	17.6324
87622.	8.160	-0.004411	484316.	-15892.	-0.000761	9832.8571	9.106E+09	94.7332
91760.	8.500	-0.007075	420267.	-15374.	-0.000559	8532.4969	9.106E+09	159.1192
95900.	8.840	-0.008971	358867.	-14619.	-0.000384	7285.9133	9.106E+09	210.8547
100046.	9.180	-0.0102	300977.	-13678.	-0.000236	6110.5911	9.106E+09	250.3674
104199.	9.520	-0.0109	247254.	-12599.	-0.000114	5019.8841	9.106E+09	278.3693
108360.	9.860	-0.0111	198165.	-11428.	-1.380E-05	4023.2561	9.106E+09	295.7903
112526.	10.200	-0.0110	154000.	-10205.	6.510E-05	3126.5946	9.106E+09	303.7197
116696.	10.540	-0.0106	114891.	-8966.7348	0.000125	2332.5795	9.106E+09	303.3518
120868.	10.880	-0.009990	80832.	-7744.1870	0.000169	1641.0865	9.106E+09	295.9364
125040.	11.220	-0.009225	51698.	-6563.7008	0.000199	1049.6094	9.106E+09	282.7333
129212.	11.560	-0.008367	27272.	-5446.3787	0.000217	553.6861	9.106E+09	264.9736
133383.	11.900	-0.007458	7255.9580	-4408.4273	0.000224	147.3144	9.106E+09	243.8261
137553.	12.240	-0.006536	-8701.0118	-3461.4638	0.000224	176.6527	9.106E+09	220.3717
141722.	12.580	-0.005631	-20990.	-2612.9152	0.000217	426.1421	9.106E+09	195.5836
145888.	12.920	-0.004763	-30022.	-1866.4825	0.000206	609.5312	9.106E+09	170.3148
150054.	13.260	-0.003951	-36220.	-1222.6457	0.000191	735.3600	9.106E+09	145.2914
154219.	13.600	-0.003204	-39999.	-679.1857	0.000174	812.0854	9.106E+09	121.1106
158382.	13.940	-0.002531	-41762.	-231.7025	0.000156	847.8799	9.106E+09	98.2439
162545.	14.280	-0.001934	-41890.	125.8855	0.000137	850.4713	9.106E+09	77.0443
166708.	14.620	-0.001414	-40735.	400.8768	0.000118	827.0246	9.106E+09	57.7553
170870.	14.960	-0.000968	-38619.	601.3649	0.000101	784.0585	9.106E+09	40.5231
175032.	15.300	-0.000592	-35828.	735.8681	8.396E-05	727.3972	9.106E+09	25.4098
179194.	15.640	-0.000282	-32614.	813.0151	6.863E-05	662.1482	9.106E+09	12.4074
183355.	15.980	-3.232E-05	-29194.	841.2888	5.478E-05	592.7059	9.106E+09	1.4523
106744.	16.320	0.000164	-25749.	835.4718	4.247E-05	522.7729	9.106E+09	-4.3038
108409.	16.660	0.000314	-22376.	809.6587	3.169E-05	454.2943	9.106E+09	-8.3497

17.000	0.000423	-19142.	769.3403	2.239E-05	388.6377	9.106E+09	-11.4142
110073.	0.000						
17.340	0.000497	-16098.	718.2925	1.449E-05	326.8387	9.106E+09	-13.6092
111738.	0.000						
17.680	0.000541	-13281.	659.8348	7.911E-06	269.6391	9.106E+09	-15.0465
113402.	0.000						
18.020	0.000561	-10714.	596.8358	2.535E-06	217.5246	9.106E+09	-15.8353
115067.	0.000						
18.360	0.000562	-8410.8649	531.7282	-1.749E-06	170.7620	9.106E+09	-16.0802
116732.	0.000						
18.700	0.000547	-6375.2526	466.5308	-5.062E-06	129.4339	9.106E+09	-15.8793
118396.	0.000						
19.040	0.000521	-4603.9739	402.8772	-7.521E-06	93.4724	9.106E+09	-15.3234
120061.	0.000						
19.380	0.000486	-3087.7747	342.0481	-9.244E-06	62.6897	9.106E+09	-14.4948
121726.	0.000						
19.720	0.000445	-1812.8616	285.0061	-1.034E-05	36.8057	9.106E+09	-13.4670
123390.	0.000						
20.060	0.000401	-762.1253	232.4322	-1.092E-05	15.4731	9.106E+09	-12.3045
125055.	0.000						
20.400	0.000356	83.7850	184.7624	-1.107E-05	1.7010	9.106E+09	-11.0630
126720.	0.000						
20.740	0.000311	745.5362	142.2236	-1.089E-05	15.1363	9.106E+09	-9.7894
128384.	0.000						
21.080	0.000267	1244.3293	104.8675	-1.044E-05	25.2631	9.106E+09	-8.5224
130049.	0.000						
21.420	0.000226	1601.2551	72.6037	-9.802E-06	32.5096	9.106E+09	-7.2932
131714.	0.000						
21.760	0.000187	1836.7756	45.2290	-9.032E-06	37.2912	9.106E+09	-6.1258
133378.	0.000						
22.100	0.000152	1970.3234	22.4545	-8.179E-06	40.0026	9.106E+09	-5.0382
135043.	0.000						
22.440	0.000121	2020.0040	3.9300	-7.285E-06	41.0112	9.106E+09	-4.0425
136708.	0.000						
22.780	9.277E-05	2002.3920	-10.7351	-6.384E-06	40.6537	9.106E+09	-3.1463
138372.	0.000						
23.120	6.855E-05	1932.4059	-21.9535	-5.502E-06	39.2328	9.106E+09	-2.3530
140037.	0.000						
23.460	4.787E-05	1823.2513	-30.1453	-4.661E-06	37.0166	9.106E+09	-1.6626
141701.	0.000						
23.800	3.052E-05	1686.4206	-35.7247	-3.875E-06	34.2386	9.106E+09	-1.0724
143366.	0.000						
24.140	1.625E-05	1531.7375	-39.0911	-3.154E-06	31.0982	9.106E+09	-0.5777
145031.	0.000						
24.480	4.786E-06	1367.4372	-40.6207	-2.504E-06	27.7625	9.106E+09	-0.1721
146695.	0.000						
24.820	-4.182E-06	1200.2727	-40.6615	-1.929E-06	24.3686	9.106E+09	0.1521
148360.	0.000						
25.160	-1.096E-05	1035.6396	-39.5295	-1.428E-06	21.0261	9.106E+09	0.4028
150025.	0.000						
25.500	-1.584E-05	877.7124	-37.5066	-9.995E-07	17.8198	9.106E+09	0.5887
151689.	0.000						
25.840	-1.911E-05	729.5857	-34.8402	-6.394E-07	14.8124	9.106E+09	0.7183
153354.	0.000						
26.180	-2.105E-05	593.4167	-31.7429	-3.430E-07	12.0479	9.106E+09	0.7999
155019.	0.000						
26.520	-2.191E-05	470.5633	-28.3946	-1.047E-07	9.5536	9.106E+09	0.8414
156683.	0.000						
26.860	-2.191E-05	361.7166	-24.9436	8.179E-08	7.3438	9.106E+09	0.8502
158348.	0.000						
27.200	-2.124E-05	267.0233	-21.5096	2.226E-07	5.4213	9.106E+09	0.8331
160013.	0.000						
27.540	-2.009E-05	186.1984	-18.1859	3.242E-07	3.7803	9.106E+09	0.7961
161677.	0.000						
27.880	-1.860E-05	118.6261	-15.0430	3.925E-07	2.4084	9.106E+09	0.7446
163342.	0.000						
28.220	-1.689E-05	63.4478	-12.1308	4.333E-07	1.2882	9.106E+09	0.6830
165006.	0.000						
28.560	-1.506E-05	19.6389	-9.4823	4.519E-07	0.3987	9.106E+09	0.6153
166671.	0.000						
28.900	-1.320E-05	-13.9274	-7.1160	4.532E-07	0.2828	9.106E+09	0.5446
168336.	0.000						
29.240	-1.136E-05	-38.4274	-5.0389	4.414E-07	0.7802	9.106E+09	0.4735
170000.	0.000						
29.580	-9.599E-06	-55.0450	-3.2491	4.205E-07	1.1176	9.106E+09	0.4039
171665.	0.000						
29.920	-7.933E-06	-64.9399	-1.7377	3.936E-07	1.3184	9.106E+09	0.3370
173330.	0.000						

30.260	-6.387E-06	-69.2245	-0.4913	3.635E-07	1.4054	9.106E+09	0.2739
174994.	0.000						
30.600	-4.967E-06	-68.9492	0.5062	3.326E-07	1.3998	9.106E+09	0.2151
176659.	0.000						
30.940	-3.673E-06	-65.0940	1.2724	3.026E-07	1.3216	9.106E+09	0.1605
178324.	0.000						
31.280	-2.498E-06	-58.5666	1.8246	2.749E-07	1.1891	9.106E+09	0.1102
179988.	0.000						
31.620	-1.430E-06	-50.2050	2.1793	2.505E-07	1.0193	9.106E+09	0.0637
181653.	0.000						
31.960	-4.537E-07	-40.7837	2.3507	2.301E-07	0.8280	9.106E+09	0.0204
183317.	0.000						
32.300	4.478E-07	-31.0230	2.3509	2.140E-07	0.6298	9.106E+09	-0.0203
184982.	0.000						
32.640	1.293E-06	-21.6004	2.1888	2.022E-07	0.4385	9.106E+09	-0.0591
186647.	0.000						
32.980	2.098E-06	-13.1621	1.8707	1.944E-07	0.2672	9.106E+09	-0.0968
188311.	0.000						
33.320	2.879E-06	-6.3358	1.3996	1.901E-07	0.1286	9.106E+09	-0.1341
189976.	0.000						
33.660	3.649E-06	-1.7413	0.7764	1.883E-07	0.0354	9.106E+09	-0.1714
191641.	0.000						
34.000	4.416E-06	0.000	0.000	1.879E-07	0.000	9.106E+09	-0.2092
96653.	0.000						

* The above values of total stress are combined axial and bending stresses.

Output Summary for Load Case No. 3:

Pile-head deflection	=	0.4655426 inches
Computed slope at pile head	=	-0.0078828 radians
Maximum bending moment	=	948855. inch-lbs
Maximum shear force	=	23100. lbs
Depth of maximum bending moment	=	4.7600000 feet below pile head
Depth of maximum shear force	=	0.3400000 feet below pile head
Number of iterations	=	13
Number of zero deflection points	=	4

 Computed Values of Pile Loading and Deflection
 for Lateral Loading for Load Case Number 4

Pile-head conditions are Shear and Moment (Loading Type 1)

Shear force at pile head	=	30400.0 lbs
Applied moment at pile head	=	0.0 in-lbs
Axial thrust load on pile head	=	0.0 lbs

Depth Distrib.	Deflect. y	Bending Moment	Shear Force	Slope S	Total Stress	Bending Stiffness	Soil Res. p	Soil Spr. Es*h
X Lat. Load feet lb/inch	inches	in-lbs	lbs	radians	psi*	lb-in ²	lb/in	lb/inch
0.000	0.000	-3.644E-07	30400.	-0.0116	7.398E-09	9.106E+09	0.000	
0.000	0.340	0.6745	124032.	30400.	-0.0116	2518.1656	9.106E+09	0.000
0.000	0.680	0.6272	248064.	30400.	-0.0115	5036.3312	9.106E+09	0.000
27.7760	1.020	0.5803	372096.	30392.	-0.0114	7554.4968	9.106E+09	-3.9508
696.4317	1.360	0.5342	496062.	30198.	-0.0112	10071.	9.106E+09	-91.1784
1725.3168	1.700	0.4889	618511.	29590.	-0.0110	12557.	9.106E+09	-206.7416
3087.8758	2.040	0.4448	737518.	28482.	-0.0107	14973.	9.106E+09	-336.6134
4735.9072	2.380	0.4020	850921.	26843.	-0.0103	17276.	9.106E+09	-466.6047
6588.5339	2.720	0.3608	956557.	24703.	-0.009891	19421.	9.106E+09	-582.5563
	0.000							

3.060	0.3213	1052496.	22146.	-0.009441	21368.	9.106E+09	-670.7453
8518.1426	0.000						
3.400	0.2837	1137269.	19313.	-0.008950	23089.	9.106E+09	-718.1371
10327.	0.000						
3.740	0.2482	1210088.	16395.	-0.008424	24568.	9.106E+09	-712.0373
11703.	0.000						
4.080	0.2150	1271054.	13245.	-0.007868	25806.	9.106E+09	-832.3531
15797.	0.000						
4.420	0.1840	1318165.	9560.6110	-0.007288	26762.	9.106E+09	-973.5508
21584.	0.000						
4.760	0.1555	1349069.	5357.2735	-0.006691	27390.	9.106E+09	-1086.9088
28518.	0.000						
5.100	0.1294	1361880.	796.5091	-0.006084	27650.	9.106E+09	-1148.7600
36211.	0.000						
5.440	0.1059	1355568.	-3880.0307	-0.005475	27521.	9.106E+09	-1143.6614
44079.	0.000						
5.780	0.0848	1330219.	-8398.8853	-0.004873	27007.	9.106E+09	-1071.4634
51576.	0.000						
6.120	0.0661	1287034.	-12514.	-0.004287	26130.	9.106E+09	-945.6599
58377.	0.000						
6.460	0.0498	1228106.	-16046.	-0.003723	24934.	9.106E+09	-785.8484
64410.	0.000						
6.800	0.0357	1156097.	-18895.	-0.003189	23472.	9.106E+09	-610.6937
69772.	0.000						
7.140	0.0238	1073923.	-21027.	-0.002690	21803.	9.106E+09	-434.5327
74630.	0.000						
7.480	0.0138	984515.	-22458.	-0.002228	19988.	9.106E+09	-266.9964
79146.	0.000						
7.820	0.005572	890662.	-23236.	-0.001808	18083.	9.106E+09	-113.9600
83450.	0.000						
8.160	-0.000992	794912.	-23425.	-0.001431	16139.	9.106E+09	21.3136
87638.	0.000						
8.500	-0.006103	699518.	-23101.	-0.001096	14202.	9.106E+09	137.2739
91770.	0.000						
8.840	-0.009935	606408.	-22345.	-0.000803	12312.	9.106E+09	233.4873
95886.	0.000						
9.180	-0.0127	517185.	-21235.	-0.000552	10500.	9.106E+09	310.2700
100004.	0.000						
9.520	-0.0144	433127.	-19851.	-0.000339	8793.5756	9.106E+09	368.4669
104135.	0.000						
9.860	-0.0154	355202.	-18264.	-0.000162	7211.5100	9.106E+09	409.3103
108281.	0.000						
10.200	-0.0158	284091.	-16543.	-1.893E-05	5767.7767	9.106E+09	434.3183
112440.	0.000						
10.540	-0.0156	220210.	-14749.	9.405E-05	4470.8275	9.106E+09	445.2124
116611.	0.000						
10.880	-0.0150	163740.	-12935.	0.000180	3324.3442	9.106E+09	443.8429
120788.	0.000						
11.220	-0.0141	114659.	-11148.	0.000242	2327.8640	9.106E+09	432.1211
124970.	0.000						
11.560	-0.0130	72770.	-9426.3448	0.000284	1477.4252	9.106E+09	411.9556
129153.	0.000						
11.900	-0.0118	37740.	-7800.1517	0.000309	766.2128	9.106E+09	385.1978
133335.	0.000						
12.240	-0.0105	9121.1971	-6293.0158	0.000320	185.1835	9.106E+09	353.5943
137515.	0.000						
12.580	-0.009178	-13611.	-4921.4332	0.000319	276.3435	9.106E+09	318.7502
141692.	0.000						
12.920	-0.007891	-31038.	-3695.6946	0.000309	630.1443	9.106E+09	282.1021
145867.	0.000						
13.260	-0.006660	-43768.	-2620.6089	0.000292	888.6048	9.106E+09	244.9008
150039.	0.000						
13.600	-0.005509	-52422.	-1696.2777	0.000270	1064.2974	9.106E+09	208.2027
154208.	0.000						
13.940	-0.004453	-57610.	-918.8894	0.000246	1169.6250	9.106E+09	172.8700
158376.	0.000						
14.280	-0.003504	-59920.	-281.5000	0.000219	1216.5287	9.106E+09	139.5758
162541.	0.000						
14.620	-0.002663	-59907.	225.2213	0.000193	1216.2608	9.106E+09	108.8170
166705.	0.000						
14.960	-0.001932	-58082.	612.3024	0.000166	1179.2166	9.106E+09	80.9287
170869.	0.000						
15.300	-0.001308	-54910.	891.8488	0.000141	1114.8214	9.106E+09	56.1038
175031.	0.000						
15.640	-0.000784	-50805.	1076.5032	0.000117	1031.4651	9.106E+09	34.4130
179193.	0.000						
15.980	-0.000352	-46126.	1178.9916	9.540E-05	936.4784	9.106E+09	15.8264
183355.	0.000						

16.320	-5.117E-06	-41184.	1211.5506	7.584E-05	836.1430	9.106E+09	0.1339
106744.	0.000						
16.660	0.000267	-36240.	1197.3703	5.849E-05	735.7623	9.106E+09	-7.0850
108409.	0.000						
17.000	0.000472	-31414.	1156.9307	4.333E-05	637.7761	9.106E+09	-12.7383
110073.	0.000						
17.340	0.000620	-26799.	1096.2920	3.029E-05	544.0950	9.106E+09	-16.9866
111738.	0.000						
17.680	0.000719	-22468.	1020.8515	1.926E-05	456.1547	9.106E+09	-19.9940
113402.	0.000						
18.020	0.000777	-18469.	935.3389	1.008E-05	374.9717	9.106E+09	-21.9239
115067.	0.000						
18.360	0.000802	-14835.	843.8262	2.623E-06	301.1983	9.106E+09	-22.9352
116732.	0.000						
18.700	0.000799	-11584.	749.7525	-3.296E-06	235.1761	9.106E+09	-23.1793
118396.	0.000						
19.040	0.000775	-8717.5103	655.9588	-7.844E-06	176.9877	9.106E+09	-22.7980
120061.	0.000						
19.380	0.000735	-6230.9505	564.7309	-1.119E-05	126.5042	9.106E+09	-21.9216
121726.	0.000						
19.720	0.000683	-4109.3058	477.8482	-1.351E-05	83.4294	9.106E+09	-20.6680
123390.	0.000						
20.060	0.000625	-2331.7095	396.6349	-1.495E-05	47.3396	9.106E+09	-19.1424
125055.	0.000						
20.400	0.000561	-872.7647	322.0146	-1.567E-05	17.7193	9.106E+09	-17.4363
126720.	0.000						
20.740	0.000497	295.9292	254.5626	-1.580E-05	6.0081	9.106E+09	-15.6284
128384.	0.000						
21.080	0.000432	1204.4663	194.5592	-1.546E-05	24.4537	9.106E+09	-13.7850
130049.	0.000						
21.420	0.000370	1883.5326	142.0388	-1.477E-05	38.2405	9.106E+09	-11.9603
131714.	0.000						
21.760	0.000312	2363.5031	96.8368	-1.382E-05	47.9851	9.106E+09	-10.1976
133378.	0.000						
22.100	0.000258	2673.7210	58.6325	-1.269E-05	54.2833	9.106E+09	-8.5301
135043.	0.000						
22.440	0.000208	2841.9441	26.9877	-1.146E-05	57.6987	9.106E+09	-6.9821
136708.	0.000						
22.780	0.000164	2893.9407	1.3814	-1.017E-05	58.7544	9.106E+09	-5.5700
138372.	0.000						
23.120	0.000125	2853.2161	-18.7608	-8.883E-06	57.9276	9.106E+09	-4.3036
140037.	0.000						
23.460	9.175E-05	2740.8527	-34.0406	-7.630E-06	55.6463	9.106E+09	-3.1865
141701.	0.000						
23.800	6.312E-05	2575.4450	-45.0661	-6.439E-06	52.2881	9.106E+09	-2.2181
143366.	0.000						
24.140	3.921E-05	2373.1137	-52.4341	-5.330E-06	48.1803	9.106E+09	-1.3937
145031.	0.000						
24.480	1.963E-05	2147.5824	-56.7170	-4.318E-06	43.6014	9.106E+09	-0.7057
146695.	0.000						
24.820	3.976E-06	1910.3030	-58.4516	-3.409E-06	38.7840	9.106E+09	-0.1446
148360.	0.000						
25.160	-8.185E-06	1670.6171	-58.1326	-2.606E-06	33.9178	9.106E+09	0.3010
150025.	0.000						
25.500	-1.729E-05	1435.9413	-56.2071	-1.910E-06	29.1533	9.106E+09	0.6429
151689.	0.000						
25.840	-2.377E-05	1211.9671	-53.0727	-1.317E-06	24.6060	9.106E+09	0.8936
153354.	0.000						
26.180	-2.804E-05	1002.8676	-49.0765	-8.210E-07	20.3608	9.106E+09	1.0654
155019.	0.000						
26.520	-3.047E-05	811.5025	-44.5160	-4.145E-07	16.4756	9.106E+09	1.1702
156683.	0.000						
26.860	-3.142E-05	639.6174	-39.6409	-8.939E-08	12.9859	9.106E+09	1.2195
158348.	0.000						
27.200	-3.120E-05	488.0326	-34.6568	1.632E-07	9.9083	9.106E+09	1.2237
160013.	0.000						
27.540	-3.009E-05	356.8180	-29.7280	3.525E-07	7.2443	9.106E+09	1.1924
161677.	0.000						
27.880	-2.833E-05	245.4519	-24.9822	4.874E-07	4.9833	9.106E+09	1.1340
163342.	0.000						
28.220	-2.611E-05	152.9628	-20.5145	5.767E-07	3.1055	9.106E+09	1.0561
165006.	0.000						
28.560	-2.362E-05	78.0533	-16.3918	6.284E-07	1.5847	9.106E+09	0.9649
166671.	0.000						
28.900	-2.098E-05	19.2056	-12.6572	6.502E-07	0.3899	9.106E+09	0.8658
168336.	0.000						
29.240	-1.831E-05	-25.2298	-9.3344	6.489E-07	0.5122	9.106E+09	0.7631
170000.	0.000						

29.580	-1.569E-05	-56.9628	-6.4310	6.305E-07	1.1565	9.106E+09	0.6601
171665.	0.000						
29.920	-1.317E-05	-77.7069	-3.9430	6.003E-07	1.5776	9.106E+09	0.5595
173330.	0.000						
30.260	-1.079E-05	-89.1379	-1.8575	5.629E-07	1.8097	9.106E+09	0.4628
174994.	0.000						
30.600	-8.576E-06	-92.8643	-0.1558	5.221E-07	1.8854	9.106E+09	0.3713
176659.	0.000						
30.940	-6.530E-06	-90.4095	1.1839	4.811E-07	1.8355	9.106E+09	0.2854
178324.	0.000						
31.280	-4.650E-06	-83.2035	2.1847	4.422E-07	1.6892	9.106E+09	0.2051
179988.	0.000						
31.620	-2.922E-06	-72.5825	2.8686	4.073E-07	1.4736	9.106E+09	0.1301
181653.	0.000						
31.960	-1.327E-06	-59.7959	3.2556	3.776E-07	1.2140	9.106E+09	0.0596
183317.	0.000						
32.300	1.593E-07	-46.0169	3.3625	3.539E-07	0.9343	9.106E+09	-0.007224
184982.	0.000						
32.640	1.561E-06	-32.3581	3.2020	3.364E-07	0.6570	9.106E+09	-0.0714
186647.	0.000						
32.980	2.904E-06	-19.8883	2.7829	3.247E-07	0.4038	9.106E+09	-0.1340
188311.	0.000						
33.320	4.211E-06	-9.6498	2.1095	3.180E-07	0.1959	9.106E+09	-0.1961
189976.	0.000						
33.660	5.499E-06	-2.6749	1.1826	3.153E-07	0.0543	9.106E+09	-0.2583
191641.	0.000						
34.000	6.783E-06	0.000	0.000	3.147E-07	0.000	9.106E+09	-0.3214
96653.	0.000						

* The above values of total stress are combined axial and bending stresses.

Output Summary for Load Case No. 4:

Pile-head deflection	=	0.7220183 inches
Computed slope at pile head	=	-0.0116497 radians
Maximum bending moment	=	1361880. inch-lbs
Maximum shear force	=	30400. lbs
Depth of maximum bending moment	=	5.1000000 feet below pile head
Depth of maximum shear force	=	0.3400000 feet below pile head
Number of iterations	=	16
Number of zero deflection points	=	4

 Computed Values of Pile Loading and Deflection
 for Lateral Loading for Load Case Number 5

Pile-head conditions are Shear and Moment (Loading Type 1)

Shear force at pile head	=	35100.0 lbs
Applied moment at pile head	=	0.0 in-lbs
Axial thrust load on pile head	=	0.0 lbs

Depth Distrib. X Lat. Load lb/inch	Deflect. y inches	Bending Moment in-lbs	Shear Force lbs	Slope S radians	Total Stress psi*	Bending Stiffness lb-in ²	Soil Res. p lb/in	Soil Spr. Es*h lb/inch
0.000	0.000	0.000	35100.	-0.0144	0.000	9.106E+09	0.000	
0.000	0.000	143208.	35100.	-0.0144	2907.4873	9.106E+09	0.000	
0.000	0.000	286416.	35100.	-0.0143	5814.9745	9.106E+09	0.000	
21.6723	0.000	429624.	35092.	-0.0141	8722.4618	9.106E+09	-3.9508	
541.8288	0.000	572766.	34898.	-0.0139	11629.	9.106E+09	-91.1790	
1338.0895	0.000	714391.	34290.	-0.0136	14504.	9.106E+09	-206.7607	
2387.1467	0.000	852573.	33181.	-0.0132	17309.	9.106E+09	-336.7756	

2.380	0.5223	985150.	31541.	-0.0128	20001.	9.106E+09	-467.2697
3649.9728	0.000						
2.720	0.4708	1109948.	29396.	-0.0124	22535.	9.106E+09	-584.2705
5062.8805	0.000						
3.060	0.4214	1225020.	26829.	-0.0118	24871.	9.106E+09	-673.8806
6524.6134	0.000						
3.400	0.3742	1328875.	23981.	-0.0113	26980.	9.106E+09	-722.3721
7876.5466	0.000						
3.740	0.3294	1420704.	21046.	-0.0107	28844.	9.106E+09	-716.1020
8869.6596	0.000						
4.080	0.2872	1500613.	17863.	-0.0100	30466.	9.106E+09	-844.6241
11998.	0.000						
4.420	0.2478	1566462.	14081.	-0.009316	31803.	9.106E+09	-1009.2851
16619.	0.000						
4.760	0.2112	1615510.	9638.8077	-0.008603	32799.	9.106E+09	-1168.0359
22564.	0.000						
5.100	0.1776	1645115.	4610.0689	-0.007872	33400.	9.106E+09	-1297.0321
29800.	0.000						
5.440	0.1470	1653129.	-825.8855	-0.007134	33563.	9.106E+09	-1367.6514
37969.	0.000						
5.780	0.1194	1638376.	-6387.5423	-0.006396	33263.	9.106E+09	-1358.6510
46438.	0.000						
6.120	0.0948	1601006.	-11744.	-0.005670	32505.	9.106E+09	-1267.0188
54547.	0.000						
6.460	0.0731	1542545.	-16590.	-0.004966	31318.	9.106E+09	-1108.2932
61860.	0.000						
6.800	0.0542	1465636.	-20702.	-0.004292	29756.	9.106E+09	-907.4485
68252.	0.000						
7.140	0.0381	1373620.	-23958.	-0.003656	27888.	9.106E+09	-688.9234
73827.	0.000						
7.480	0.0244	1270136.	-26325.	-0.003064	25787.	9.106E+09	-471.3785
78785.	0.000						
7.820	0.0131	1158806.	-27831.	-0.002520	23527.	9.106E+09	-266.9627
83330.	0.000						
8.160	0.003849	1043031.	-28545.	-0.002027	21176.	9.106E+09	-82.6730
87626.	0.000						
8.500	-0.003466	925881.	-28554.	-0.001585	18798.	9.106E+09	77.9671
91790.	0.000						
8.840	-0.009088	810028.	-27960.	-0.001197	16446.	9.106E+09	213.6064
95898.	0.000						
9.180	-0.0132	697731.	-26862.	-0.000859	14166.	9.106E+09	324.2299
99993.	0.000						
9.520	-0.0161	590831.	-25363.	-0.000570	11995.	9.106E+09	410.6682
104098.	0.000						
9.860	-0.0179	490767.	-23558.	-0.000328	9963.8273	9.106E+09	474.3171
108224.	0.000						
10.200	-0.0188	398599.	-21536.	-0.000129	8092.5833	9.106E+09	516.9704
112370.	0.000						
10.540	-0.0189	315037.	-19378.	3.132E-05	6396.0569	9.106E+09	540.7058
116535.	0.000						
10.880	-0.0185	240476.	-17157.	0.000156	4882.2697	9.106E+09	547.7922
120713.	0.000						
11.220	-0.0177	175033.	-14937.	0.000249	3553.6168	9.106E+09	540.6075
124900.	0.000						
11.560	-0.0165	118590.	-12770.	0.000315	2407.6699	9.106E+09	521.5604
129091.	0.000						
11.900	-0.0151	70828.	-10700.	0.000357	1437.9918	9.106E+09	493.0195
133283.	0.000						
12.240	-0.0136	31274.	-8761.9165	0.000380	634.9367	9.106E+09	457.2496
137473.	0.000						
12.580	-0.0120	-669.0939	-6979.7530	0.000387	13.5843	9.106E+09	416.3600
141659.	0.000						
12.920	-0.0104	-25681.	-5370.9601	0.000381	521.3905	9.106E+09	372.2640
145842.	0.000						
13.260	-0.008884	-44496.	-3945.1736	0.000365	903.3848	9.106E+09	326.6509
150021.	0.000						
13.600	-0.007434	-57874.	-2705.6273	0.000342	1174.9827	9.106E+09	280.9699
154195.	0.000						
13.940	-0.006091	-66574.	-1650.1426	0.000314	1351.6228	9.106E+09	236.4246
158367.	0.000						
14.280	-0.004869	-71339.	-772.1228	0.000283	1448.3598	9.106E+09	193.9772
162536.	0.000						
14.620	-0.003778	-72875.	-61.5153	0.000251	1479.5394	9.106E+09	154.3598
166702.	0.000						
14.960	-0.002820	-71841.	494.2852	0.000219	1458.5509	9.106E+09	118.0915
170867.	0.000						
15.300	-0.001993	-68841.	909.6129	0.000187	1397.6518	9.106E+09	85.5005
175030.	0.000						

15.640	-0.001292	-64418.	1199.8023	0.000157	1307.8565	9.106E+09	56.7492
179193.	0.000						
15.980	-0.000709	-59051.	1380.5641	0.000130	1198.8820	9.106E+09	31.8596
183355.	0.000						
16.320	-0.000234	-53153.	1458.0315	0.000105	1079.1401	9.106E+09	6.1146
106744.	0.000						
16.660	0.000144	-47153.	1462.6815	8.210E-05	957.3317	9.106E+09	-3.8352
108409.	0.000						
17.000	0.000436	-41217.	1430.8509	6.230E-05	836.8194	9.106E+09	-11.7680
110073.	0.000						
17.340	0.000653	-35478.	1370.3783	4.512E-05	720.2843	9.106E+09	-17.8754
111738.	0.000						
17.680	0.000804	-30035.	1288.3047	3.044E-05	609.7905	9.106E+09	-22.3568
113402.	0.000						
18.020	0.000901	-24965.	1190.8535	1.812E-05	506.8525	9.106E+09	-25.4134
115067.	0.000						
18.360	0.000952	-20318.	1083.4338	7.975E-06	412.5032	9.106E+09	-27.2433
116731.	0.000						
18.700	0.000966	-16124.	970.6619	-1.894E-07	327.3613	9.106E+09	-28.0370
118396.	0.000						
19.040	0.000951	-12397.	856.3977	-6.579E-06	251.6949	9.106E+09	-27.9748
120061.	0.000						
19.380	0.000912	-9135.9433	743.7925	-1.140E-05	185.4829	9.106E+09	-27.2238
121725.	0.000						
19.720	0.000858	-6327.8589	635.3455	-1.487E-05	128.4717	9.106E+09	-25.9365
123390.	0.000						
20.060	0.000791	-3951.5244	532.9650	-1.717E-05	80.2260	9.106E+09	-24.2499
125055.	0.000						
20.400	0.000718	-1978.8641	438.0342	-1.850E-05	40.1760	9.106E+09	-22.2848
126719.	0.000						
20.740	0.000640	-377.1652	351.4761	-1.903E-05	7.6574	9.106E+09	-20.1457
128384.	0.000						
21.080	0.000562	889.1811	273.8191	-1.891E-05	18.0526	9.106E+09	-17.9215
130049.	0.000						
21.420	0.000486	1857.1988	205.2594	-1.830E-05	37.7059	9.106E+09	-15.6862
131714.	0.000						
21.760	0.000413	2564.0979	145.7205	-1.731E-05	52.0577	9.106E+09	-13.4996
133378.	0.000						
22.100	0.000345	3046.2778	94.9079	-1.605E-05	61.8472	9.106E+09	-11.4086
135043.	0.000						
22.440	0.000282	3338.5463	52.3596	-1.462E-05	67.7810	9.106E+09	-9.4484
136708.	0.000						
22.780	0.000225	3473.5324	17.4908	-1.309E-05	70.5216	9.106E+09	-7.6441
138372.	0.000						
23.120	0.000175	3481.2712	-10.3669	-1.153E-05	70.6787	9.106E+09	-6.0116
140037.	0.000						
23.460	0.000131	3388.9384	-31.9311	-9.996E-06	68.8041	9.106E+09	-4.5591
141701.	0.000						
23.800	9.359E-05	3220.7133	-47.9401	-8.515E-06	65.3887	9.106E+09	-3.2885
143366.	0.000						
24.140	6.179E-05	2997.7470	-59.1292	-7.122E-06	60.8619	9.106E+09	-2.1964
145031.	0.000						
24.480	3.547E-05	2738.2188	-66.2116	-5.837E-06	55.5928	9.106E+09	-1.2754
146695.	0.000						
24.820	1.416E-05	2457.4600	-69.8639	-4.673E-06	49.8927	9.106E+09	-0.5149
148360.	0.000						
25.160	-2.657E-06	2168.1293	-70.7151	-3.636E-06	44.0185	9.106E+09	0.0977
150025.	0.000						
25.500	-1.551E-05	1880.4252	-69.3392	-2.729E-06	38.1774	9.106E+09	0.5767
151689.	0.000						
25.840	-2.493E-05	1602.3215	-66.2511	-1.949E-06	32.5312	9.106E+09	0.9370
153354.	0.000						
26.180	-3.142E-05	1339.8160	-61.9044	-1.290E-06	27.2017	9.106E+09	1.1937
155019.	0.000						
26.520	-3.546E-05	1097.1816	-56.6914	-7.442E-07	22.2756	9.106E+09	1.3616
156683.	0.000						
26.860	-3.749E-05	877.2138	-50.9454	-3.018E-07	17.8097	9.106E+09	1.4550
158348.	0.000						
27.200	-3.792E-05	681.4670	-44.9433	4.735E-08	13.8355	9.106E+09	1.4872
160013.	0.000						
27.540	-3.710E-05	510.4764	-38.9100	3.144E-07	10.3640	9.106E+09	1.4703
161677.	0.000						
27.880	-3.535E-05	363.9611	-33.0232	5.103E-07	7.3893	9.106E+09	1.4154
163342.	0.000						
28.220	-3.294E-05	241.0074	-27.4180	6.458E-07	4.8931	9.106E+09	1.3322
165006.	0.000						
28.560	-3.008E-05	140.2299	-22.1932	7.312E-07	2.8470	9.106E+09	1.2290
166671.	0.000						

28.900	-2.697E-05	59.9106	-17.4158	7.761E-07	1.2163	9.106E+09	1.1129
168336.	0.000						
29.240	-2.375E-05	-1.8831	-13.1266	7.891E-07	0.0382	9.106E+09	0.9897
170000.	0.000						
29.580	-2.053E-05	-47.2023	-9.3451	7.781E-07	0.9583	9.106E+09	0.8640
171665.	0.000						
29.920	-1.740E-05	-78.1391	-6.0743	7.500E-07	1.5864	9.106E+09	0.7393
173330.	0.000						
30.260	-1.441E-05	-96.7685	-3.3048	7.108E-07	1.9646	9.106E+09	0.6183
174994.	0.000						
30.600	-1.160E-05	-105.1060	-1.0186	6.656E-07	2.1339	9.106E+09	0.5024
176659.	0.000						
30.940	-8.984E-06	-105.0804	0.8073	6.185E-07	2.1334	9.106E+09	0.3927
178324.	0.000						
31.280	-6.556E-06	-98.5184	2.1984	5.729E-07	2.0002	9.106E+09	0.2892
179988.	0.000						
31.620	-4.309E-06	-87.1418	3.1798	5.313E-07	1.7692	9.106E+09	0.1919
181653.	0.000						
31.960	-2.221E-06	-72.5714	3.7748	4.955E-07	1.4734	9.106E+09	0.0998
183317.	0.000						
32.300	-2.659E-07	-56.3397	4.0030	4.666E-07	1.1438	9.106E+09	0.0121
184982.	0.000						
32.640	1.586E-06	-39.9073	3.8795	4.451E-07	0.8102	9.106E+09	-0.0726
186647.	0.000						
32.980	3.366E-06	-24.6830	3.4146	4.306E-07	0.5011	9.106E+09	-0.1553
188311.	0.000						
33.320	5.100E-06	-12.0446	2.6132	4.224E-07	0.2445	9.106E+09	-0.2375
189976.	0.000						
33.660	6.812E-06	-3.3591	1.4760	4.189E-07	0.0682	9.106E+09	-0.3200
191641.	0.000						
34.000	8.518E-06	0.000	0.000	4.182E-07	0.000	9.106E+09	-0.4036
96653.	0.000						

* The above values of total stress are combined axial and bending stresses.

Output Summary for Load Case No. 5:

Pile-head deflection	=	0.9190116 inches
Computed slope at pile head	=	-0.0144024 radians
Maximum bending moment	=	1653129. inch-lbs
Maximum shear force	=	35100. lbs
Depth of maximum bending moment	=	5.4400000 feet below pile head
Depth of maximum shear force	=	0.6800000 feet below pile head
Number of iterations	=	17
Number of zero deflection points	=	4

 Computed Values of Pile Loading and Deflection
 for Lateral Loading for Load Case Number 6

Pile-head conditions are Shear and Moment (Loading Type 1)

Shear force at pile head	=	42000.0 lbs
Applied moment at pile head	=	0.0 in-lbs
Axial thrust load on pile head	=	0.0 lbs

Depth Distrib. X	Deflect. y	Bending Moment	Shear Force	Slope S	Total Stress	Bending Stiffness	Soil Res. p	Soil Spr. Es*h
Lat. Load feet lb/inch	inches	in-lbs	lbs	radians	psi*	lb-in^2	lb/in	lb/inch
0.00	1.2501	3.644E-07	42000.	-0.0188	7.398E-09	9.106E+09	0.000	
0.000	0.000							
0.340	1.1732	171360.	42000.	-0.0188	3479.0446	9.106E+09	0.000	
0.000	0.000							
0.680	1.0966	342720.	42000.	-0.0187	6958.0892	9.106E+09	0.000	
0.000	0.000							
1.020	1.0207	514080.	41992.	-0.0185	10437.	9.106E+09	-3.9508	
15.7927	0.000							
1.360	0.9457	685374.	41798.	-0.0182	13915.	9.106E+09	-91.1787	
393.3791	0.000							

1.700	0.8719	855151.	41190.	-0.0179	17362.	9.106E+09	-206.7611
967.4962	0.000						
2.040	0.7997	1021485.	40081.	-0.0175	20739.	9.106E+09	-336.7897
1718.1860	0.000						
2.380	0.7294	1182214.	38441.	-0.0170	24002.	9.106E+09	-467.3550
2614.1390	0.000						
2.720	0.6613	1335162.	36295.	-0.0164	27107.	9.106E+09	-584.5450
3606.6459	0.000						
3.060	0.5955	1478380.	33727.	-0.0158	30015.	9.106E+09	-674.4503
4620.5565	0.000						
3.400	0.5325	1610371.	30875.	-0.0151	32695.	9.106E+09	-723.1730
5540.5941	0.000						
3.740	0.4725	1730323.	27938.	-0.0143	35130.	9.106E+09	-716.8209
6190.1891	0.000						
4.080	0.4156	1838343.	24746.	-0.0135	37323.	9.106E+09	-847.6561
8322.4580	0.000						
4.420	0.3620	1932253.	20932.	-0.0127	39230.	9.106E+09	-1021.9801
11518.	0.000						
4.760	0.3120	2009150.	16383.	-0.0118	40791.	9.106E+09	-1207.8887
15796.	0.000						
5.100	0.2657	2065941.	11074.	-0.0109	41944.	9.106E+09	-1394.8649
21423.	0.000						
5.440	0.2231	2099511.	5044.1172	-0.009962	42625.	9.106E+09	-1560.8001
28545.	0.000						
5.780	0.1844	2107101.	-1550.9042	-0.009020	42780.	9.106E+09	-1672.0535
37003.	0.000						
6.120	0.1495	2086856.	-8417.7331	-0.008080	42368.	9.106E+09	-1694.0391
46236.	0.000						
6.460	0.1184	2038412.	-15156.	-0.007156	41385.	9.106E+09	-1608.9056
55430.	0.000						
6.800	0.0911	1963185.	-21347.	-0.006260	39858.	9.106E+09	-1425.8719
63864.	0.000						
7.140	0.0673	1864223.	-26652.	-0.005402	37848.	9.106E+09	-1174.9648
71181.	0.000						
7.480	0.0470	1745702.	-30868.	-0.004593	35442.	9.106E+09	-891.7112
77390.	0.000						
7.820	0.0299	1612337.	-33923.	-0.003841	32735.	9.106E+09	-605.4807
82716.	0.000						
8.160	0.0157	1468893.	-35843.	-0.003151	29822.	9.106E+09	-335.7573
87435.	0.000						
8.500	0.004155	1319859.	-36718.	-0.002526	26797.	9.106E+09	-93.4658
91786.	0.000						
8.840	-0.004945	1169270.	-36672.	-0.001968	23739.	9.106E+09	116.2919
95943.	0.000						
9.180	-0.0119	1020617.	-35839.	-0.001478	20721.	9.106E+09	291.9108
100018.	0.000						
9.520	-0.0170	876823.	-34359.	-0.001053	17802.	9.106E+09	433.7711
104077.	0.000						
9.860	-0.0205	740250.	-32365.	-0.000691	15029.	9.106E+09	543.3806
108154.	0.000						
10.200	-0.0226	612722.	-29986.	-0.000387	12440.	9.106E+09	622.9224
112263.	0.000						
10.540	-0.0237	495563.	-27338.	-0.000139	10061.	9.106E+09	675.0165
116404.	0.000						
10.880	-0.0238	389641.	-24528.	5.920E-05	7910.7108	9.106E+09	702.5775
120572.	0.000						
11.220	-0.0232	295415.	-21649.	0.000213	5997.6719	9.106E+09	708.7101
124761.	0.000						
11.560	-0.0220	212986.	-18782.	0.000327	4324.1517	9.106E+09	696.6148
128963.	0.000						
11.900	-0.0205	142153.	-15995.	0.000406	2886.0624	9.106E+09	669.4977
133170.	0.000						
12.240	-0.0187	82465.	-13343.	0.000456	1674.2395	9.106E+09	630.4839
137378.	0.000						
12.580	-0.0168	33272.	-10869.	0.000482	675.4977	9.106E+09	582.5404
141583.	0.000						
12.920	-0.0148	-6224.1589	-8602.3680	0.000488	126.3663	9.106E+09	528.4108
145782.	0.000						
13.260	-0.0128	-36924.	-6564.4555	0.000479	749.6462	9.106E+09	470.5659
149976.	0.000						
13.600	-0.0109	-59790.	-4765.7146	0.000457	1213.8917	9.106E+09	411.1699
154163.	0.000						
13.940	-0.009071	-75812.	-3208.7199	0.000427	1539.1764	9.106E+09	352.0628
158344.	0.000						
14.280	-0.007400	-85973.	-1889.2083	0.000390	1745.4764	9.106E+09	294.7566
162520.	0.000						
14.620	-0.005885	-91228.	-797.4002	0.000351	1852.1592	9.106E+09	240.4434
166692.	0.000						

14.960	-0.004537	-92480.	80.7312	0.000310	1877.5808	9.106E+09	190.0132
170861.	0.000						
15.300	-0.003359	-90569.	762.2801	0.000269	1838.7846	9.106E+09	144.0794
175027.	0.000						
15.640	-0.002345	-86260.	1266.3402	0.000229	1751.2947	9.106E+09	103.0089
179191.	0.000						
15.980	-0.001490	-80236.	1613.0693	0.000192	1628.9916	9.106E+09	66.9563
183354.	0.000						
16.320	-0.000781	-73097.	1791.3486	0.000157	1484.0595	9.106E+09	20.4355
106744.	0.000						
16.660	-0.000206	-65618.	1844.1978	0.000126	1332.2210	9.106E+09	5.4710
108409.	0.000						
17.000	0.000249	-58049.	1841.6359	9.857E-05	1178.5335	9.106E+09	-6.7268
110073.	0.000						
17.340	0.000598	-50591.	1794.4782	7.424E-05	1027.1194	9.106E+09	-16.3898
111738.	0.000						
17.680	0.000855	-43406.	1712.5582	5.318E-05	881.2445	9.106E+09	-23.7671
113402.	0.000						
18.020	0.001032	-36616.	1604.6770	3.525E-05	743.4020	9.106E+09	-29.1159
115067.	0.000						
18.360	0.001143	-30311.	1478.5840	2.026E-05	615.3996	9.106E+09	-32.6943
116731.	0.000						
18.700	0.001198	-24551.	1340.9877	7.966E-06	498.4467	9.106E+09	-34.7549
118396.	0.000						
19.040	0.001208	-19369.	1197.5871	-1.874E-06	393.2398	9.106E+09	-35.5395
120060.	0.000						
19.380	0.001182	-14779.	1053.1234	-9.524E-06	300.0439	9.106E+09	-35.2760
121725.	0.000						
19.720	0.001130	-10776.	911.4436	-1.525E-05	218.7701	9.106E+09	-34.1748
123390.	0.000						
20.060	0.001058	-7341.2541	775.5756	-1.931E-05	149.0462	9.106E+09	-32.4271
125055.	0.000						
20.400	0.000972	-4446.8031	647.8085	-2.195E-05	90.2814	9.106E+09	-30.2038
126719.	0.000						
20.740	0.000879	-2055.1366	529.7767	-2.340E-05	41.7245	9.106E+09	-27.6549
128384.	0.000						
21.080	0.000781	-123.8251	422.5445	-2.389E-05	2.5140	9.106E+09	-24.9099
130049.	0.000						
21.420	0.000684	1392.8263	326.6889	-2.361E-05	28.2779	9.106E+09	-22.0781
131713.	0.000						
21.760	0.000589	2541.9565	242.3797	-2.273E-05	51.6082	9.106E+09	-19.2499
133378.	0.000						
22.100	0.000498	3370.6447	169.4540	-2.140E-05	68.4327	9.106E+09	-16.4980
135043.	0.000						
22.440	0.000414	3924.7010	107.4855	-1.977E-05	79.6814	9.106E+09	-13.8787
136707.	0.000						
22.780	0.000337	4247.7266	55.8475	-1.794E-05	86.2397	9.106E+09	-11.4340
138372.	0.000						
23.120	0.000268	4380.4167	13.7684	-1.600E-05	88.9336	9.106E+09	-9.1930
140037.	0.000						
23.460	0.000207	4360.0765	-19.6193	-1.405E-05	88.5207	9.106E+09	-7.1735
141701.	0.000						
23.800	0.000153	4220.3232	-45.2368	-1.212E-05	85.6833	9.106E+09	-5.3841
143366.	0.000						
24.140	0.000108	3990.9442	-64.0242	-1.028E-05	81.0263	9.106E+09	-3.8254
145031.	0.000						
24.480	6.930E-05	3697.8861	-76.9113	-8.562E-06	75.0765	9.106E+09	-2.4918
146695.	0.000						
24.820	3.775E-05	3363.3483	-84.7950	-6.980E-06	68.2845	9.106E+09	-1.3728
148360.	0.000						
25.160	1.235E-05	3005.9589	-88.5217	-5.553E-06	61.0286	9.106E+09	-0.4541
150025.	0.000						
25.500	-7.560E-06	2641.0109	-88.8746	-4.288E-06	53.6193	9.106E+09	0.2811
151689.	0.000						
25.840	-2.264E-05	2280.7418	-86.5653	-3.185E-06	46.3049	9.106E+09	0.8510
153354.	0.000						
26.180	-3.355E-05	1934.6384	-82.2287	-2.241E-06	39.2781	9.106E+09	1.2748
155019.	0.000						
26.520	-4.093E-05	1609.7556	-76.4219	-1.447E-06	32.6821	9.106E+09	1.5717
156683.	0.000						
26.860	-4.536E-05	1311.0355	-69.6246	-7.925E-07	26.6174	9.106E+09	1.7604
158348.	0.000						
27.200	-4.739E-05	1041.6193	-62.2417	-2.654E-07	21.1475	9.106E+09	1.8587
160013.	0.000						
27.540	-4.752E-05	803.1436	-54.6082	1.478E-07	16.3059	9.106E+09	1.8832
161677.	0.000						
27.880	-4.619E-05	596.0166	-46.9943	4.613E-07	12.1007	9.106E+09	1.8491
163342.	0.000						

28.220	-4.376E-05	419.6699	-39.6119	6.888E-07	8.5204	9.106E+09	1.7698
165006.	0.000						
28.560	-4.057E-05	272.7834	-32.6210	8.440E-07	5.5382	9.106E+09	1.6571
166671.	0.000						
28.900	-3.687E-05	153.4823	-26.1369	9.395E-07	3.1161	9.106E+09	1.5213
168336.	0.000						
29.240	-3.290E-05	59.5059	-20.2369	9.872E-07	1.2081	9.106E+09	1.3708
170000.	0.000						
29.580	-2.882E-05	-11.6511	-14.9670	9.979E-07	0.2365	9.106E+09	1.2125
171665.	0.000						
29.920	-2.476E-05	-62.6245	-10.3479	9.813E-07	1.2714	9.106E+09	1.0517
173330.	0.000						
30.260	-2.081E-05	-96.0900	-6.3815	9.457E-07	1.9509	9.106E+09	0.8926
174994.	0.000						
30.600	-1.704E-05	-114.6973	-3.0555	8.985E-07	2.3286	9.106E+09	0.7378
176659.	0.000						
30.940	-1.348E-05	-121.0226	-0.3485	8.457E-07	2.4571	9.106E+09	0.5891
178324.	0.000						
31.280	-1.014E-05	-117.5410	1.7658	7.922E-07	2.3864	9.106E+09	0.4473
179988.	0.000						
31.620	-7.015E-06	-106.6135	3.3154	7.420E-07	2.1645	9.106E+09	0.3123
181653.	0.000						
31.960	-4.085E-06	-90.4871	4.3269	6.978E-07	1.8371	9.106E+09	0.1835
183317.	0.000						
32.300	-1.320E-06	-71.3056	4.8235	6.616E-07	1.4477	9.106E+09	0.0599
184982.	0.000						
32.640	1.314E-06	-51.1277	4.8229	6.342E-07	1.0380	9.106E+09	-0.0601
186647.	0.000						
32.980	3.855E-06	-31.9505	4.3374	6.156E-07	0.6487	9.106E+09	-0.1779
188311.	0.000						
33.320	6.337E-06	-15.7347	3.3725	6.049E-07	0.3195	9.106E+09	-0.2951
189976.	0.000						
33.660	8.790E-06	-4.4308	1.9283	6.004E-07	0.0900	9.106E+09	-0.4129
191641.	0.000						
34.000	1.124E-05	0.000	0.000	5.994E-07	0.000	9.106E+09	-0.5323
96653.	0.000						

* The above values of total stress are combined axial and bending stresses.

Output Summary for Load Case No. 6:

Pile-head deflection = 1.2500705 inches
 Computed slope at pile head = -0.0188436 radians
 Maximum bending moment = 2107101. inch-lbs
 Maximum shear force = 42000. lbs
 Depth of maximum bending moment = 5.7800000 feet below pile head
 Depth of maximum shear force = 0.6800000 feet below pile head
 Number of iterations = 19
 Number of zero deflection points = 4

 Computed Values of Pile Loading and Deflection
 for Lateral Loading for Load Case Number 7

Pile-head conditions are Shear and Moment (Loading Type 1)

Shear force at pile head = 47600.0 lbs
 Applied moment at pile head = 0.0 in-lbs
 Axial thrust load on pile head = 0.0 lbs

Depth Distrib.	Deflect. X	Bending Moment	Shear Force	Slope S	Total Stress	Bending Stiffness	Soil Res. p	Soil Spr. Es*h
Lat. Load	y	in-lbs	lbs	radians	psi*	lb-in ²	lb/in	lb/inch
feet	inches							
lb/inch								
0.000	0.000	6.073E-07	47600.	-0.0228	1.233E-08	9.106E+09	0.000	
0.000	0.340	194208.	47600.	-0.0227	3942.9172	9.106E+09	0.000	
0.000	0.680	388416.	47600.	-0.0226	7885.8344	9.106E+09	0.000	
0.000	0.000							

1.020	1.2773	582624.	47592.	-0.0224	11829.	9.106E+09	-3.9508
12.6196	0.000						
1.360	1.1865	776766.	47398.	-0.0221	15770.	9.106E+09	-91.1787
313.5277	0.000						
1.700	1.0972	969391.	46790.	-0.0217	19681.	9.106E+09	-206.7610
768.8851	0.000						
2.040	1.0096	1158573.	45681.	-0.0212	23522.	9.106E+09	-336.7899
1361.1008	0.000						
2.380	0.9241	1342150.	44041.	-0.0207	27249.	9.106E+09	-467.3570
2063.4997	0.000						
2.720	0.8410	1517946.	41895.	-0.0200	30818.	9.106E+09	-584.5543
2835.7536	0.000						
3.060	0.7608	1684012.	39326.	-0.0193	34190.	9.106E+09	-674.4734
3617.1206	0.000						
3.400	0.6836	1838850.	36475.	-0.0185	37333.	9.106E+09	-723.2069
4316.3333	0.000						
3.740	0.6098	1981649.	33537.	-0.0176	40233.	9.106E+09	-716.8476
4796.2697	0.000						
4.080	0.5396	2112516.	30346.	-0.0167	42889.	9.106E+09	-847.8401
6410.6236	0.000						
4.420	0.4733	2229269.	26528.	-0.0158	45260.	9.106E+09	-1023.2652
8821.3976	0.000						
4.760	0.4110	2328988.	21964.	-0.0147	47284.	9.106E+09	-1214.1055
12052.	0.000						
5.100	0.3530	2408497.	16597.	-0.0137	48899.	9.106E+09	-1417.0844
16378.	0.000						
5.440	0.2994	2464416.	10397.	-0.0126	50034.	9.106E+09	-1622.0695
22102.	0.000						
5.780	0.2503	2493334.	3403.1859	-0.0115	50621.	9.106E+09	-1806.1363
29437.	0.000						
6.120	0.2058	2492186.	-4221.7428	-0.0104	50598.	9.106E+09	-1931.5738
38293.	0.000						
6.460	0.1658	2458885.	-12152.	-0.009247	49922.	9.106E+09	-1955.9799
48124.	0.000						
6.800	0.1303	2393023.	-19924.	-0.008160	48584.	9.106E+09	-1853.8228
58026.	0.000						
7.140	0.0992	2296302.	-27037.	-0.007110	46621.	9.106E+09	-1632.6844
67122.	0.000						
7.480	0.0723	2172403.	-33078.	-0.006108	44105.	9.106E+09	-1328.4696
74932.	0.000						
7.820	0.0494	2026389.	-37799.	-0.005168	41141.	9.106E+09	-985.9580
81435.	0.000						
8.160	0.0302	1863963.	-41121.	-0.004296	37843.	9.106E+09	-642.4327
86891.	0.000						
8.500	0.0143	1690842.	-43089.	-0.003500	34328.	9.106E+09	-322.0894
91636.	0.000						
8.840	0.001607	1512360.	-43823.	-0.002782	30705.	9.106E+09	-37.7905
95960.	0.000						
9.180	-0.008362	1333249.	-43481.	-0.002145	27068.	9.106E+09	205.1083
100071.	0.000						
9.520	-0.0159	1157552.	-42236.	-0.001587	23501.	9.106E+09	405.5540
104103.	0.000						
9.860	-0.0213	988606.	-40256.	-0.001106	20071.	9.106E+09	564.7789
108131.	0.000						
10.200	-0.0249	829062.	-37706.	-0.000699	16832.	9.106E+09	685.2099
112190.	0.000						
10.540	-0.0270	680924.	-34738.	-0.000360	13824.	9.106E+09	769.9306
116293.	0.000						
10.880	-0.0279	545602.	-31489.	-8.568E-05	11077.	9.106E+09	822.4203
120439.	0.000						
11.220	-0.0277	423971.	-28085.	0.000132	8607.6945	9.106E+09	846.4122
124620.	0.000						
11.560	-0.0268	316430.	-24633.	0.000297	6424.3296	9.106E+09	845.7897
128824.	0.000						
11.900	-0.0253	222968.	-21225.	0.000418	4526.8115	9.106E+09	824.4884
133043.	0.000						
12.240	-0.0234	143230.	-17939.	0.000500	2907.9410	9.106E+09	786.3984
137267.	0.000						
12.580	-0.0212	76584.	-14835.	0.000550	1554.8451	9.106E+09	735.2680
141490.	0.000						
12.920	-0.0189	22177.	-11959.	0.000572	450.2436	9.106E+09	674.6171
145708.	0.000						
13.260	-0.0165	-21000.	-9342.9835	0.000572	426.3614	9.106E+09	607.6654
149918.	0.000						
13.600	-0.0142	-54062.	-7007.2975	0.000555	1097.5972	9.106E+09	537.2788
154120.	0.000						
13.940	-0.0120	-78180.	-4960.7397	0.000525	1587.2519	9.106E+09	465.9359
158313.	0.000						

14.280	-0.009936	-94542.	-3202.9759	0.000487	1919.4369	9.106E+09	395.7130
162499.	0.000						
14.620	-0.008036	-104316.	-1726.0182	0.000442	2117.8850	9.106E+09	328.2859
166678.	0.000						
14.960	-0.006327	-108626.	-515.8279	0.000395	2205.3843	9.106E+09	264.9447
170852.	0.000						
15.300	-0.004817	-108525.	446.1658	0.000346	2203.3416	9.106E+09	206.6208
175021.	0.000						
15.640	-0.003505	-104985.	1181.6700	0.000298	2131.4685	9.106E+09	153.9205
179188.	0.000						
15.980	-0.002385	-98883.	1714.2823	0.000252	2007.5758	9.106E+09	107.1640
183353.	0.000						
16.320	-0.001445	-90997.	2010.0381	0.000210	1847.4654	9.106E+09	37.8143
106743.	0.000						
16.660	-0.000672	-82481.	2123.6282	0.000171	1674.5752	9.106E+09	17.8671
108408.	0.000						
17.000	-5.029E-05	-73668.	2162.8451	0.000136	1495.6465	9.106E+09	1.3568
110073.	0.000						
17.340	0.000437	-64832.	2141.1882	0.000105	1316.2593	9.106E+09	-11.9729
111738.	0.000						
17.680	0.000806	-56196.	2071.0545	7.784E-05	1140.9185	9.106E+09	-22.4063
113402.	0.000						
18.020	0.001072	-47932.	1963.6491	5.451E-05	973.1502	9.106E+09	-30.2434
115067.	0.000						
18.360	0.001251	-40172.	1828.9392	3.478E-05	815.6031	9.106E+09	-35.7908
116731.	0.000						
18.700	0.001356	-33008.	1675.6460	1.838E-05	670.1520	9.106E+09	-39.3529
118396.	0.000						
19.040	0.001401	-26499.	1511.2668	5.049E-06	538.0009	9.106E+09	-41.2252
120060.	0.000						
19.380	0.001397	-20676.	1342.1224	-5.519E-06	419.7823	9.106E+09	-41.6888
121725.	0.000						
19.720	0.001356	-15547.	1173.4245	-1.363E-05	315.6531	9.106E+09	-41.0063
123390.	0.000						
20.060	0.001286	-11101.	1009.3569	-1.960E-05	225.3825	9.106E+09	-39.4189
125054.	0.000						
20.400	0.001196	-7311.1079	853.1679	-2.373E-05	148.4341	9.106E+09	-37.1443
126719.	0.000						
20.740	0.001092	-4139.3421	707.2675	-2.629E-05	84.0392	9.106E+09	-34.3755
128384.	0.000						
21.080	0.000981	-1539.8052	573.3279	-2.757E-05	31.2620	9.106E+09	-31.2811
130049.	0.000						
21.420	0.000867	539.0138	452.3839	-2.779E-05	10.9434	9.106E+09	-28.0052
131713.	0.000						
21.760	0.000755	2151.6472	344.9295	-2.719E-05	43.6839	9.106E+09	-24.6685
133378.	0.000						
22.100	0.000646	3353.6381	251.0109	-2.595E-05	68.0874	9.106E+09	-21.3700
135043.	0.000						
22.440	0.000543	4199.8962	170.3129	-2.426E-05	85.2686	9.106E+09	-18.1879
136707.	0.000						
22.780	0.000448	4743.3917	102.2379	-2.226E-05	96.3029	9.106E+09	-15.1823
138372.	0.000						
23.120	0.000361	5034.1571	45.9769	-2.007E-05	102.2062	9.106E+09	-12.3966
140037.	0.000						
23.460	0.000284	5118.5634	0.5734	-1.779E-05	103.9199	9.106E+09	-9.8600
141701.	0.000						
23.800	0.000216	5038.8357	-35.0230	-1.552E-05	102.3012	9.106E+09	-7.5892
143366.	0.000						
24.140	0.000157	4832.7755	-61.9092	-1.331E-05	98.1177	9.106E+09	-5.5903
145031.	0.000						
24.480	0.000107	4533.6564	-81.1904	-1.121E-05	92.0448	9.106E+09	-3.8612
146695.	0.000						
24.820	6.580E-05	4170.2618	-93.9486	-9.259E-06	84.6669	9.106E+09	-2.3928
148360.	0.000						
25.160	3.184E-05	3767.0359	-101.2182	-7.481E-06	76.4804	9.106E+09	-1.1707
150025.	0.000						
25.500	4.761E-06	3344.3215	-103.9676	-5.888E-06	67.8982	9.106E+09	-0.1770
151689.	0.000						
25.840	-1.620E-05	2918.6606	-103.0862	-4.484E-06	59.2562	9.106E+09	0.6090
153354.	0.000						
26.180	-3.183E-05	2503.1381	-99.3764	-3.270E-06	50.8201	9.106E+09	1.2095
155019.	0.000						
26.520	-4.289E-05	2107.7489	-93.5494	-2.237E-06	42.7927	9.106E+09	1.6469
156683.	0.000						
26.860	-5.009E-05	1739.7749	-86.2243	-1.375E-06	35.3219	9.106E+09	1.9438
158348.	0.000						
27.200	-5.410E-05	1404.1590	-77.9301	-6.706E-07	28.5080	9.106E+09	2.1219
160013.	0.000						

27.540	-5.556E-05	1103.8653	-69.1102	-1.087E-07	22.4113	9.106E+09	2.2016
161677.	0.000						
27.880	-5.499E-05	840.2196	-60.1278	3.268E-07	17.0586	9.106E+09	2.2016
163342.	0.000						
28.220	-5.289E-05	613.2223	-51.2730	6.524E-07	12.4500	9.106E+09	2.1390
165006.	0.000						
28.560	-4.967E-05	421.8322	-42.7702	8.843E-07	8.5643	9.106E+09	2.0290
166671.	0.000						
28.900	-4.567E-05	264.2172	-34.7868	1.038E-06	5.3643	9.106E+09	1.8845
168336.	0.000						
29.240	-4.120E-05	137.9719	-27.4407	1.128E-06	2.8012	9.106E+09	1.7166
170000.	0.000						
29.580	-3.647E-05	40.3014	-20.8086	1.168E-06	0.8182	9.106E+09	1.5344
171665.	0.000						
29.920	-3.167E-05	-31.8264	-14.9340	1.170E-06	0.6462	9.106E+09	1.3453
173330.	0.000						
30.260	-2.692E-05	-81.5601	-9.8340	1.145E-06	1.6559	9.106E+09	1.1547
174994.	0.000						
30.600	-2.233E-05	-112.0718	-5.5062	1.101E-06	2.2753	9.106E+09	0.9667
176659.	0.000						
30.940	-1.794E-05	-126.4909	-1.9348	1.048E-06	2.5681	9.106E+09	0.7840
178324.	0.000						
31.280	-1.378E-05	-127.8598	0.9044	9.907E-07	2.5959	9.106E+09	0.6078
179988.	0.000						
31.620	-9.852E-06	-119.1111	3.0392	9.354E-07	2.4183	9.106E+09	0.4387
181653.	0.000						
31.960	-6.145E-06	-103.0602	4.4973	8.856E-07	2.0924	9.106E+09	0.2761
183317.	0.000						
32.300	-2.626E-06	-82.4134	5.3033	8.441E-07	1.6732	9.106E+09	0.1190
184982.	0.000						
32.640	7.429E-07	-59.7850	5.4769	8.122E-07	1.2138	9.106E+09	-0.0340
186647.	0.000						
32.980	4.002E-06	-37.7223	5.0307	7.904E-07	0.7659	9.106E+09	-0.1847
188311.	0.000						
33.320	7.192E-06	-18.7345	3.9707	7.777E-07	0.3804	9.106E+09	-0.3349
189976.	0.000						
33.660	1.035E-05	-5.3216	2.2959	7.723E-07	0.1080	9.106E+09	-0.4861
191641.	0.000						
34.000	1.349E-05	0.000	0.000	7.712E-07	0.000	9.106E+09	-0.6394
96653.	0.000						

* The above values of total stress are combined axial and bending stresses.

Output Summary for Load Case No. 7:

Pile-head deflection = 1.5546696 inches
 Computed slope at pile head = -0.0227753 radians
 Maximum bending moment = 2493334. inch-lbs
 Maximum shear force = 47600. lbs
 Depth of maximum bending moment = 5.7800000 feet below pile head
 Depth of maximum shear force = 0.0000000 feet below pile head
 Number of iterations = 20
 Number of zero deflection points = 4

 Computed Values of Pile Loading and Deflection
 for Lateral Loading for Load Case Number 8

Pile-head conditions are Shear and Moment (Loading Type 1)

Shear force at pile head = 50200.0 lbs
 Applied moment at pile head = 0.0 in-lbs
 Axial thrust load on pile head = 0.0 lbs

Depth Distrib. X Lat. Load lb/inch	Deflect. y inches	Bending Moment in-lbs	Shear Force lbs	Slope S radians	Total Stress psi*	Bending Stiffness lb-in^2	Soil Res. p lb/in	Soil Spr. Es*h lb/inch
0.000	1.7070	0.000	50200.	-0.0247	0.000	9.106E+09	0.000	

0.000	0.340	1.6062	204816.	50200.	-0.0247	4158.2866	9.106E+09	0.000
0.000	0.680	1.5059	409632.	50200.	-0.0245	8316.5732	9.106E+09	0.000
11.4629	1.020	1.4062	614448.	50192.	-0.0243	12475.	9.106E+09	-3.9508
284.4765	1.360	1.3077	819198.	49998.	-0.0240	16632.	9.106E+09	-91.1785
696.7874	1.700	1.2107	1022431.	49390.	-0.0236	20758.	9.106E+09	-206.7607
1231.7958	2.040	1.1155	1222221.	48281.	-0.0230	24814.	9.106E+09	-336.7892
1864.6526	2.380	1.0226	1416406.	46641.	-0.0225	28757.	9.106E+09	-467.3562
2558.2089	2.720	0.9323	1602810.	44495.	-0.0218	32541.	9.106E+09	-584.5534
3257.0573	3.060	0.8449	1779484.	41926.	-0.0210	36128.	9.106E+09	-674.4729
3878.6747	3.400	0.7607	1944930.	39075.	-0.0202	39487.	9.106E+09	-723.2067
4300.0845	3.740	0.6802	2098338.	36137.	-0.0193	42602.	9.106E+09	-716.8469
5732.8228	4.080	0.6034	2239812.	32946.	-0.0183	45474.	9.106E+09	-847.8480
7866.8909	4.420	0.5307	2367173.	29128.	-0.0173	48060.	9.106E+09	-1023.3685
10719.	4.760	0.4624	2477498.	24562.	-0.0162	50300.	9.106E+09	-1214.8276
14540.	5.100	0.3986	2567602.	19186.	-0.0151	52129.	9.106E+09	-1420.5476
19640.	5.440	0.3395	2634058.	12954.	-0.0139	53478.	9.106E+09	-1634.3393
26316.	5.780	0.2852	2673308.	5867.2805	-0.0127	54275.	9.106E+09	-1839.6326
34671.	6.120	0.2358	2681935.	-1973.5164	-0.0115	54450.	9.106E+09	-2003.8953
44395.	6.460	0.1913	2657204.	-10308.	-0.0103	53948.	9.106E+09	-2081.7130
54692.	6.800	0.1517	2597820.	-18702.	-0.009135	52742.	9.106E+09	-2033.1082
64554.	7.140	0.1168	2504592.	-26619.	-0.007992	50850.	9.106E+09	-1847.5921
73226.	7.480	0.0865	2380609.	-33554.	-0.006897	48332.	9.106E+09	-1551.6663
80459.	7.820	0.0605	2230796.	-39152.	-0.005864	45291.	9.106E+09	-1192.9006
86422.	8.160	0.0386	2061125.	-43254.	-0.004903	41846.	9.106E+09	-817.7140
91466.	8.500	0.0205	1877842.	-45859.	-0.004020	38125.	9.106E+09	-459.2403
95936.	8.840	0.005799	1686915.	-47074.	-0.003222	34249.	9.106E+09	-136.3562
100098.	9.180	-0.005803	1493718.	-47062.	-0.002509	30326.	9.106E+09	142.3792
104130.	9.520	-0.0147	1302891.	-46007.	-0.001883	26452.	9.106E+09	374.5396
108135.	9.860	-0.0212	1118298.	-44099.	-0.001340	22704.	9.106E+09	560.9538
112166.	10.200	-0.0256	943044.	-41518.	-0.000878	19146.	9.106E+09	704.0876
116246.	10.540	-0.0283	779510.	-38435.	-0.000492	15826.	9.106E+09	807.2405
120375.	10.880	-0.0296	629414.	-35005.	-0.000177	12779.	9.106E+09	874.1739
124547.	11.220	-0.0298	493869.	-31367.	7.483E-05	10027.	9.106E+09	908.9307
128750.	11.560	-0.0290	373455.	-27645.	0.000269	7582.0912	9.106E+09	915.7249
132972.	11.900	-0.0276	268285.	-23943.	0.000413	5446.8619	9.106E+09	898.8438
137203.	12.240	-0.0256	178077.	-20350.	0.000513	3615.4097	9.106E+09	862.5483
141436.	12.580	-0.0234	102227.	-16936.	0.000576	2075.4681	9.106E+09	810.9703
145663.	12.920	-0.0210	39877.	-13756.	0.000608	809.6055	9.106E+09	748.0174
149883.	13.260	-0.0184	-10021.	-10848.	0.000614	203.4539	9.106E+09	677.2890

13.600	-0.0159	-48645.	-8238.4908	0.000601	987.6137	9.106E+09	602.0130
154093.	0.000						
13.940	-0.0135	-77247.	-5939.3797	0.000573	1568.3147	9.106E+09	525.0023
158293.	0.000						
14.280	-0.0113	-97110.	-3953.1642	0.000534	1971.5836	9.106E+09	448.6328
162485.	0.000						
14.620	-0.009176	-109505.	-2273.2778	0.000488	2223.2306	9.106E+09	374.8409
166668.	0.000						
14.960	-0.007287	-115660.	-886.1254	0.000437	2348.1947	9.106E+09	305.1358
170845.	0.000						
15.300	-0.005609	-116736.	227.2284	0.000385	2370.0339	9.106E+09	240.6259
175017.	0.000						
15.640	-0.004145	-113806.	1089.4947	0.000333	2310.5501	9.106E+09	182.0537
179186.	0.000						
15.980	-0.002889	-107846.	1725.7523	0.000284	2189.5386	9.106E+09	129.8373
183352.	0.000						
16.320	-0.001830	-99724.	2088.3014	0.000237	2024.6468	9.106E+09	47.8828
106743.	0.000						
16.660	-0.000954	-90805.	2237.6688	0.000195	1843.5723	9.106E+09	25.3365
108408.	0.000						
17.000	-0.000243	-81464.	2302.7228	0.000156	1653.9349	9.106E+09	6.5527
110073.	0.000						
17.340	0.000319	-72015.	2298.2760	0.000122	1462.0830	9.106E+09	-8.7325
111738.	0.000						
17.680	0.000749	-62710.	2237.9949	9.137E-05	1273.1823	9.106E+09	-20.8170
113402.	0.000						
18.020	0.001064	-53753.	2134.2888	6.528E-05	1091.3171	9.106E+09	-30.0193
115067.	0.000						
18.360	0.001282	-45295.	1998.2477	4.309E-05	919.5973	9.106E+09	-36.6675
116731.	0.000						
18.700	0.001416	-37447.	1839.6218	2.455E-05	760.2698	9.106E+09	-41.0903
118396.	0.000						
19.040	0.001482	-30283.	1666.8369	9.377E-06	614.8294	9.106E+09	-43.6082
120060.	0.000						
19.380	0.001493	-23846.	1487.0382	-2.750E-06	484.1269	9.106E+09	-44.5284
121725.	0.000						
19.720	0.001459	-18149.	1306.1570	-1.216E-05	368.4735	9.106E+09	-44.1389
123389.	0.000						
20.060	0.001393	-13187.	1128.9944	-1.918E-05	267.7375	9.106E+09	-42.7055
125054.	0.000						
20.400	0.001303	-8936.5339	959.3174	-2.413E-05	181.4344	9.106E+09	-40.4694
126719.	0.000						
20.740	0.001196	-5359.3541	799.9628	-2.734E-05	108.8085	9.106E+09	-37.6456
128384.	0.000						
21.080	0.001080	-2408.8378	652.9440	-2.908E-05	48.9055	9.106E+09	-34.4224
130048.	0.000						
21.420	0.000959	-31.3313	519.5595	-2.962E-05	0.6361	9.106E+09	-30.9621
131713.	0.000						
21.760	0.000838	1830.7673	400.4981	-2.922E-05	37.1692	9.106E+09	-27.4013
133378.	0.000						
22.100	0.000721	3236.7328	295.9401	-2.809E-05	65.7139	9.106E+09	-23.8526
135043.	0.000						
22.440	0.000609	4245.6382	205.6520	-2.641E-05	86.1973	9.106E+09	-20.4062
136707.	0.000						
22.780	0.000505	4914.8530	129.0739	-2.436E-05	99.7840	9.106E+09	-17.1320
138372.	0.000						
23.120	0.000410	5298.8815	65.3986	-2.207E-05	107.5808	9.106E+09	-14.0814
140037.	0.000						
23.460	0.000325	5448.5055	13.6414	-1.966E-05	110.6185	9.106E+09	-11.2898
141701.	0.000						
23.800	0.000250	5410.1956	-27.2980	-1.723E-05	109.8408	9.106E+09	-8.7786
143366.	0.000						
24.140	0.000184	5225.7534	-58.5840	-1.485E-05	106.0961	9.106E+09	-6.5576
145031.	0.000						
24.480	0.000129	4932.1505	-81.4002	-1.257E-05	100.1352	9.106E+09	-4.6268
146695.	0.000						
24.820	8.190E-05	4561.5282	-96.9145	-1.044E-05	92.6106	9.106E+09	-2.9783
148360.	0.000						
25.160	4.346E-05	4141.3282	-106.2506	-8.494E-06	84.0795	9.106E+09	-1.5982
150025.	0.000						
25.500	1.260E-05	3694.5236	-110.4662	-6.738E-06	75.0082	9.106E+09	-0.4683
151689.	0.000						
25.840	-1.152E-05	3239.9239	-110.5381	-5.185E-06	65.7787	9.106E+09	0.4330
153354.	0.000						
26.180	-2.971E-05	2792.5324	-107.3517	-3.833E-06	56.6955	9.106E+09	1.1290
155019.	0.000						
26.520	-4.280E-05	2363.9339	-101.6955	-2.678E-06	47.9939	9.106E+09	1.6437
156683.	0.000						

26.860	-5.157E-05	1962.6968	-94.2596	-1.709E-06	39.8477	9.106E+09	2.0014
158348.	0.000						
27.200	-5.675E-05	1594.7754	-85.6368	-9.120E-07	32.3780	9.106E+09	2.2255
160013.	0.000						
27.540	-5.901E-05	1263.9008	-76.3265	-2.715E-07	25.6604	9.106E+09	2.3383
161677.	0.000						
27.880	-5.896E-05	971.9513	-66.7408	2.294E-07	19.7331	9.106E+09	2.3605
163342.	0.000						
28.220	-5.714E-05	719.2960	-57.2113	6.082E-07	14.6035	9.106E+09	2.3108
165006.	0.000						
28.560	-5.400E-05	505.1073	-47.9972	8.825E-07	10.2550	9.106E+09	2.2059
166671.	0.000						
28.900	-4.994E-05	327.6388	-39.2942	1.069E-06	6.6519	9.106E+09	2.0603
168336.	0.000						
29.240	-4.527E-05	184.4669	-31.2428	1.184E-06	3.7451	9.106E+09	1.8865
170000.	0.000						
29.580	-4.028E-05	72.6977	-23.9374	1.241E-06	1.4759	9.106E+09	1.6946
171665.	0.000						
29.920	-3.514E-05	-10.8624	-17.4346	1.255E-06	0.2205	9.106E+09	1.4930
173330.	0.000						
30.260	-3.003E-05	-69.5686	-11.7610	1.237E-06	1.4124	9.106E+09	1.2881
174994.	0.000						
30.600	-2.505E-05	-106.8319	-6.9206	1.198E-06	2.1690	9.106E+09	1.0846
176659.	0.000						
30.940	-2.026E-05	-126.0410	-2.9018	1.146E-06	2.5590	9.106E+09	0.8855
178324.	0.000						
31.280	-1.570E-05	-130.5102	0.3176	1.088E-06	2.6497	9.106E+09	0.6926
179988.	0.000						
31.620	-1.138E-05	-123.4496	2.7642	1.031E-06	2.5063	9.106E+09	0.5067
181653.	0.000						
31.960	-7.286E-06	-107.9545	4.4656	9.794E-07	2.1918	9.106E+09	0.3274
183317.	0.000						
32.300	-3.389E-06	-87.0100	5.4469	9.357E-07	1.7665	9.106E+09	0.1536
184982.	0.000						
32.640	3.494E-07	-63.5079	5.7277	9.020E-07	1.2894	9.106E+09	-0.0160
186647.	0.000						
32.980	3.971E-06	-40.2719	5.3212	8.787E-07	0.8176	9.106E+09	-0.1833
188311.	0.000						
33.320	7.520E-06	-20.0871	4.2330	8.652E-07	0.4078	9.106E+09	-0.3501
189976.	0.000						
33.660	1.103E-05	-5.7308	2.4617	8.594E-07	0.1164	9.106E+09	-0.5182
191641.	0.000						
34.000	1.453E-05	0.000	0.000	8.581E-07	0.000	9.106E+09	-0.6885
96653.	0.000						

* The above values of total stress are combined axial and bending stresses.

Output Summary for Load Case No. 8:

Pile-head deflection = 1.7070015 inches
 Computed slope at pile head = -0.0246968 radians
 Maximum bending moment = 2681935. inch-lbs
 Maximum shear force = 50200. lbs
 Depth of maximum bending moment = 6.1200000 feet below pile head
 Depth of maximum shear force = 0.6800000 feet below pile head
 Number of iterations = 21
 Number of zero deflection points = 4

 Computed Values of Pile Loading and Deflection
 for Lateral Loading for Load Case Number 9

Pile-head conditions are Shear and Moment (Loading Type 1)

Shear force at pile head = 54800.0 lbs
 Applied moment at pile head = 0.0 in-lbs
 Axial thrust load on pile head = 0.0 lbs

Depth Distrib.	Deflect. X	Bending Moment	Shear Force	Slope S	Total Stress	Bending Stiffness	Soil Res. p	Soil Spr. Es*h
Lat. Load	feet	in-lbs	lbs	radians	psi*	lb-in ²	lb/in	lb/inch
lb/inch	inches							

0.00	1.9934	9.717E-07	54800.	-0.0282	1.973E-08	9.106E+09	0.000	
0.000	0.000							
0.000	0.340	1.8782	223584.	54800.	-0.0282	4539.3248	9.106E+09	0.000
0.000	0.000							
0.000	0.680	1.7634	447168.	54800.	-0.0280	9078.6497	9.106E+09	0.000
0.000	0.000							
9.7727	1.020	1.6494	670752.	54792.	-0.0278	13618.	9.106E+09	-3.9508
	0.000							
242.0926	1.360	1.5366	894270.	54598.	-0.0274	18156.	9.106E+09	-91.1784
	0.000							
591.7816	1.700	1.4255	1116271.	53990.	-0.0270	22663.	9.106E+09	-206.7605
	0.000							
1043.8311	2.040	1.3164	1334829.	52881.	-0.0264	27100.	9.106E+09	-336.7890
	0.000							
1576.2127	2.380	1.2097	1547782.	51241.	-0.0258	31424.	9.106E+09	-467.3558
	0.000							
2156.5638	2.720	1.1059	1752954.	49095.	-0.0251	35589.	9.106E+09	-584.5531
	0.000							
2737.3621	3.060	1.0053	1948396.	46526.	-0.0242	39557.	9.106E+09	-674.4726
	0.000							
3248.8247	3.400	0.9082	2132610.	43675.	-0.0233	43297.	9.106E+09	-723.2064
	0.000							
3588.3312	3.740	0.8151	2304786.	40738.	-0.0223	46793.	9.106E+09	-716.8465
	0.000							
4764.0005	4.080	0.7261	2465028.	37546.	-0.0212	50046.	9.106E+09	-847.8502
	0.000							
6507.2118	4.420	0.6417	2611157.	33728.	-0.0201	53013.	9.106E+09	-1023.4111
	0.000							
8822.0740	4.760	0.5620	2740250.	29161.	-0.0189	55634.	9.106E+09	-1215.2093
	0.000							
11912.	5.100	0.4873	2849114.	23780.	-0.0177	57844.	9.106E+09	-1422.8181
	0.000							
16052.	5.440	0.4179	2934293.	17523.	-0.0164	59574.	9.106E+09	-1644.0731
	0.000							
21578.	5.780	0.3538	2992104.	10352.	-0.0150	60747.	9.106E+09	-1871.2137
	0.000							
28804.	6.120	0.2952	3018767.	2283.6405	-0.0137	61289.	9.106E+09	-2083.9363
	0.000							
37808.	6.460	0.2421	3010739.	-6544.0581	-0.0123	61126.	9.106E+09	-2243.3670
	0.000							
48192.	6.800	0.1945	2965367.	-15807.	-0.0110	60205.	9.106E+09	-2297.2821
	0.000							
59022.	7.140	0.1523	2881754.	-24988.	-0.009691	58507.	9.106E+09	-2203.4507
	0.000							
69191.	7.480	0.1154	2761461.	-33476.	-0.008427	56065.	9.106E+09	-1957.1743
	0.000							
77937.	7.820	0.0836	2608588.	-40725.	-0.007224	52961.	9.106E+09	-1595.9952
	0.000							
85086.	8.160	0.0565	2429148.	-46382.	-0.006096	49318.	9.106E+09	-1177.4467
	0.000							
90897.	8.500	0.0338	2230108.	-50321.	-0.005052	45277.	9.106E+09	-753.2632
	0.000							
95783.	8.840	0.0152	2018528.	-52588.	-0.004100	40981.	9.106E+09	-357.7400
	0.000							
100123.	9.180	0.000356	1800993.	-53335.	-0.003244	36565.	9.106E+09	-8.7310
	0.000							
104194.	9.520	-0.0112	1583313.	-52768.	-0.002486	32145.	9.106E+09	286.9037
	0.000							
108170.	9.860	-0.0199	1370409.	-51104.	-0.001824	27823.	9.106E+09	528.3997
	0.000							
112149.	10.200	-0.0261	1166301.	-48562.	-0.001256	23679.	9.106E+09	718.0014
	0.000							
116176.	10.540	-0.0302	974145.	-45344.	-0.000777	19778.	9.106E+09	859.3488
	0.000							
120265.	10.880	-0.0325	796294.	-41639.	-0.000380	16167.	9.106E+09	956.7360
	0.000							
124412.	11.220	-0.0333	634369.	-37617.	-5.938E-05	12879.	9.106E+09	1014.7968
	0.000							
128605.	11.560	-0.0329	489337.	-33429.	0.000192	9934.7958	9.106E+09	1038.3613
	0.000							
132830.	11.900	-0.0317	361590.	-29205.	0.000383	7341.2052	9.106E+09	1032.3611
	0.000							
137073.	12.240	-0.0298	251028.	-25055.	0.000520	5096.5159	9.106E+09	1001.7333
	0.000							
141321.	12.580	-0.0275	157142.	-21071.	0.000612	3190.3767	9.106E+09	951.3151
	0.000							

12.920	-0.0248	79091.	-17323.	0.000665	1605.7480	9.106E+09	885.7345
145568.	0.000						
13.260	-0.0220	15785.	-13865.	0.000686	320.4660	9.106E+09	809.3084
149806.	0.000						
13.600	-0.0192	-34050.	-10733.	0.000682	691.2986	9.106E+09	725.9575
154033.	0.000						
13.940	-0.0165	-71800.	-7948.5451	0.000658	1457.7154	9.106E+09	639.1441
158249.	0.000						
14.280	-0.0139	-98910.	-5518.9496	0.000620	2008.1244	9.106E+09	551.8341
162453.	0.000						
14.620	-0.0114	-116834.	-3441.5820	0.000571	2372.0331	9.106E+09	466.4834
166646.	0.000						
14.960	-0.009196	-126993.	-1704.4670	0.000517	2578.2871	9.106E+09	385.0436
170831.	0.000						
15.300	-0.007203	-130743.	-288.6465	0.000459	2654.4101	9.106E+09	308.9861
175008.	0.000						
15.640	-0.005450	-129349.	829.9334	0.000401	2626.1068	9.106E+09	239.3374
179180.	0.000						
15.980	-0.003933	-123970.	1678.7001	0.000344	2516.9161	9.106E+09	176.7247
183348.	0.000						
16.320	-0.002642	-115650.	2180.2254	0.000290	2347.9986	9.106E+09	69.1210
106741.	0.000						
16.660	-0.001563	-106180.	2405.9463	0.000241	2155.7208	9.106E+09	41.5266
108408.	0.000						
17.000	-0.000678	-96018.	2527.9662	0.000195	1949.4084	9.106E+09	18.2871
110073.	0.000						
17.340	3.169E-05	-85552.	2563.5014	0.000155	1736.9157	9.106E+09	-0.8678
111738.	0.000						
17.680	0.000585	-75100.	2528.5714	0.000119	1524.7162	9.106E+09	-16.2548
113402.	0.000						
18.020	0.001001	-64918.	2437.8406	8.738E-05	1318.0103	9.106E+09	-28.2211
115067.	0.000						
18.360	0.001298	-55207.	2304.5216	6.047E-05	1120.8421	9.106E+09	-37.1313
116731.	0.000						
18.700	0.001494	-46114.	2140.3286	3.777E-05	936.2230	9.106E+09	-43.3554
118395.	0.000						
19.040	0.001606	-37742.	1955.4751	1.898E-05	766.2565	9.106E+09	-47.2590
120060.	0.000						
19.380	0.001649	-30157.	1758.7076	3.771E-06	612.2618	9.106E+09	-49.1956
121725.	0.000						
19.720	0.001637	-23391.	1557.3685	-8.226E-06	474.8935	9.106E+09	-49.5000
123389.	0.000						
20.060	0.001582	-17449.	1357.4812	-1.737E-05	354.2545	9.106E+09	-48.4839
125054.	0.000						
20.400	0.001495	-12314.	1163.8522	-2.404E-05	250.0013	9.106E+09	-46.4323
126719.	0.000						
20.740	0.001386	-7951.7356	980.1833	-2.858E-05	161.4405	9.106E+09	-43.6015
128383.	0.000						
21.080	0.001262	-4315.4919	809.1913	-3.133E-05	87.6155	9.106E+09	-40.2181
130048.	0.000						
21.420	0.001130	-1348.7348	652.7293	-3.260E-05	27.3828	9.106E+09	-36.4790
131713.	0.000						
21.760	0.000996	1010.7790	511.9068	-3.268E-05	20.5214	9.106E+09	-32.5517
133378.	0.000						
22.100	0.000863	2828.4250	387.2065	-3.182E-05	57.4242	9.106E+09	-28.5760
135043.	0.000						
22.440	0.000736	4170.3840	278.5939	-3.025E-05	84.6694	9.106E+09	-24.6655
136707.	0.000						
22.780	0.000617	5101.7515	185.6205	-2.817E-05	103.5786	9.106E+09	-20.9097
138372.	0.000						
23.120	0.000506	5685.0473	107.5166	-2.575E-05	115.4209	9.106E+09	-17.3765
140037.	0.000						
23.460	0.000406	5979.0870	43.2756	-2.314E-05	121.3907	9.106E+09	-14.1142
141701.	0.000						
23.800	0.000317	6038.1758	-8.2726	-2.045E-05	122.5904	9.106E+09	-11.1545
143366.	0.000						
24.140	0.000240	5911.5824	-48.3975	-1.777E-05	120.0202	9.106E+09	-8.5146
145031.	0.000						
24.480	0.000172	5643.2519	-78.4145	-1.518E-05	114.5724	9.106E+09	-6.1996
146695.	0.000						
24.820	0.000116	5271.7197	-99.6401	-1.274E-05	107.0293	9.106E+09	-4.2051
148360.	0.000						
25.160	6.849E-05	4830.1885	-113.3562	-1.047E-05	98.0651	9.106E+09	-2.5185
150025.	0.000						
25.500	3.017E-05	4346.7330	-120.7824	-8.418E-06	88.2498	9.106E+09	-1.1218
151689.	0.000						
25.840	-2.011E-07	3844.6040	-123.0554	-6.583E-06	78.0553	9.106E+09	0.007560
153354.	0.000						

26.180	-2.355E-05	3342.6008	-121.2149	-4.973E-06	67.8633	9.106E+09	0.8946
155019.	0.000						
26.520	-4.078E-05	2855.4903	-116.1949	-3.585E-06	57.9737	9.106E+09	1.5661
156683.	0.000						
26.860	-5.280E-05	2394.4501	-108.8199	-2.408E-06	48.6134	9.106E+09	2.0491
158348.	0.000						
27.200	-6.043E-05	1967.5196	-99.8047	-1.431E-06	39.9457	9.106E+09	2.3702
160013.	0.000						
27.540	-6.448E-05	1580.0436	-89.7575	-6.365E-07	32.0789	9.106E+09	2.5549
161677.	0.000						
27.880	-6.563E-05	1235.0982	-79.1856	-5.782E-09	25.0756	9.106E+09	2.6274
163342.	0.000						
28.220	-6.452E-05	933.8893	-68.5024	4.801E-07	18.9603	9.106E+09	2.6095
165006.	0.000						
28.560	-6.171E-05	676.1185	-58.0365	8.408E-07	13.7269	9.106E+09	2.5209
166671.	0.000						
28.900	-5.766E-05	460.3114	-48.0407	1.095E-06	9.3455	9.106E+09	2.3790
168336.	0.000						
29.240	-5.277E-05	284.1066	-38.7019	1.262E-06	5.7681	9.106E+09	2.1988
170000.	0.000						
29.580	-4.736E-05	144.5041	-30.1511	1.358E-06	2.9338	9.106E+09	1.9927
171665.	0.000						
29.920	-4.169E-05	38.0734	-22.4730	1.399E-06	0.7730	9.106E+09	1.7710
173330.	0.000						
30.260	-3.595E-05	-38.8760	-15.7150	1.399E-06	0.7893	9.106E+09	1.5417
174994.	0.000						
30.600	-3.027E-05	-90.1614	-9.8960	1.370E-06	1.8305	9.106E+09	1.3108
176659.	0.000						
30.940	-2.477E-05	-119.6270	-5.0138	1.323E-06	2.4287	9.106E+09	1.0824
178324.	0.000						
31.280	-1.948E-05	-131.0739	-1.0528	1.267E-06	2.6611	9.106E+09	0.8592
179988.	0.000						
31.620	-1.443E-05	-128.2178	2.0105	1.209E-06	2.6031	9.106E+09	0.6424
181653.	0.000						
31.960	-9.614E-06	-114.6683	4.2021	1.154E-06	2.3281	9.106E+09	0.4319
183317.	0.000						
32.300	-5.009E-06	-93.9283	5.5466	1.108E-06	1.9070	9.106E+09	0.2271
184982.	0.000						
32.640	-5.755E-07	-69.4082	6.0635	1.071E-06	1.4092	9.106E+09	0.0263
186647.	0.000						
32.980	3.731E-06	-44.4498	5.7660	1.046E-06	0.9024	9.106E+09	-0.1722
188311.	0.000						
33.320	7.956E-06	-22.3580	4.6590	1.031E-06	0.4539	9.106E+09	-0.3705
189976.	0.000						
33.660	1.214E-05	-6.4328	2.7399	1.024E-06	0.1306	9.106E+09	-0.5702
191641.	0.000						
34.000	1.631E-05	0.000	0.000	1.023E-06	0.000	9.106E+09	-0.7729
96653.	0.000						

* The above values of total stress are combined axial and bending stresses.

Output Summary for Load Case No. 9:

Pile-head deflection = 1.9934477 inches
 Computed slope at pile head = -0.0282414 radians
 Maximum bending moment = 3018767. inch-lbs
 Maximum shear force = 54800. lbs
 Depth of maximum bending moment = 6.1200000 feet below pile head
 Depth of maximum shear force = 0.6800000 feet below pile head
 Number of iterations = 22
 Number of zero deflection points = 4

 Computed Values of Pile Loading and Deflection
 for Lateral Loading for Load Case Number 10

Pile-head conditions are Shear and Moment (Loading Type 1)

Shear force at pile head = 59200.0 lbs
 Applied moment at pile head = 0.0 in-lbs
 Axial thrust load on pile head = 0.0 lbs

Depth Distrib.	Deflect.	Bending	Shear	Slope	Total	Bending	Soil Res.	Soil Spr.
----------------	----------	---------	-------	-------	-------	---------	-----------	-----------

Lat.	X feet lb/inch	Load lb/inch	y inches	Moment in-lbs	Force lbs	S radians	Stress psi*	Stiffness lb-in ²	p lb/in	Es*h lb/inch
0.000	0.000	0.000	2.2877	9.717E-07	59200.	-0.0318	1.973E-08	9.106E+09	0.000	
0.000	0.340	0.000	2.1579	241536.	59200.	-0.0317	4903.7962	9.106E+09	0.000	
0.000	0.680	0.000	2.0286	483072.	59200.	-0.0316	9807.5924	9.106E+09	0.000	
8.4829	1.020	0.000	1.9002	724608.	59192.	-0.0313	14711.	9.106E+09	-3.9508	
209.8063	1.360	0.000	1.7731	966078.	58998.	-0.0309	19614.	9.106E+09	-91.1784	
511.9555	1.700	0.000	1.6478	1206031.	58390.	-0.0304	24485.	9.106E+09	-206.7604	
901.2643	2.040	0.000	1.5246	1442541.	57281.	-0.0299	29287.	9.106E+09	-336.7887	
1357.9919	2.380	0.000	1.4041	1673446.	55641.	-0.0292	33975.	9.106E+09	-467.3555	
1853.5523	2.720	0.000	1.2867	1896570.	53495.	-0.0284	38505.	9.106E+09	-584.5526	
2346.5159	3.060	0.000	1.1727	2109964.	50926.	-0.0275	42838.	9.106E+09	-674.4721	
2776.7803	3.400	0.000	1.0626	2312130.	48075.	-0.0265	46942.	9.106E+09	-723.2058	
3056.9684	3.740	0.000	0.9567	2502258.	45138.	-0.0254	50802.	9.106E+09	-716.8459	
4043.8324	4.080	0.000	0.8554	2680452.	41946.	-0.0242	54420.	9.106E+09	-847.8496	
5501.1930	4.420	0.000	0.7590	2844533.	38128.	-0.0230	57751.	9.106E+09	-1023.4149	
7424.6773	4.760	0.000	0.6678	2991578.	33561.	-0.0217	60737.	9.106E+09	-1215.2696	
9976.6714	5.100	0.000	0.5821	3118393.	28179.	-0.0203	63311.	9.106E+09	-1423.3207	
13384.	5.440	0.000	0.5020	3221515.	21915.	-0.0189	65405.	9.106E+09	-1646.9196	
17955.	5.780	0.000	0.4279	3297221.	14714.	-0.0174	66942.	9.106E+09	-1882.9797	
24054.	6.120	0.000	0.3598	3341583.	6546.1266	-0.0159	67843.	9.106E+09	-2120.9937	
31993.	6.460	0.000	0.2977	3350638.	-2543.6213	-0.0144	68026.	9.106E+09	-2334.7651	
41783.	6.800	0.000	0.2419	3320827.	-12359.	-0.0130	67421.	9.106E+09	-2476.8025	
52864.	7.140	0.000	0.1920	3249786.	-22488.	-0.0115	65979.	9.106E+09	-2488.1541	
64129.	7.480	0.000	0.1482	3137327.	-32314.	-0.0101	63696.	9.106E+09	-2328.7194	
74400.	7.820	0.000	0.1100	2986103.	-41157.	-0.008680	60625.	9.106E+09	-2006.1487	
82992.	8.160	0.000	0.0773	2801484.	-48459.	-0.007383	56877.	9.106E+09	-1572.9822	
89869.	8.500	0.000	0.0498	2590680.	-53904.	-0.006175	52597.	9.106E+09	-1096.2169	
95406.	8.840	0.000	0.0269	2361628.	-57425.	-0.005066	47947.	9.106E+09	-629.9706	
100070.	9.180	0.008431	0.000	2122089.	-59132.	-0.004061	43084.	9.106E+09	-206.7886	
104257.	9.520	-0.006199	0.000	1879109.	-59231.	-0.003165	38151.	9.106E+09	158.4083	
108236.	9.860	0.000	-0.0174	1638765.	-57966.	-0.002377	33271.	9.106E+09	461.4401	
112167.	10.200	0.000	-0.0256	1406102.	-55590.	-0.001695	28547.	9.106E+09	703.6145	
116134.	10.540	0.000	-0.0312	1185152.	-52341.	-0.001114	24062.	9.106E+09	888.7206	
120171.	10.880	0.000	-0.0347	978996.	-48444.	-0.000629	19876.	9.106E+09	1021.5867	
124281.	11.220	0.000	-0.0364	789846.	-44101.	-0.000233	16036.	9.106E+09	1107.4788	
128455.	11.560	0.000	-0.0366	619131.	-39492.	8.264E-05	12570.	9.106E+09	1151.8724	
132675.	11.900	0.000	-0.0357	467591.	-34775.	0.000326	9493.2869	9.106E+09	1160.3507	

12.240	-0.0339	335366.	-30085.	0.000506	6808.7922	9.106E+09	1138.5233
136925.	0.000						
12.580	-0.0316	222094.	-25535.	0.000631	4509.0778	9.106E+09	1091.9276
141188.	0.000						
12.920	-0.0288	126999.	-21215.	0.000709	2578.3960	9.106E+09	1025.9152
145453.	0.000						
13.260	-0.0258	48981.	-17193.	0.000749	994.4370	9.106E+09	945.5358
149712.	0.000						
13.600	-0.0227	-13297.	-13519.	0.000756	269.9648	9.106E+09	855.4307
153959.	0.000						
13.940	-0.0196	-61335.	-10224.	0.000740	1245.2614	9.106E+09	759.7502
158192.	0.000						
14.280	-0.0166	-96726.	-7323.5973	0.000704	1963.7895	9.106E+09	662.0959
162411.	0.000						
14.620	-0.0138	-121096.	-4819.3178	0.000656	2458.5529	9.106E+09	565.4921
166616.	0.000						
14.960	-0.0113	-136052.	-2702.0531	0.000598	2762.2001	9.106E+09	472.3827
170810.	0.000						
15.300	-0.008968	-143145.	-953.7077	0.000535	2906.1988	9.106E+09	384.6493
174995.	0.000						
15.640	-0.006914	-143834.	450.4150	0.000471	2920.1997	9.106E+09	303.6461
179172.	0.000						
15.980	-0.005124	-139469.	1539.5572	0.000408	2831.5790	9.106E+09	230.2471
183344.	0.000						
16.320	-0.003588	-131271.	2200.7510	0.000347	2665.1431	9.106E+09	93.8675
106738.	0.000						
16.660	-0.002292	-121511.	2516.4884	0.000290	2466.9833	9.106E+09	60.9057
108406.	0.000						
17.000	-0.001219	-110737.	2707.8048	0.000238	2248.2395	9.106E+09	32.8768
110073.	0.000						
17.340	-0.000347	-99415.	2794.2839	0.000191	2018.3846	9.106E+09	9.5149
111738.	0.000						
17.680	0.000342	-87935.	2794.3007	0.000149	1785.3139	9.106E+09	-9.5067
113403.	0.000						
18.020	0.000871	-76614.	2724.8104	0.000112	1555.4561	9.106E+09	-24.5572
115067.	0.000						
18.360	0.001259	-65701.	2601.2086	8.054E-05	1333.8979	9.106E+09	-36.0319
116731.	0.000						
18.700	0.001528	-55388.	2437.2529	5.341E-05	1124.5171	9.106E+09	-44.3385
118395.	0.000						
19.040	0.001695	-45813.	2245.0378	3.074E-05	930.1211	9.106E+09	-49.8846
120060.	0.000						
19.380	0.001779	-37068.	2035.0131	1.217E-05	752.5844	9.106E+09	-53.0687
121724.	0.000						
19.720	0.001795	-29207.	1816.0388	-2.676E-06	592.9830	9.106E+09	-54.2716
123389.	0.000						
20.060	0.001757	-22250.	1595.4686	-1.420E-05	451.7234	9.106E+09	-53.8510
125054.	0.000						
20.400	0.001679	-16188.	1379.2542	-2.281E-05	328.6636	9.106E+09	-52.1364
126718.	0.000						
20.740	0.001571	-10995.	1172.0653	-2.890E-05	223.2240	9.106E+09	-49.4268
128383.	0.000						
21.080	0.001443	-6624.2407	977.4183	-3.285E-05	134.4890	9.106E+09	-45.9884
130048.	0.000						
21.420	0.001303	-3019.1449	797.8103	-3.501E-05	61.2963	9.106E+09	-42.0547
131713.	0.000						
21.760	0.001157	-114.1089	634.8530	-3.571E-05	2.3167	9.106E+09	-37.8263
133378.	0.000						
22.100	0.001011	2161.2560	489.4045	-3.526E-05	43.8790	9.106E+09	-33.4721
135042.	0.000						
22.440	0.000869	3879.4315	361.6937	-3.390E-05	78.7623	9.106E+09	-29.1312
136707.	0.000						
22.780	0.000735	5112.6766	251.4390	-3.189E-05	103.8004	9.106E+09	-24.9152
138372.	0.000						
23.120	0.000609	5931.1738	157.9559	-2.941E-05	120.4179	9.106E+09	-20.9099
140037.	0.000						
23.460	0.000495	6401.5964	80.2548	-2.665E-05	129.9687	9.106E+09	-17.1788
141701.	0.000						
23.800	0.000392	6586.0530	17.1283	-2.374E-05	133.7137	9.106E+09	-13.7655
143366.	0.000						
24.140	0.000301	6541.3635	-32.7735	-2.080E-05	132.8063	9.106E+09	-10.6962
145031.	0.000						
24.480	0.000222	6318.6213	-70.8783	-1.792E-05	128.2841	9.106E+09	-7.9827
146695.	0.000						
24.820	0.000155	5962.9964	-98.6376	-1.517E-05	121.0640	9.106E+09	-5.6248
148360.	0.000						
25.160	9.825E-05	5513.7388	-117.4823	-1.260E-05	111.9429	9.106E+09	-3.6128
150025.	0.000						

25.500	5.190E-05	5004.3406	-128.7888	-1.024E-05	101.6009	9.106E+09	-1.9296
151689.	0.000						
25.840	1.469E-05	4462.8222	-133.8518	-8.119E-06	90.6067	9.106E+09	-0.5523
153354.	0.000						
26.180	-1.435E-05	3912.1099	-133.8660	-6.243E-06	79.4258	9.106E+09	0.5453
155019.	0.000						
26.520	-3.625E-05	3370.4755	-129.9138	-4.611E-06	68.4292	9.106E+09	1.3920
156683.	0.000						
26.860	-5.198E-05	2852.0134	-122.9584	-3.217E-06	57.9031	9.106E+09	2.0175
158348.	0.000						
27.200	-6.250E-05	2367.1347	-113.8422	-2.048E-06	48.0589	9.106E+09	2.4513
160013.	0.000						
27.540	-6.870E-05	1923.0607	-103.2885	-1.087E-06	39.0430	9.106E+09	2.7222
161677.	0.000						
27.880	-7.137E-05	1524.3008	-91.9062	-3.147E-07	30.9472	9.106E+09	2.8574
163342.	0.000						
28.220	-7.126E-05	1173.1060	-80.1977	2.896E-07	23.8170	9.106E+09	2.8821
165006.	0.000						
28.560	-6.901E-05	869.8875	-68.5673	7.472E-07	17.6609	9.106E+09	2.8191
166671.	0.000						
28.900	-6.517E-05	613.5968	-57.3315	1.080E-06	12.4576	9.106E+09	2.6887
168336.	0.000						
29.240	-6.020E-05	402.0627	-46.7296	1.307E-06	8.1629	9.106E+09	2.5083
170000.	0.000						
29.580	-5.450E-05	232.2835	-36.9347	1.449E-06	4.7159	9.106E+09	2.2931
171665.	0.000						
29.920	-4.837E-05	100.6755	-28.0645	1.524E-06	2.0440	9.106E+09	2.0551
173330.	0.000						
30.260	-4.207E-05	3.2772	-20.1915	1.547E-06	0.0665	9.106E+09	1.8042
174994.	0.000						
30.600	-3.575E-05	-64.0875	-13.3532	1.533E-06	1.3011	9.106E+09	1.5479
176659.	0.000						
30.940	-2.955E-05	-105.6848	-7.5605	1.495E-06	2.1457	9.106E+09	1.2916
178324.	0.000						
31.280	-2.355E-05	-125.7812	-2.8065	1.444E-06	2.5537	9.106E+09	1.0388
179988.	0.000						
31.620	-1.777E-05	-128.5857	0.9268	1.387E-06	2.6106	9.106E+09	0.7913
181653.	0.000						
31.960	-1.223E-05	-118.2186	3.6622	1.331E-06	2.4001	9.106E+09	0.5496
183317.	0.000						
32.300	-6.909E-06	-98.7025	5.4223	1.283E-06	2.0039	9.106E+09	0.3132
184982.	0.000						
32.640	-1.765E-06	-73.9723	6.2260	1.244E-06	1.5018	9.106E+09	0.0808
186647.	0.000						
32.980	3.243E-06	-47.8980	6.0854	1.217E-06	0.9725	9.106E+09	-0.1497
188311.	0.000						
33.320	8.163E-06	-24.3151	5.0047	1.201E-06	0.4937	9.106E+09	-0.3801
189976.	0.000						
33.660	1.304E-05	-7.0598	2.9798	1.194E-06	0.1433	9.106E+09	-0.6125
191641.	0.000						
34.000	1.790E-05	0.000	0.000	1.192E-06	0.000	9.106E+09	-0.8482
96653.	0.000						

* The above values of total stress are combined axial and bending stresses.

Output Summary for Load Case No. 10:

Pile-head deflection = 2.2876901 inches
 Computed slope at pile head = -0.0318018 radians
 Maximum bending moment = 3350638. inch-lbs
 Maximum shear force = -59231. lbs
 Depth of maximum bending moment = 6.4600000 feet below pile head
 Depth of maximum shear force = 9.5200000 feet below pile head
 Number of iterations = 23
 Number of zero deflection points = 4

 Computed Values of Pile Loading and Deflection
 for Lateral Loading for Load Case Number 11

Pile-head conditions are Shear and Moment (Loading Type 1)

Shear force at pile head = 63500.0 lbs
 Applied moment at pile head = 0.0 in-lbs

Axial thrust load on pile head

= 0.0 lbs

Depth Distrib. X Lat. Load feet lb/inch	Deflect. y inches	Bending Moment in-lbs	Shear Force lbs	Slope S radians	Total Stress psi*	Bending Stiffness lb-in ²	Soil Res. p lb/in	Soil Spr. Es*h lb/inch
0.000	0.000	1.700E-06	63500.	-0.0354	3.452E-08	9.106E+09	0.000	
0.000	0.000	259080.	63500.	-0.0354	5259.9841	9.106E+09	0.000	
0.000	0.000	518160.	63500.	-0.0352	10520.	9.106E+09	0.000	
7.4540	0.000	777240.	63492.	-0.0349	15780.	9.106E+09	-3.9508	
184.0935	0.000	1036254.	63298.	-0.0345	21039.	9.106E+09	-91.1785	
448.4982	0.000	1293751.	62690.	-0.0340	26266.	9.106E+09	-206.7606	
788.1626	0.000	1547805.	61581.	-0.0334	31424.	9.106E+09	-336.7891	
1185.2640	0.000	1796254.	59941.	-0.0326	36469.	9.106E+09	-467.3560	
1614.3134	0.000	2036922.	57795.	-0.0317	41355.	9.106E+09	-584.5533	
2038.7902	0.000	2267860.	55226.	-0.0308	46043.	9.106E+09	-674.4729	
2406.2777	0.000	2487570.	52375.	-0.0297	50504.	9.106E+09	-723.2068	
2641.3472	0.000	2695242.	49437.	-0.0286	54720.	9.106E+09	-716.8468	
3482.6999	0.000	2890980.	46246.	-0.0273	58694.	9.106E+09	-847.8508	
4720.6929	0.000	3072605.	42428.	-0.0260	62382.	9.106E+09	-1023.4168	
6345.5208	0.000	3237194.	37861.	-0.0246	65723.	9.106E+09	-1215.2802	
8488.3081	0.000	3381552.	32478.	-0.0231	68654.	9.106E+09	-1423.4239	
11333.	0.000	3502216.	26213.	-0.0215	71104.	9.106E+09	-1647.6811	
15139.	0.000	3595452.	19002.	-0.0199	72997.	9.106E+09	-1886.9954	
20251.	0.000	3657276.	10794.	-0.0183	74252.	9.106E+09	-2136.7100	
27062.	0.000	3683532.	1575.9173	-0.0167	74785.	9.106E+09	-2381.9967	
35859.	0.000	3670135.	-8563.3952	-0.0150	74513.	9.106E+09	-2588.2545	
46524.	0.000	3613654.	-19346.	-0.0134	73366.	9.106E+09	-2697.5000	
58274.	0.000	3512269.	-30247.	-0.0118	71308.	9.106E+09	-2645.8595	
69818.	0.000	3366840.	-40544.	-0.0102	68355.	9.106E+09	-2401.7091	
79970.	0.000	3181432.	-49506.	-0.008783	64591.	9.106E+09	-1991.5888	
88205.	0.000	2962870.	-56598.	-0.007406	60154.	9.106E+09	-1484.8719	
94675.	0.000	2719591.	-61576.	-0.006133	55215.	9.106E+09	-955.4519	
99865.	0.000	2460407.	-64456.	-0.004973	49953.	9.106E+09	-456.1956	
104285.	0.000	2193629.	-65418.	-0.003930	44536.	9.106E+09	-15.2965	
108321.	0.000	1926596.	-64722.	-0.003007	39115.	9.106E+09	356.5796	
112222.	0.000	1665499.	-62651.	-0.002202	33814.	9.106E+09	658.4327	
116127.	0.000	1415362.	-59485.	-0.001512	28735.	9.106E+09	893.7525	
120100.	0.000	1180104.	-55483.	-0.000931	23959.	9.106E+09	1067.8419	
124160.	0.000	962621.	-50884.	-0.000451	19544.	9.106E+09	1186.6568	

11.560	-0.0400	764891.	-45900.	-6.353E-05	15529.	9.106E+09	1256.3806
128302.	0.000						
11.900	-0.0395	588076.	-40719.	0.000240	11939.	9.106E+09	1283.2870
132509.	0.000						
12.240	-0.0380	432623.	-35503.	0.000468	8783.3515	9.106E+09	1273.6734
136760.	0.000						
12.580	-0.0357	298372.	-30388.	0.000632	6057.7140	9.106E+09	1233.7839
141035.	0.000						
12.920	-0.0328	184659.	-25485.	0.000740	3749.0514	9.106E+09	1169.7026
145319.	0.000						
13.260	-0.0297	90418.	-20880.	0.000802	1835.7066	9.106E+09	1087.2302
149599.	0.000						
13.600	-0.0263	14274.	-16639.	0.000825	289.8069	9.106E+09	991.7603
153868.	0.000						
13.940	-0.0229	-45359.	-12804.	0.000818	920.9133	9.106E+09	888.1734
158121.	0.000						
14.280	-0.0196	-90209.	-9399.6595	0.000788	1831.4625	9.106E+09	780.7577
162358.	0.000						
14.620	-0.0165	-122061.	-6433.6632	0.000740	2478.1435	9.106E+09	673.1621
166578.	0.000						
14.960	-0.0136	-142707.	-3900.9200	0.000681	2897.3197	9.106E+09	568.3787
170783.	0.000						
15.300	-0.0109	-153892.	-1785.1696	0.000615	3124.4042	9.106E+09	468.7538
174977.	0.000						
15.640	-0.008563	-157274.	-61.8340	0.000545	3193.0666	9.106E+09	376.0185
179160.	0.000						
15.980	-0.006483	-154397.	1299.5710	0.000475	3134.6482	9.106E+09	291.3368
183337.	0.000						
16.320	-0.004686	-146670.	2143.9837	0.000408	2977.7683	9.106E+09	122.5910
106734.	0.000						
16.660	-0.003157	-136902.	2565.1816	0.000344	2779.4570	9.106E+09	83.8786
108404.	0.000						
17.000	-0.001878	-125738.	2839.6508	0.000285	2552.7977	9.106E+09	50.6652
110072.	0.000						
17.340	-0.000829	-113730.	2989.3183	0.000232	2309.0155	9.106E+09	22.7012
111738.	0.000						
17.680	1.226E-05	-101345.	3034.9337	0.000183	2057.5610	9.106E+09	-0.3407
113403.	0.000						
18.020	0.000668	-88965.	2995.7970	0.000141	1806.2217	9.106E+09	-18.8440
115067.	0.000						
18.360	0.001161	-76899.	2889.5674	0.000104	1561.2509	9.106E+09	-33.2293
116731.	0.000						
18.700	0.001514	-65386.	2732.1467	7.180E-05	1327.5105	9.106E+09	-43.9377
118395.	0.000						
19.040	0.001747	-54605.	2537.6241	4.491E-05	1108.6195	9.106E+09	-51.4165
120060.	0.000						
19.380	0.001881	-44679.	2318.2753	2.267E-05	907.1054	9.106E+09	-56.1074
121724.	0.000						
19.720	0.001932	-35688.	2084.6043	4.668E-06	724.5537	9.106E+09	-58.4371
123389.	0.000						
20.060	0.001919	-27669.	1845.4213	-9.526E-06	561.7516	9.106E+09	-58.8094
125053.	0.000						
20.400	0.001855	-20629.	1607.9466	-2.035E-05	418.8249	9.106E+09	-57.5997
126718.	0.000						
20.740	0.001753	-14548.	1377.9350	-2.823E-05	295.3650	9.106E+09	-55.1510
128383.	0.000						
21.080	0.001624	-9385.2316	1159.8130	-3.359E-05	190.5441	9.106E+09	-51.7715
130048.	0.000						
21.420	0.001479	-5084.0995	956.8230	-3.683E-05	103.2202	9.106E+09	-47.7333
131713.	0.000						
21.760	0.001324	-1577.5556	771.1712	-3.832E-05	32.0284	9.106E+09	-43.2725
133377.	0.000						
22.100	0.001166	1208.6576	604.1724	-3.841E-05	24.5388	9.106E+09	-38.5897
135042.	0.000						
22.440	0.001010	3352.4913	456.3910	-3.738E-05	68.0641	9.106E+09	-33.8522
136707.	0.000						
22.780	0.000861	4932.8080	327.7736	-3.553E-05	100.1486	9.106E+09	-29.1956
138372.	0.000						
23.120	0.000720	6027.1238	217.7727	-3.307E-05	122.3660	9.106E+09	-24.7264
140037.	0.000						
23.460	0.000591	6709.8334	125.4590	-3.022E-05	136.2267	9.106E+09	-20.5254
141701.	0.000						
23.800	0.000474	7050.8691	49.6217	-2.714E-05	143.1506	9.106E+09	-16.6497
143366.	0.000						
24.140	0.000370	7114.7468	-11.1425	-2.396E-05	144.4475	9.106E+09	-13.1366
145031.	0.000						
24.480	0.000278	6959.9466	-58.3537	-2.081E-05	141.3046	9.106E+09	-10.0061
146695.	0.000						

24.820	0.000200	6638.5807	-93.5842	-1.776E-05	134.7801	9.106E+09	-7.2638
148360.	0.000						
25.160	0.000133	6196.2996	-118.4055	-1.489E-05	125.8007	9.106E+09	-4.9035
150025.	0.000						
25.500	7.828E-05	5672.3919	-134.3457	-1.223E-05	115.1640	9.106E+09	-2.9103
151689.	0.000						
25.840	3.357E-05	5100.0384	-142.8569	-9.815E-06	103.5438	9.106E+09	-1.2619
153354.	0.000						
26.180	-1.812E-06	4506.6795	-145.2907	-7.663E-06	91.4971	9.106E+09	0.0688
155019.	0.000						
26.520	-2.896E-05	3914.4664	-142.8818	-5.776E-06	79.4736	9.106E+09	1.1120
156683.	0.000						
26.860	-4.895E-05	3340.7643	-136.7380	-4.151E-06	67.8260	9.106E+09	1.8996
158348.	0.000						
27.200	-6.283E-05	2798.6840	-127.8363	-2.775E-06	56.8204	9.106E+09	2.4640
160013.	0.000						
27.540	-7.159E-05	2297.6205	-117.0222	-1.634E-06	46.6475	9.106E+09	2.8370
161677.	0.000						
27.880	-7.616E-05	1843.7828	-105.0148	-7.059E-07	37.4335	9.106E+09	3.0490
163342.	0.000						
28.220	-7.735E-05	1440.6998	-92.4130	2.990E-08	29.2499	9.106E+09	3.1284
165006.	0.000						
28.560	-7.591E-05	1089.6931	-79.7047	5.968E-07	22.1235	9.106E+09	3.1012
166671.	0.000						
28.900	-7.248E-05	790.3095	-67.2775	1.018E-06	16.0453	9.106E+09	2.9906
168336.	0.000						
29.240	-6.761E-05	540.7085	-55.4300	1.316E-06	10.9778	9.106E+09	2.8170
170000.	0.000						
29.580	-6.174E-05	338.0005	-44.3837	1.513E-06	6.8623	9.106E+09	2.5979
171665.	0.000						
29.920	-5.526E-05	178.5376	-34.2948	1.629E-06	3.6248	9.106E+09	2.3477
173330.	0.000						
30.260	-4.845E-05	58.1552	-25.2659	1.682E-06	1.1807	9.106E+09	2.0782
174994.	0.000						
30.600	-4.154E-05	-27.6324	-17.3572	1.689E-06	0.5610	9.106E+09	1.7986
176659.	0.000						
30.940	-3.468E-05	-83.4799	-10.5964	1.664E-06	1.6949	9.106E+09	1.5155
178324.	0.000						
31.280	-2.796E-05	-114.0992	-4.9882	1.619E-06	2.3165	9.106E+09	1.2336
179988.	0.000						
31.620	-2.146E-05	-124.1835	-0.5225	1.566E-06	2.5212	9.106E+09	0.9555
181653.	0.000						
31.960	-1.518E-05	-118.3624	2.8185	1.512E-06	2.4031	9.106E+09	0.6823
183317.	0.000						
32.300	-9.125E-06	-101.1842	5.0543	1.463E-06	2.0543	9.106E+09	0.4137
184982.	0.000						
32.640	-3.251E-06	-77.1190	6.2017	1.423E-06	1.5657	9.106E+09	0.1487
186647.	0.000						
32.980	2.483E-06	-50.5785	6.2712	1.394E-06	1.0269	9.106E+09	-0.1146
188311.	0.000						
33.320	8.124E-06	-25.9457	5.2658	1.377E-06	0.5268	9.106E+09	-0.3783
189976.	0.000						
33.660	1.372E-05	-7.6099	3.1796	1.369E-06	0.1545	9.106E+09	-0.6443
191641.	0.000						
34.000	1.930E-05	0.000	0.000	1.368E-06	0.000	9.106E+09	-0.9143
96653.	0.000						

* The above values of total stress are combined axial and bending stresses.

Output Summary for Load Case No. 11:

Pile-head deflection = 2.5943642 inches
 Computed slope at pile head = -0.0354377 radians
 Maximum bending moment = 3683532. inch-lbs
 Maximum shear force = -65418. lbs
 Depth of maximum bending moment = 6.4600000 feet below pile head
 Depth of maximum shear force = 9.5200000 feet below pile head
 Number of iterations = 23
 Number of zero deflection points = 4

 Summary of Pile Response(s)

Definitions of Pile-head Loading Conditions:

Load Type 1: Load 1 = Shear, lbs, and Load 2 = Moment, in-lbs
 Load Type 2: Load 1 = Shear, lbs, and Load 2 = Slope, radians
 Load Type 3: Load 1 = Shear, lbs, and Load 2 = Rotational Stiffness, in-lbs/radian
 Load Type 4: Load 1 = Top Deflection, inches, and Load 2 = Moment, in-lbs
 Load Type 5: Load 1 = Top Deflection, inches, and Load 2 = Slope, radians

Maximum Load Shear Case Pile No.	Load Type No.	Pile-head Condition 1 Pile-head V(lbs) or Rotation y(inches)	Pile-head Condition 2 in-lb, rad., or in-lb/rad.	Axial Loading lbs	Pile-head Deflection inches	Maximum Moment in Pile in-lbs	in lbs
1	1	V = 9500.0000	M = 0.000	0.0000000	0.14868850	338185.	
9500.0000		-0.00270257					
2	1	V = 15900.	M = 0.000	0.0000000	0.27522117	600952.	
15900.		-0.00486723					
3	1	V = 23100.	M = 0.000	0.0000000	0.46554263	948855.	
23100.		-0.00788283					
4	1	V = 30400.	M = 0.000	0.0000000	0.72201835	1361880.	
30400.		-0.01164971					
5	1	V = 35100.	M = 0.000	0.0000000	0.91901162	1653129.	
35100.		-0.01440237					
6	1	V = 42000.	M = 0.000	0.0000000	1.25007047	2107101.	
42000.		-0.01884360					
7	1	V = 47600.	M = 0.000	0.0000000	1.55466958	2493334.	
47600.		-0.02277532					
8	1	V = 50200.	M = 0.000	0.0000000	1.70700147	2681935.	
50200.		-0.02469677					
9	1	V = 54800.	M = 0.000	0.0000000	1.99344768	3018767.	
54800.		-0.02824142					
10	1	V = 59200.	M = 0.000	0.0000000	2.28769011	3350638.	-
59231.		-0.03180176					
11	1	V = 63500.	M = 0.000	0.0000000	2.59436421	3683532.	-
65418.		-0.03543775					

The analysis ended normally.